Ψ_k Newsletter

AB INITIO (FROM ELECTRONIC STRUCTURE) CALCULATION OF COMPLEX PROCESSES IN MATERIALS

Number 45 June 2001

Editor: Z. (Dzidka) Szotek
E-mail: psik-coord@dl.ac.uk

Contents

1 Editorial

We start this newsletter with a call for abstracts of newly submitted papers and scientific highlights. Please do read this and try to respond positively. In this newsletter we publish a number of reports on collaborative visits, visits to conferences, and workshop reports including abstracts of presented papers. Please see the **TMR1**, **TMR2**, and **ESF** sections for details. The workshop/conference announcements can be found in the **RTN**, **TMR2**, **ESF**, and **General Workshop/Conference** sections. Note that in the **ESF** section we publish a call for proposals for 2002 workshops to be funded by the ESF Programme. A few position announcements can as usual be found in the **General Job Announcments** section. As always, the abstracts of newly submitted papers are placed in the usual **Abstracts** section. In the **Book Announcement** section, S. Goedecker (CEA Grenoble) writes about his and A. Hoisie's new book on "Performance optimization of numerically intensive codes". The newsletter is finished with the scientific highlight of the month by O.K. Andersen, T. Saha-Dasgupta, S. Ezhov, L. Tsetseris, O. Jepsen, R.W. Tank, C. Arcangeli, and G. Krier (MPI Stuttgart) on **"Third-generation MTOs"**. Please see the table of contents for further details.

The *Networks* have a home page on World Wide Web (WWW). Its *Uniform Resource Locator* (URL) is:

http://psi-k.dl.ac.uk/

The above contains pointers to home pages of some of the members of our electronic structure community. If you maintain a home page on your activities we will be happy to include a pointer from the *Networks'* home page to your home page.

Please note that the home page of the Psi-k Networks has recently been updated. It contains useful information regarding funding of workshops and collaborative visits within the ESF Programme. Its major new feature is a separate highlight section which contains all highlight articles of the Newsletters published so far.

Please submit all material for the next newsletters to the email address below.

The following email addresses, which remain in operation, are repeated for your convenience, and are the easiest way to contact us.

	function
psik-coord@daresbury.ac.uk	**messages to the coordinators, editor & newsletter**
psik-management@daresbury.ac.uk	**messages to the NMB of all Networks**
psik-network@daresbury.ac.uk	**messages to the whole Ψ_k community**

Dzidka Szotek and Walter Temmerman
e-mail: psik-coord@dl.ac.uk

2 General News

2.1 Call for Abstracts of Newly Submitted Papers and Scientific Highlights

Recently we have noticed a sharp decline in submissions of abstracts to the Psi-k newsletters. The purpose of the **Abstracts** section is to keep the whole Psi-k community aware of our common interests and research efforts at any particular time, and to stimulate more collaboration and enhance collaborative visits between scientific institutions across Europe. So, we would like to encourage you all to send us your abstracts. The abstract template is available in every LaTeX file of the Psi-k newsletter. If you feel however that it takes too much of your effort, then just extract your abstract from your article and send it to us anyway. Do not wait until your paper is accepted or published, because it misses the point of the **Abstracts** section.

As you are fully aware, we publish six Psi-k newsletters a year and in each of them there is a scientific highlight. Six highlights a year may not seem that many, but it is increasingly harder to find volunteers for writing them. In addition, we find that there are only a few European groups who are willing to contribute a highlight from time to time. However, it would be beneficial to the whole community if also, until now, less visible groups would like to share the effort of producing exciting Psi-k newsletters by contributing a scientific highlight. There are many interesting things happening across the Psi-k community and it would be nice if all of it was well represented in the Psi-k newsletters. Note that all scientific highlights published to date can, apart from the newsletters, also be viewed at a dedicated web site:
http://psi-k.dl.ac.uk/psi-k/highlights.html.
So, if you feel that you could write a scientific highlight for one of the future newsletters, please contact us on psik-coord@dl.ac.uk suggesting a topic and preferred dates. We shall get back to you with exact dates and other details as soon as possible.

3 News from the TMR1 Network

"Interface Magnetism"

3.1 Reports on Visits to Conferences

Reports on a Conference Participation:

March Meeting of the APS

Seattle, Washington

March 12-16, 2001

This year's APS March Meeting was again very hectic, with more than 5,000 contributions offered in more than 30 parallel sessions. Having an invited talk on "Complex Band Structure and Resonant States in the Barrier-Problem", I could attend the meeting on the funds of the TMR-Network on "Interface Magnetism". Being myself mostly interested in magnetism and spin electronics, there was a huge amount of material presented, 12 dedicated sessions on Magnetic Nanostructures and several sessions on magnetic tunnel junctions and spindependent transport, all very well attended. Noteworthy are in particular the strong activities on the semiconductor side, filling seven well attended sessions on Spindependent Phenomena in Semiconductors. There were quite a few good ab-initio papers on magnetic semiconductors, so that I fear we will have problems in competing with these US activities in the future.

Let me shortly mention some personal highlights: Firstly Peter Levy's talk on Current induced Interlayer Coupling, secondly two new effects based on pure spin currents (without charge): a Dissipationless Spin Current (J. Knig et al. cond-mat. (0011504)) and a Spin Hall Effect (Shufeng Zhang, PRL 2000). Thus the spin is everywhere!

Finally, I should say that Seattle and the country around there are beautiful and very worthwhile to visit, but preferably not in March.

Peter H. Dederichs

The annual March Meeting 2001 of The American Physical Society was held March 12-16, 2001 in Seattle, Washington. During the outstanding scientific meeting approximately 5,000 papers were presented consisting of more than 90 invited sessions and 550 contributed sessions. Participating APS divisions ranged from Condensed Matter Physics, Materials Physics,

Chemical and Biological Physics to Computational Physics. More than 30 sessions were held in parallel in a very active but still relaxed atmosphere. Highlights of the conference have been the spin-dependent phenomena in semiconductors and magnetic nanostructures, properties of nanoparticles and nanowires and the session on "the history of electronic structure theory in atoms" with papers given by Kohn, Freeman and Kleinman.

There were a lot of activities of the TMR network on "Interface Magnetism", e. g. papers given by members of the groups in Jülich, Vienna, Twente and many more. The contributions from Dresden were "GMR in Co/Cu and Fe/Cr multilayers – a comparison" and "Ab initio calculated electronic structure of metallic nanowires".

Finally, I would like to acknowledge funding by the TMR network which made my visit to the 2001 March Meeting of the APS possible.

Jörg Binder

4 News from the Research Training Network (RTN)

COMPUTATIONAL MAGNETOELECTRONICS

4.1 RTN Workshop/Conference Announcements

4.1.1 First Annual Meeting

Second Announcement

1st Annual Meeting

of the Research Training Network

Computational Magnetoelectronics

Budapest, September 27-30, 2001

organized by the Hungarian Partner

Objective: The purpose of the meeting is to provide an overview on the activity of all the partners of the Network during the first year, Oct 2000 – Sept 2001. On average 5–10 members per each node (in total up to 80 participants) are expected, with special attention to young researchers for whom a session of tutorial lectures given by senior researchers is scheduled. We also plan to invite a limited number of overseas participants (non-members of the Network). All participants are invited to give oral contributions covering the topics of the scientific projects of the Network. Plans on research and training collaborations within the Network, on future workshops and realization of the scientific programs will be extensively discussed.

Timetable:	Sept 27, Thu Morning	Arrival
	Sept 27, Thu 2 p.m. – Sept 30, Sun 12 a.m.,	Meeting
	Sept 30, Sun Afternoon	Departure

Venue: The meeting will be held in the conference room of Hotel *AGRO, H-1121 Budapest, Normafa u. 54*, which is located at the attractive, hilly side of Budapest. Accommodation will be provided in single and double rooms in the same hotel or nearby.

Attendance: In order to get a quick overview on how many people are expected, we ask the node leaders (spokespersons) for sending us a list of the scheduled participants from the corresponding node. Please, also make notes on the list about the need for single and double

rooms (and the tentative sharing). Please, also mark on the list the tentative time of arrival and departure of the participants.

Further details and the scheduled program will be announced in the forthcoming Newsletters. The abstracts of the contributions will be collected into an abstract booklet which will be distributed prior the meeting.

Contact: János Kollár `jk@szfki.hu`
László Szunyogh `szunyogh@heisenberg.phy.bme.hu`

5 News from the TMR2 Network

'Electronic Structure calculations of materials properties and processes for industry and basic science'

5.1 Reports on Workshops/Conferences

5.1.1 Report on Workshop on f-Electron Systems

The Physics of f-Electron Systems

Daresbury Laboratory

6th - 8th April 2001

Workshop Sponsored by:

ESF Programme:

"Electronic Structure calculations for elucidating the complex atomistic behaviour of solids and surfaces"

TMR Network:

"Electronic Structure Calculations of Materials Properties and Processes for Industry and Basic Science"

Conference Organisers

Olle Eriksson, Axel Svane, Walter Temmerman

Shirley Miller, Damian Jones

The Physics of f-Electron Systems

Daresbury Laboratory, Tower Seminar Room, 6-8 April 2001

'The physics of f-electron systems' workshop took place in Daresbury from April 6-8, 2001. The workshop was sponsored by the ESF Programme and TMR Network. It brought together 35 participants, mostly from Europe, but also from as far a field as the US, Australia and Brazil. The physics of the f-electron systems, the rare earths and actinides, is dominated by the anomalous behaviour of the volume per atom in both the rare earth and actinide series. The opening talk by Borje Johansson exposed these fundamental issues of the lattice parameters and structures of the f-electron systems in a masterly fashion. Three themes were running through this workshop, all addressing the volume per atom anomalies. The first theme was a critical assessment of the present state of the art electronic structure calculations. Talks by Per Soderlind (GGA+OP), Victor Antonov (LSDA+U), Rajeev Ahuja (GGA), Peter Oppeneer (fully relativistic LSDA), Leon Petit (SIC-LSD), Mike Brooks (nature of exchange interactions) covered this topic exhaustively. Surprisingly, a lot of properties could be calculated successfully, most notably the elastic constants, by these 'modified' band theory methods which have in common a mean field approach to the electron-electron interaction problem. The second theme was to present the latest experimental data on the actinides and Pu in particular, highlighting the intricate correlated behaviour of the f-electrons. Talks by Peter Wachter, Gerry Lander, Thomas Gouder and Zygmunt Henkie covered this comprehensively. The third theme was to review progress in ab initio many body theory for f-electron systems. This session was dominated by the huge success of Dynamical Mean Field Theory (DMFT) in describing the electronic properties of fluctuating electron systems. Talks by Antoine Georges, Gabi Kotliar, Jesper Laersgaard, Balazs Gyorffy and Urban Lundin resulted in a deeper understanding of the problem of fluctuating f-electrons. In particular the DMFT was introduced by Antoine Georges and Gabi Kotliar presented the first results for an ab initio calculation on Pu (This is now published in the April 12 issue of Nature). The enthusiasm for DMFT spilled over into the satellite meeting which was a Question & Answer session on DMFT. All in all this was a most stimulating meeting with plenty of time for lively discussions and one felt that many more exciting results will be generated in the foreseeable future.

The Organizers:

Olle Eriksson, Axel Svane and Walter Temmerman

Programme

· Friday April 6th

Chair: Walter Temmerman

10:00 - 13:30 Coffee and Buffet Lunch in Science Centre

13:30 - 14:20 B. Johansson "*Electronic structure of actinides*"

14:20 - 15:10 P. Wachter "*The physics of the actinide tellurides up to AmTe*"

15:10 - 15:40 Coffee

15:40 - 16:30 P. Oppeneer "*Theoretical results on the Pu monochalcogenides and on intermetallic U compounds*"

16:30 - 17:20 L. Petit "*SIC-LSD theory of actnide pnictides and chalcogenides*"

17:20 - 18:10 R. Ahuja "*Structural Phase Transformations in Americium, Thorium Pnictides and Chalcogenides and Elastic constants of AnTe where An=Th, U, Pu, Np and Am*"

19:30 - Closing Ring O'Bells Pub, Daresbury

· Saturday April 7th

Chair: Axel Svane

9:00 - 9:50 A. Georges "*Kondo physics: from single impurity to Dynamical Mean Field Theory*"

9:50 - 10:20 Coffee

10:20 - 11:10 J. Lægsgaard "*Excitation spectra of the Ce monopnictides within dynamical mean-field theory*"

11:10 - 12:00 B. Gyorffy "*Non-local coherent potential approximation*"

12:00 - 13:00 Buffet Lunch

Chair: Gerrit van der Laan

13:00 - 13:50 P. Wachter "*Recent developments in the d-phase of Pu metal*"

13:50 - 14:40 G. Kotliar "*Dynamical Mean Field Theory of Pu*"

14:40 - 15:30 T. Gouder "*Spectroscopy study of thin films of plutonium*"

15:30 - 16:00 Coffee

16:00 - 16:50 G. Lander "*X-ray magnetic scattering from f-electron materials*"

16:50 - 17:40 P. Söderlind "*GGA+OP theory for f-electron metals*"

17:40 - 18:30 M. Brooks "*Exchange enhanced spin-orbit interaction and screened exchange interactions*"

19:30 - Closing Conference Dinner at Daresbury Cantina

· Sunday April 8th

Chair: Olle Eriksson

9:00 - 9:50 V. Antonov "*The electronic structure and magneto-optical Kerr effect of Tm monochalcogenides*"

9:50 - 10:20 Coffee

10:20 - 11:10 Z. Henkie "*Nonmagnetic Kondo-like behaviour in actnides: Atomic disorder versus band structure tuning effect*"

11:10 - 12:00 M. Biasini "*Positron annihilation studies of the fermi surface of rare-earth intermetallic compounds*"

12:00 - 12:50 U. Lundin "*Using pertubation theory from the atomic limit in electronic structure calculations*"

12:50 End of Meeting (Lunch available at Daresbury Cantina)

· Satellite Meeting: Sunday April 8th

14:00 - 17:00 Informal discussions on the dynamical mean field approach to f-electron systems

Friday 13:30 - 14:20

Electronic structure of Actinides

Borje Johansson

Condensed Matter Theory Group, Department of Physics, Uppsala University,

SE-751 21 Uppsala, Sweden

and

Applied Materials Physics, Department of Materials and Engineering, Brinellvägen 23,
Royal Institute of Technology (KTH), SE-100 44 Stockholm, Sweden

The series of heavy radioactive elements known as the actinides all have similar chemical properties. However,when the volume per atom in the solid state is plotted as a function of atomic number, one of the most dramatic anomalies in the entire periodic table occurs. The atomic volume of americium, the seventh element in the series, is almost 50% larger than the volume of the sixth, plutonium. Recent experiments at the European Synchrotron Radiation Facility (ESRF) in Grenoble, France, have shed new light on the properties of americium. These have shown that americium becomes more like plutonium under very high pressures (S. Heathman et al. Phys. Rev. Lett. 85, 2961 (2000)). This and other features of the actinide elements related to their electronic structure will be discussed in terms of density functional theory.

14:20 - 15:10

The Physics of the Actinide Tellurides up to AmTe

P. Wachter and M. Filzmoser

Laboratorium für Festkörperphysik, ETH Zürich, 8093 Zürich, Switzerland

J. Rebizant

European Institute for Transuranium Elements, 76125 Karlsruhe, Germany

The elastic constants c_{11}, c_{12} and c_{44} of U, Np, Pu, and Am telluride single crystals have been obtained by Brillouin scattering from the measured sound velocities in prominent crystallographic directions. In case of the U chalcogenides also by ultrasound techniques. The Cauchy pressure, the Poisson ratio, the anisotropy ratio and the bulk modulus and the Debye temperature have been derived from these data. U and Pu telluride have a negative c_{12}, implying intermediate valence. AmTe has a very low bulk modulus, but a positive c_{12}. It is extremely soft, with a very low sound velocity. For AmTe also the LO and TO phonon frequencies could be determined. The elastic data point to a divalent Am state.

The optical reflectivity of the light actinide tellurides (and sometimes of all chalcogenides) has been measured between UV and infrared wavelengths, in the case of AmTe down to the far infrared. The plasma edge of the free carriers has been determined, which yields the ratio of $n/m*$. Together with the γ value of the specific heat and magnetic data a consistent proposal for the electronic structure of the light actinide chalcogenides can be given. Thus the Pu chalcogenides are intermediate valent and represent the high pressure phase of the corresponding Sm chalcogenides. AmTe, as judged by the electronic, optic and magnetic properties seems to be in the $5f^7$ configuration, i.e. divalent Am, but with a narrow, half filled (24 meV) wide $5f$ band, about 0.1 eV below the bottom of the $6d$ conduction band. We thus propose a new kind of unhybridized heavy fermion. Also AmTe seems to represent a high pressure phase of EuTe.

15:40 - 16:30

Theoretical results on the Pu monochalcogenides and on intermetallic U compounds

P.M. Oppeneer

Institute of Solid State and Materials Research, P.O. Box 270016,

D-01171 Dresden, Germany

The anomalous properties of the Pu monochalcogenides are studied on the basis of electronic structure calculations. As a surprise, it is found that most of the anomalous properties of the Pu monochalcogenides can be explained by the LSDA approach valid for delocalized $5f$ electrons. In particular, it turns out that the Pu monochalcogenides are semimetallic as observed

experimentally, because, first the large spin-orbit interaction of the Pu $5f$ states splits the $5f_{5/2}$ and $5f_{7/2}$ subbands away from the Fermi energy, and second the hybridization between Pu $6d$, chalcogenide p and Pu $5f$ bands leads to the formation of a hybridization gap. The anomalous lattice constants, which correspond neither to Pu^{2+} nor to Pu^{3+} are consistent with the energy band approach, as is the lattice constant where the transition to Pu^{2+} is expected. The calculations suggest that Pu has a $5f^{6-x}6d^x$ configuration, where $x \approx 0.4$, depending on the lattice parameter. This finding is reminiscent of the mixed-valence model to the Pu monochalcogenides, but there exist also differences. On the basis of the calculations a magnetic phase transition under pressure is predicted. Calculated physical properties of several ternary uranium intermetallics will also be presented. For URhAl, where a sizable induced moment on Rh has been reported, we compare the spin and orbital moments as computed with both the ASW and FLAPW methods. The obtained theoretical moments are very consistent, the deviation per individual moment being less than $0.04\mu_B$. Furthermore, the x-ray magnetic circular dichroism at the M-edges in UrhAl is computed and found to be in good agreement with the available experimental spectrum. The orbital U moment, as derived experimentally from the sum rule, however, is not in good correspondence with that obtained from neutron scattering experiments.

Work done in collaboration with T. Kraft, M.S.S. Brooks, J. Kune, P. Novák, G. Varelogiannis, and M. Divi.

16:30 - 17:20

SIC-LSD Theory of Actinide Pnictides and Chalcogenides

Leon Petit

University of Aarhus, Denmark

We use the ab-initio self-interaction-corrected local spin-density approximation (SIC-LSD), to investigate the electronic and magnetic properties of the transuranium pnictides and chalcogenides, i.e. NpX, PuX, AmX and CmX (X = N, P, As, Sb, Bi, O, S, Se, Te). The f-electron manifold is considered to be consisting of both localized and delocalized states, and by varying their relative proportions we establish the energetically favourable groundstate configuration. We find the Neptunium pnictides to be tetravalent up to NpAs. NpSb becomes trivalent. The corresponding Np chalcogenides follow the same trend. The increased f-electron localization makes the Pu pnictides and chalcogenides more trivalent, but still a considerable trend towards tetravalency is observed for small Pu-Pu distances. The Am pnictides are found to be trivalent, whereas in the Am chalcogenides we notice a transition to a divalent configuration around AmTe. In the Cm compounds, the favourable half-filled 5f shell results in a preferred trivalent configuration for both the pnictides and the chalcogenides. Generally, for the pnictides, our calculations are in good agreement with the experimental results. In the chalcogenides, many-body effects which can not be accounted for in the LSD tend to make the compounds intermediate valent, and the calculations become less reliable.

17:20 - 18:10

Structural Phase Transformations in Americium, Thorium Pnictides and Chalcogenides and Elastic constants of AnTe where An=Th, U, Pu, Np and Am

R. Ahuja

Condensed Matter Theory Group, Department of Physics, University of Uppsala

Box 530, Uppsala, Sweden

Density-functional electronic structure calculations have been used to investigate the high pressure behavior of Am. The phase transition from fcc to the low symmetry structure is shown to originate from a drastic change in the nature of the electronic structure induced by the elevated pressure. For the low density phase, an orbital polarization correction to the local spin density (LSD) theory was applied. Gradient terms of the electron density were included in the calculation of the exchange/correlation energy and potential, according to the generalized gradient approximation (GGA). Theory compares rather well with recent experimental data of S.Heathman et al.(Phys.Rev.Lett. 85, 2961 (2000)) which implies that electron correlation effects are reasonably modeled in our orbital polarization scheme.

Using the same approach, we have looked in to the elastic constants of AnTe where An = Th, U, Pu, Am and Np. They compare very well with the recent experimental data. In addition, we will also present our results for high pressure structural phase transition in thorium pnictides and chalcogenides. We compare the calculated structural stabilities with experimental data. For most of the compounds LDA gives the correct ground state but it fails in case of ThSe, ThAs and ThSb. If we instead use the GGA, the correct ground state is obtained also for these compunds. At high pressure all the compounds show a NaCl $\rightarrow$ CsCl phase transition except ThTe and ThBi which are stable in the CsCl structure already at ambient pressure.

Saturday 9:00 - 9:50

Kondo physics: from single impurity to Dynamical Mean Field Theory

Antoine Georges

Laboratoire de Physique Theorique de l'Ecole Normale Superieure - Paris

and

Laboratoire de Physique des Solides - Orsay

Dynamical Mean Field Theory (DMFT) describes f-electron materials by embedding an impurity problem in a crystal in a self-consistent manner. This self-consistent embedding allows to address several phenomena which cannot be understood in a simple single-impurity picture.

In particular, I will emphasize that two distinct energy scales emerge: one associated with the onset of screening of local moments, and a lower one associated with the onset of Fermi liquid coherence. For low densities of conduction electrons (the so-called "exhaustion" limit) the latter becomes very small. I will also review what has been learned from DMFT on the ordered phases of Kondo and Anderson lattice models. Finally, I will emphasize some limitations of the method, particularly regarding the Kondo vs. RKKY competition, and possible improvements.

10:20 - 11:10

Excitation spectra of the Ce monopnictides within dynamical mean-field theory

J.Lægsgaard and A.Svane

Institute of Physics and Astronomy, University of Aarhus,DK-8000 Aarhus C, Denmark

A lattice tight-binding model of the Ce monopnictides CeN, CeP, CeAs including local Coulomb correlations is studied within dynamical mean-field theory. The impurity problem is solved in a finite-U extension of the non-crossing approximation, including lowest-order crossing diagrams in an approximate way. Parametrization of the model by means of ab initio calculations is attempted and discussed. It is shown that the model gives a good account for the various features of Ce monopnictide photoemission spectra. In particular, dispersive quasiparticle peak positions are found close to the Fermi edge in CeP. CeN shows metallic Fermi-liquid behavior with a correlation-induced mass enhancement factor of ~ 5 around the Fermi level.

11:10 - 12:00

Non-Local Coherent Potential Approximation

R.Marodian[1], B.L.Gyorffy[1], J.F.Annett[1] and M.Jarrell[2]

[1] H.H.Wills Physics Laboratory, University of Bristol, Tyndall Ave, Bristol BS8 1TL

[2] Department of Physics, University of Cincinnati, Cincinnati OH 45221,USA

Over the past 30 years or so the Coherent Potential Approximation (CPA) has proved itself to be a generally reliable method for dealing with electrons, and other elementary excitations such as phonons and spin-waves, in disordered systems. [1] However, it is well known to be only a mean field theory for the problems at hand [2] and hence much effort have gone into finding a systematic and effective method for improving on it [3]. Suprisingly, this turned out to be a very difficult problem and what appears to be a viable solution to it has been proposed only recently. The new method is the Dynamical Cluster Approximation (DCA) adopted for the static problem of electrons in a disordered potential, by Jarrell et al.[4] In this talk we recall this work and report on some more recent investigations of the new approach.

[1]H. Ehrenreich and L. Schwartz, "Solid State Physics", 31 (1976)

[2]R. Valming and D. Vollhardt, Phys.Rev.45, 4637 (1992)

[3]B.G. Nickel and W.H.Butler, Phys. Rev. Lett. 30, (1973)

Robert Mills and Pisishta Ratanavararaksa Phys. Rev. B 18, 5291 (1978)

[4]M. Jarrell and A H.R. Krishnamurthy, Cond-mat/0006431

13:00 - 13:50

Recent developments in the d-Phase of Pu Metal

P. Wachter

Laboratorium für Festkörperphysik, ETH Zürich, 8093 Zürich, Switzerland

There has been a renewed interest in the various crystallograhic phases of Pu metal, especially in its high temperature fcc d-phase. In the recent 2 or 3 years many significant experiments have been carried out, but clear statements as to itinerant or localized $5f$ states have been avoided. Especially there has not been a correlation of the various experiments, which would support any of the above premisses. Thus theories are en vogue which propose even an inhomogeneous alloy between localized and itinerant $5f$ states in $\delta-$Pu[1].

All experiments to be discussed have been performed on Ga stabilized $\delta-$Pu at low temperatures. Al and Ga stabilization results in a smaller lattice constant of $\delta-$Pu, Ce and Am substitution in a larger lattice constant. These experiments thus correspond to positive or negative pressures, but the statements regarding the $5f$ state hardly depend on these substitutions, thus the $5f$ state is in a stable configuration.

Arko et al. [2] have performed unique photoemission experiments with 40.8 He II excitation. Usually this group works with in ultrahigh vacuum in situ cleaved single crystals at low temperatures and they perform ARPES i.e. angular resolved photoemission with high spectral resolution. This is necessary because the f electrons are only strongly emitted at certain $\mathbf{k}$ values i.e. certain emission angles. For $\delta-$Pu no single crystals are available and one could not cleave them anyhow because of the plastic deformity of Pu. In this case a low temperature laser ablation was performed with successive laser annealing and partial recristallisation with preferential orientation. Under this condition a clearly discernable $5f$ peak at the Fermi level E_F cold be observed with a half width of about $50-100$ meV. This is a clear indication of a narrow $5f$ band. Localized $5f$ states would give a completely different picture with fingerprint like multiplet spectra of the $5f^{n-1}$ final state. The question is now, whether this band like $5f$ state is the result of hybridization of an initially localized $5f$ state with a broad $6d$ band, where the $5f$ band has acquired a width corresponding to the hybridization energy. In this case photoemission would show a combined spectrum of final $5f^{n-1}$ states where n corresponds to the trivalent or the divalent valence. Experimentally this spectrum would look like the one of Intermediate valent SmB_6, but it is not the case. Thus the narrow $5f$ band is the result of direct $5f$ overlap in $\delta-$Pu.

This statement is supported by the measurement of the elastic moduli on $\delta-$Pu single crystals [3] where it is found that c_{12} is positive. A negative c_{12} would be an unmistakable sign of intermediate valence.

Because of the narrow $5f$ band the magnetic moments are quenched nearly completely. Thus experimentally only a temperature independent Pauli magnetic susceptibility prevails [4]. The Pauli susceptibility depends only on the density of states at E_F, and this must be large in order to dominate the susceptibility. This implies a narrow partially filled $5f$ band. The value of the Pauli susceptibility is between the one of PuTe and AmTe, the up to date record holders, with AmTe having the maximum value ever found. An estimate of the band width of the $5f$ band in $\delta-$Pu yields a width between 24 and 40 meV, the band widths of AmTe and PuTe, respectively. This compares well with the band width estimated from photoemission.

The γ value of the specific heat has been measured to be 53 mJ/molK^2 for $\delta-$Pu and 22 mJ/molK^2 for $\alpha-$Pu. The mere existence of a large γ value necessitates a narrow $5f$ band because also the γ value is proportional to the density of states at E_F. The Wilson ratio remains constant. A value of 53 mJ/molK^2 for $\delta-$Pu corresponds to a band width of about 30 meV. Thus all estimates of the band width from various experiments center around about 40 meV.

The conclusion is then that in $\delta-$Pu a narrow itinerant $5f$ band exists through direct $5f$ overlap, not withstanding the hybridization of this $5f$ band with the $6d$ band, making the material a light weight heavy fermion. The existence of localized $5f$ states can be experimentally excluded.

[1] B.R. Cooper, Y.L.Lin and A. Setty, Journeés des Actinides 2000, Dresden, S 15

[2] A.L. Arko, J.J. Joyce, L. Morales and J. Lashey, Journeés des Actinides 2000, Dresden P 11

[3] H.M. Ledbetter and R.L. Moment, Acta Metallurgica 24, (1976) 891

[4] M. Dormeval and N. Baclet, Journeés des Actinides 2000, Dresden, S 11

13:50 - 14:40

Dynamical Mean Field Theory of Pu

Gabriel Kotliar

Rutgers University, Department of Physics and Astronomy, 136 Frelinghuysen Road, POBox 9019, Piscataway N.J 08854, USA

We describe recent advances in the integration of the Dynamical Mean Field Method with realistic electronic structure calculations. A new functional approach is used to derive the total energy of the solid, its minimization leads to a fully integrated DMFT LDA loop, which is implemented within a full potential LMTO method for the one electron part, and a new extension of the interpolative perturbation theory (which is benchmarked against the QMC method) for the many body part of the loop.

Results for the total energy as a function of volume of fcc δ plutonium will be presented together with the corresponding one electron spectra which is being compared with photoemission

experiments.

This work results in new perspectives on the physics of the α and δ phases of plutonium. Both are viewed as correlated phases, on different sides of a Mott transition.

14:40 - 15:30

Spectroscopy study of thin films of plutonium

T. Gouder[1] L. Havela[1,2] F. Wastin[1] and J. Rebizant[1]

[1] European Commission, Joint Research Centre, Institute for Transuranium Elements, Post Box 2340, D-76175 Karlsruhe, Germany

[2] Department of Electronic Structures, Charles University, Ke Karlovu 5, CZ-121 16 Prague 2, Czech Republic

Photoelectron spectroscopy studies were performed on thin films of Pu, deposited on various substrates (Si, Mg and Al). We studied the evolution of the electronic structure as a function of overlayer thickness. The leading idea is that in thin overlayers, due to the reduced atomic coordination, $5f$ localisation phenomena would be emphasised.

This was confirmed experimentally. Indeed, with decreasing overlayer thickness, the $5f$ spectral response evolves from the typical $\alpha-$Pu, to the $\delta-$Pu behaviour. Around one monolayer coverage, localised $5f$ states appears, as found e.g. in PuSb or Pu_2O_3. Core level spectra (Pu-$4f$) confirm gradual retraction of the $5f$ states from bonding, by continuous increase of the poorly screened final state with decreasing overlayer thickness.

A surprising and not yet understood phenomenon is a pronounced temperature dependence of photoelectron spectra at the intermediate ($\delta-$Pu like) state of localisation, observed for PuSe compounds and Pu-Si interdiffusion layers. This may be related to many-body physics, similar to the Kondo-effect.

We could also resolve contradicting experimental results on $\alpha-$Pu. There are serious discrepancies between valence band data on $\alpha-$Pu in literature, which were shown to originate from the method of surface preparation. Those cleaning methods, which allowed the surface to rearrange lead to a $\delta-$Pu like surface (which is thermodynamically stable), while those methods which prevent rearrangement lead to a highly defective $\alpha-$Pu or amorphous surface.

16:00 - 16:50

X-ray Magnetic Scattering from f-electron materials

G. H. Lander

European Commission, ITU, Karlsruhe, Germany

The cross section for the scattering of photons from spin and orbital moments is small. This cross section may be increased by tuning the photon energy to resonant edges, i.e. when the incident photon promotes a core electron to a valence orbital. Intermediate states are then formed which can decay to give a large enhancement of the scattering cross section.

In the actinides we have examined both L_2 and L_3 edges, but most of the work has been performed at the M_i edges, where i = 2, 3, 4, & 5. Although we have a qualitative picture, much remains to be done before we can claim to understand these processes. In particular, this talk will highlight some of our recent findings such as:

(1) The unusual energy spectrum of NpO_2

(2) The unexpectedly large enhancement at the M_2 edge in comparison to that at the M_3

(3) The appearance of a new spectral feature in the Pu M_5 edge in Pu compounds

(4) The large signal at the U M_4 edge in URu_2Si_2 when the neutron moment is only $\sim 0.02\ \mu_B$

(5) The large enhancement at the K edge of anions in UGa_3 and UAs.

Since resonant scattering is more difficult in other parts of the periodic table, because the energies of the respective edges are lower and special large d-space samples, such as multilayers, have to be used, more resonant studies have actually been performed on actinides than other materials. We are therefore interested in how best to use this technique, as well as to discover new properties of actinide systems.

16:50 - 17:40

GGA+OP theory for f-electron metals

Per Söderlind

Lawrence Livermore National Laboratory, University of California,

P.O. Box 808, Livermore, CA 94550, USA

The ground state of metals from the lanthanide and actinide series has been studied using a standard density-functional technique expanded to include spin and orbital polarization (OP). For the exchange and correlation energy functional the general gradient approximation (GGA) has been used throughout all calculations. In most cases, a considerable improvement of the equation-of-state has been achieved compared to previous density-functional treatments. In particular, the abrupt change in density between Pu and Am is accurately predicted. Also the intermediate δ phase of Pu is well described within the present approach.

17:40 - 18:30

Exchange enhanced spin-orbit interaction and screened exchange interactions

M.S.S. Brooks

European Commission, Joint Research Center, Institute for Transuranium Elements, D-76125 Karlsruhe, Germany

Exchange interactions depend upon both orbital and spin quantum numbers and it is only in the uniform electron gas that the dependence upon orbital quantum numbers vanishes. The orbital dependence of the exchange interactions is retained by Hartree-Fock theory for non-uniform densities. When spin-orbit interaction is large the density matrix is off-diagonal in spin, leading to exchange interactions which are also off-diagonal in spin. In turn these exchange interactions enhance the effect of spin-orbit interaction with the result that the spin and orbital densities in the atom are non-collinear. This can lead to an enhancement of the local orbital and spin moments with a reduction in the calculated total moment. The lack of screening of the exchange interactions in Hartree-Fock theory is addressed by application of Thomas-Fermi screening to self-consistent energy band calculations, which reduces the exchange interactions particularly the spherical Coulomb integral.

Sunday 9:00 - 9:50

The electronic structure and magneto-optical Kerr effect of Tm monochalcogenides

V.N. Antonov

Institute of Metal Physics, 36 Vernadskii Street, 252142 Kiev, Ukraine

B.N. Harmon

Ames Laboratory, Iowa State University, Iowa, 5001, USA

A.N. Yaresko

Max Planck Institute for Physics of Complex Systems, D-01187 Dresden, Germany

The optical and magneto-optical (MO) spectra of Tm monochalcogenides are investigated theoretically from first principles, using the fully relativistic Dirac LMTO band structure method. The electronic structure is obtained with the local spin-density approximation (LSDA), as well as with the so-called LSDA+U approach. In contrast to LSDA, where the stable solution in TmTe is a metal, the LSDA+U gave an insulating ground state. LSDA+U theory predicts the thulium ion in TmTe to be in an integer divalent state. It also shows a gradual decreasing of the energy gap with reducing of the lattice constant. LSDA+U theoretical calculations produce a similar energy band structure in TmS and TmSe, with twelve $4f$ bands fully occupied and

hybridized with chalcogenide p states. The 14^{th} f hole level was found to be completely unoccupied and well above the Fermi level and a hole 13^{th} f level is partly occupied and pinned at the Fermi level. The occupation number of the 13^{th} f level is equal to 0.12 and 0.27 in TmS and TmSe respectively (valence 2.88+ and 2.73+). Such an energy band structure of thulium monochalcogenides describes well their measured BIS, XPS and UPS spectra as well as the optical and MO spectra. The origin of the Kerr rotation realized in the compounds is examined.

10:20 - 11:10

Nonmagnetic Kondo-like behaviour in actinides: Atomic disorder versus band structure tuning effect

Z.Henkie

W.Trzebiatowski Institute for Low Temperature and Structure Research,

50-950 Wroclaw 2, P.O. Box 1410, Poland

It has been found that electron transport properties of some actinide compounds show a nonmagnetic Kondo-like behaviour which presumably is due to the deviation of the compound's composition from the stoichiometric one. The temperature dependent electrical resistivity of the compounds can be resolved into several contributions: a phonon resistivity, a magnetic resistivity and single-ion Kondo-like resistivity. The Kondo-like resistivity is scaled with the Kondo temperature T_K that assumes values between 20 K and 50 K, depending on a particular compound. The thermoelectric power shows pronounced peak at T_K while the temperature dependence of the Hall coefficient reveals the skew -scattering-like component.

The presented group of compounds includes the semimetallic antiferromagnet USb_{1+x}, crystallising in a cubic structure, and some uranium and thorium pnictidochalcogenides crystallising in the tetragonal structure of the PbFCl type. The uranium compounds from the latter group - UPS, UAsS, $UAs_{1-x}Se_{1+x}$ - are highly anisotropic ferromagnets with Curie temperature of about 110 K. The Hall carrier concentration for uranium arsenoselenide was found to be equal $\sim$ 0.5 per formula unit (f.u.). The ARPES spectra examination done by Arko and coworkers shows the d-like band crossing the Fermi energy and hybridising with the narrow f-like band thus pulling it from above to below the Fermi energy E_F and leaving the high density of states at E_F. On the other hand, the examined here thorium arsenochalkogenides show weak and temperature independent diamagnetism between 20 and 300 K. The transport properties show that the main charge carriers in ThAsSe and $ThAs_{1.23}S_{0.77}$ are light electrons. An estimation done for the last compound shows that this band is characterised by the carrier density equal to 1.5 10^{22} e^-/cm^3 and effective mass between 0.2 and 0.4 of free electron mass.

The Kondo-like compounds show very different magnetic and the conduction band properties. Therefore, it is unlikely that the observed Kondo-like features may be related to their magnetic or band properties. On the other hand, atomic disorder turned out to be the common property of all these systems that is presumably created by the deviation of the compounds' composition from the stoichiometric one. Anomalous large anisotropic displacement factors have been observed

for composing atoms. The displacement factor, equal 0.033 Å^2 for As in ThAsSe, decreases with decreasing x through the $UAs_{1-x}Se_{1+x}$ series down to 0.007 Å^2 in UAsS. The decrease of the displacement factor is accompanied by monotonous decrease of the Kondo-like resistivity. It is believed that the high values of the displacement factors of the considered systems reveal two level systems in them. Thus the mechanism that leads to their Kondo-like behaviour is described by the two-level system Kondo model of Cox and Zawadowski.

This work was supported by the Polish Committee for Scientific Research, Grant no. KBN-2 P03B 062 18 for years 2000-2001.

11:10 - 12:00

Positron annihilation studies of the Fermi surface of rare-earth intermetallic compounds

M Biasini[1,6], G Ferro[1,6], M Monge[1,7], M Gemmi[1],

G Kontrim-Sznajd[2], A.Czopnik[2], S. Massidda[3,6], G. Satta P[3,6]

P Lejay[4], A Continenza[5,6]

[1] ENEA via don Fiammelli 2 40128 Bologna Italy

[2] Trzebiatowski Institute of Low Temperature and Structure Research

P.O.Box 937 Wroclaw Poland

[3] Universita' di cagliari Dep.to di Fisica I-09124 Cagliari

[4] CRTBT, Av. de Martyrs BP 166, 38042 Grenoble Cedex 9, France

[5] Universita' dell'Aquila Dep.to di Fisica I-67010 Coppito(L'Aquila)

[6] Istituto nazionale di Fisica della materia

[7] Universidad Carlos III, Av. Universidad 30, 28911 Leganes (Madrid), Spain

The measurement of the 2-dimensional angular correlation of the positron annihilation radiation (2D-ACAR), providing a 2D projection of the two-photon electron-positron momentum density, $\rho(p)$, is a powerful tool to investigate the electronic structure of intermetallic compounds. Thanks to the crystal symmetry, a small number of projections of $\rho(p)$ is often sufficient to perform its 3D reconstruction using tomographic techniques [1]. From $\rho(p)$, by applying the Lock Crisp West transformation [2], the 3D **k**-space density $\rho(k)$, and, consequently, the Fermi surface (FS) can be mapped out. We present the latest results obtained with the 2D-ACAR spectrometer implemented at ENEA Bologna. (1) We carried out 2D-ACAR experiments to reconstruct the complex multi-sheet FS of the rare-earth system $TmGa_3$. The resulting FS is in fair agreement with band structure calculations, which constrain the $4f$ electrons to retain a local atomic character [3]. We discover a correlation between the antiferromagnetic structures of this compound and the nesting of the FS along the [110] directions [4]. Moreover, we propose methods to estimate the density of states at the Fermi energy (E_F) and the electronic contribution to the specific heat, γ [we obtain $N(E_F)$=13.6 states/ (Ryd cell) and γ =2.4 (mJ/mole K^2)].

(2) The heavy fermion system $CeRu_2Si_2$ is one of the key compounds to study the physics of the highly correlated f electron systems. Most of the understanding of the so called standard heavy-fermion behaviour is based upon the idea that the itinerant character of the Ce $4f$ electrons in the Kondo-lattice ground state should change to localised at temperatures higher than the Kondo temperature T_K. The 2D-ACAR measurements were performed at $T \succ T_K$ and compared to those of the reference isostructural non f-electron system $LaRu_2Si_2$. The 3D $\mathbf{k}$-space densities of the two compounds were very similar. These results are in reasonable agreement with the band structure calculated for $CeRu_2Si_2$ using the local density approximation (LDA). Conversely, a clear discrepancy between the LDA calculation for $LaRu_2Si_2$ and the experiment results unless the Fermi level is raised of 11 mRyd. After the adjustment in E_F the calculated FSs are rather similar and in agreement with both experiments. The implications of this similarity on the physics of the heavy fermions are discussed.

[1] G Kontrym-Sznajd et al Mat. Scie. Forum 255-257 (1997) 754 and references therein

[2] D G Lock, V H C Crisp and R N West, J. Phys. F 3 (1973) 561

[3] V.B. Pluzhnikov et al, Phys. Rev. B 59, 7893 (1999)

[4] M Biasini at al to appear in Phys. Rev. Lett.

12:00 - 12:50

Using perturbation theory from the atomic limit in Electronic Structure Calculations

Urban Lundin

We discuss the possibility to include strong correlations in electronic structure calculations. We start from the atomic limit and, making model calculations, investigate what terms from perturbation theory that are most important. We derive corrections to the Hamiltonian and overlap matrices in electronic structure calculations, and perform selfconsistent calculations for the light lanthanides. The results show an improvement of the equilibrium properties, such as the equilibrium volume, compared to conventional electronic structure calculations.

The Physics of f-Electron Systems

Daresbury Laboratory, 6th - 8th April 2001

List of Participants

James Annett	University of Bristol	james.annett@bristol.ac.uk
Rajeev Ahuja	University of Uppsala	rajeev@fysik.uu.se
Bernard Amadon	CEA/DAM,Ile de France	amadon@lps.u-psud.fr
Victor Antonov	Max-Plank-Institute, Dresden	anton@imp.kiev.ua
Michel Beauvy	CEA, Centre de Cadarache	beauvy@decade.cea.fr
Maurizio Biasini	ENEA, Bologna	biasini@risc990.bologna.enea.it
Mike Brooks	ITU Karlsruhe	brooks@itu.fzk.de
Klaus Capelle	University of Bristol	capelle@if.sc.usp.br
Marno Colarieti-Tosti	University of Uppsala	mamo@fysik.uu.se
John Dobson	Griffiths University, Brisbane	j.dobson@sct.gu.edu.au
Paul Durham	CLRC Daresbury Laboratory	p.j.durham@dl.ac.uk
Olle Eriksson	University of Uppsala	olle.eriksson@fysik.uu.se
Antoine Georges	Ecole Normale Superieure, Paris	Antoine.Georges@lpt.ens.fr
Thomas Gouder	ITU Karlsruhe	gouder@itu.fzk.de
Tim Gould	Griffiths University, Brisbane	
Balazs Gyorffy	University of Bristol	b.gyorffy@bristol.ac.uk
Zygmunt Henkie	Polish Academy of Sciences, Wroclaw	henkie@int.pan.wroc.pl
Danny Jervis	University of Bristol	
Borje Johansson	University of Uppsala	borje.johansson@fysik.uu.se
Gabi Kotliar	Rutgers University	kotliar@physics.rutgers.edu
Jesper Laersgaard	Technical University of Denmark, Lyngby	jl@com.dtu.dk
Gerry Lander	ITU Karlsruhe	lander@ill.fr
Martin Lueders	S.I.S.S.A, Trieste	lueders@sissa.it
Urban Lundin	University of Uppsala	urban.lundin@fysik.uu.se
Peter Oppeneer	ISSMR, Dresden	p.m.oppeneer@ifw-dresden.de
Leon Petit	University of Aarhus	lpetit@ifa.au.dk
Sa Li	University of Uppsala	lisa@fysik.uu.se
Per Soderlind	Lawrence Livermore National Laboratory	soderlind1@poptop.llnl.gov
Julie Staunton	Warwick University	phrjz@weedy.warwick.ac.uk
Paul Strange	University of Keele	p.strange@phys.keele.ac.uk
Axel Svane	University of Aarhus	svane@ifa.au.dk
Dzidka Szotek	CLRC Daresbury Laboratory	z.szotek@dl.ac.uk
Walter Temmerman	CLRC Daresbury Laboratory	w.m.temmerman@dl.ac.uk
Rik Tyer	University of Sheffield	PHP97RT@sheffield.ac.uk
Gerrit van der Laan	CLRC Daresbury Laboratory	G.van_der_Laan@dl.ac.uk
Peter Wachter	ETH Zurich	wachter@solid.phys.ethz.ch
Yi Wang	University of Uppsala	yi.wang@fysik.uu.se

5.2 TMR2 Workshop/Conference Announcements

5.2.1 WIEN2k Workshop

Seventh WIEN Workshop

Full-Potential APW+lo calculations with the new WIEN2k code

September 25-29, 2001
Vienna University of Technology, Austria
Chairman: Karlheinz Schwarz (TU-Vienna)
Email: kschwarz@theochem.tuwien.ac.at

Supported by TMR2 (LAPW) and ESF Program STRUC-Ψ_k.

First Announcement

This workshop is aimed at anyone who wants to learn how density functional calculations can be done using the full-potential Augmented Plane Wave + local orbitals (FP-APW+lo) method as embodied in the new WIEN2k code (or related topics). With this new scheme a speedup of up to an order of magnitude can be achieved.

The workshop schedule is divided between lectures and practical sessions and consists of two parts as follows:

- Part I:
  - A short introduction to the (L)APW (+lo) method and density functional theory
  - Introduction to the use of the WIEN2k program package
  - Hands-on experience
- Part II:
  - New features of WIEN2k
  - Results obtained with WIEN and related topics
  - Discussions and exchange of experience with users and developers
  - Poster session

Conference site:
The conference will take place at the TU Wien (Vienna University of Technology)
A-1040 Vienna, Favoritenstr. 11

Contact:
For further information look at our WWW-homepage
http://www.wien2k.at/ws2001/
or send an email to kschwarz@theochem.tuwien.ac.at.

6 News from the ESF Programme

"Electronic Structure Calculations for Elucidating the Complex Atomistic Behaviour of Solids and Surfaces"

6.1 Call for Workshop Proposals for 2002

It is time to consider proposals for workshops to be held in 2002 for (partial) funding by the ESF Psi-k Programme.

Proposals should be submitted by email (in the form of a single simple email letter WITHOUT ATTACHMENTS OR LATEX, just plain ascii) to the Psi-k Programme secretary, Walter Temmerman, at

psik-coord@dl.ac.uk

by August 31, 2001, and should include the following points (preferably numbered in this order).

1. Title and purpose of the workshop, with names and addresses (including email) of the organisers.
2. The scientific content and why a workshop would be useful at this time.
3. A tentative list of speakers whom it is hoped to have.
4. The number of participants it is planned to invite or attract, and their scientific involvement, eg. as simulators, related experimentalists, code developers etc., and young scientists in the subject.
5. Plans for a tutorial element and for attracting new researchers into the subject of the workshop. (If this is thought inappropriate for this workshop, please discuss why.) The purpose of the ESF Psi-k Programme is to help everyone in our community to do good quality research, and in our expanding field this implies some outreach and tutorial activity.
6. A budget, expressed in Euro, and how much is being applied for from the ESF Psi-k Programme. This support in the past has been limited to ~9k Euro.
7. A statement of other organisations which will be applied to for co-sponsorship and additional funding, eg. the RTN Network on Computational Electronics, other RTN Networks, CECAM, CCP-9 in the UK, etc..
8. Where it is hoped the Workshop would be held.

Volker Heine, chairman of ESF Psi-k Programme
e-mail: vh200@phy.cam.ac.uk

6.2 Reports on Collaborative Visits

Report on a Collaborative Visit of Adam Kiejna (Wrocław, PL) to the Department of Applied Physics, Chalmers University of Technology (Gothenburg, S)

3 – 8 April, 2001

I visited Prof. Bengt Lundqvist and the Materials and Surface Theory Group at the Department of Applied Physics at Chalmers University of Technology, from 3 to 8 April, 2001.

The aim of my visit was to discuss with Bengt Lundqvist, Elsebeth Schröder, Carlo Ruberto and various memebers of the group, the progress in the projects we are carrying out on oxygen adsorption and the early stages of oxidation of aluminum and magnesium surfaces in order to understand the structural and electronic properties of these materials by means of ab-initio simulations. This includes the character of bonding, destabilization of the surface due to subsurface oxygen, and the possibilities for the metal-oxide formation.

In particular we have discussed new results on adsorption and incorporation of oxygen at the Al(111) surface, the structural properties of adsorbed ultrathin oxide films on Al surface, and the adsorption of Al atoms on the Al(111) and TiC(111) surfaces precovered with a monolayer of O atoms. We have analyzed recent results on the O/Mg(0001) system and outlined some new calculations to be performed for this system using the pseudopotential plane-wave code.
I also had the opportunity to discuss with Göran Wahnström the relevance of different exchange-correlation functionals for the calculation of vacancies in metals, with Shiwu Gao on the efficiency of his parallelized version of the WIEN code, and various topics with some other members of the group.

The visit was very useful for the advancement of our projects.
I am very grateful to the Ψ_k-network for its support.

Adam Kiejna

Report on a Collaborative Visit of O. Bengone (Uppsala University) to G. Kresse and J. Hafner (Institute für Theoretishe Physik, Technische Universität Wien)

Visit from March 11 to 18, 2001

During my visit to Drs. G. Kresse and J. Hafner at the University of Vienna we ported the multi-orbitals Hubbard code [1], the so-called LDA+U approximation in the "Vienna ab-initio code". The code has now been successfully ported and extended to take into account the strong correlation effects either among the d or the f open-shell orbitals.

The correction ported is formulated in its rotationally invariant version, and takes into account the non-sphericity of the Coulomb and exchange interaction, i.e., the interaction's dependence on a particular d or f orbitals m and m'.

The LDA+U correction has been successfully tested for bulk NiO, which is a prototype of Mott-Hubbard compounds. The results are in excellent agreement with previous LDA+U implementations, and allow a theoretical reproduction of the experimentally observed insulating anti-ferromagnetic ground state of NiO.

[1] O. Bengone *et al.* Phys. Rev. B **62**, 16392 (2001).

Olivier Bengone

Uppsala University, May 21, 2001

Report on a Collaborative Visit of Mebarek Alouani and Sebastien Lebegue (Institut de Physique et Chimie des Materiaux de Strasbourg) to Peter Bloechl (Clausthal Technical University)

April 15 - April 21, 2001 (M. Alouani and S. Lebegue)
April 29 - May 11, 2001 (S. Lebegue)

My student (S. Lebegue) and myself visited Dr. Peter Bloechl at the Technical University of Clausthal. This visit was planned for three weeks for my student and one week for me. Because Dr. Bloechl has to be out of town for the week of April 22-28, 2001. Sebastien has to travel again to Clausthal on April 29, 2001.

The aim of our visit was to continue an ongoing collaboration with Prof. Bloechl, on further developments of the PAW and GW methods. The goal of our study is to overcome the plasmon-pole approximation [1,2], which is expected to fail for metals. The screening of the Coulomb interaction will have to be determined from the dynamical dielectric function within the random phase approximation. Because the existing GW implementation has been coded as a separate code, the first step was to incorporate the GW code into the PAW code in order to take advantages of new developments of the PAW method such as the possibility to use general k-points. The goals achieved on this short visit are :

(1) A development of a strategy to merge the PAW and GW codes. Most of the effort went on the adaptation of the GW code to the LINUX platform using the ABSOFT compiler. Initially The GW code was developed on the IBM platform and relayed heavily on the ESSL library. Now we have succeeded in adapting it to the LINUX platform and have the possibly to use either the ESSL library or the LAPACK, BLAS, and FFTW packages, however, at this time the code runs (very slowly) on LINUX-INTEL computers, and further optimization is needed.

(2) We have started implementing the tetrahedron method into the PAW code, but this part of the project turned out to be much more difficult than previously thought. One has to calculated properly the derivatives of the **k**-points weights with respect to some dynamical variables to be able to calculate properly the forces on the atoms. Nonetheless, the variable occupation approach based on the Car-Parinello algorithm was successfully tested for Al.

(3) During his stay, Lebegue has a good opportunity to learn more about how to make a good PAW simulation for a metal, and how to generate accurate pseudopotentials for PAW electronic structure calculations.

[1] B. Arnaud and M. Alouani, PRB 62, 4464, (2000).

[2] B. Arnaud and M. Alouani, PRB 63, 85208, (2001).

Mebarek Alouani

Report on a Collaborative Visit of Clemens Först and Johannes Schimpl (Technical University, Vienna) to Peter E. Blöchl (Technical University of Clausthal)

March 15 to April 5, 2001

According to the joint proposal from Peter E. Blöchl and Karlheinz Schwarz, which was approved by the ψ_k committee, we spent the time from March 15^{th} to April 5^{th} 2001 at the Technical University of Clausthal, Germany. Our basic objectives for this visit were

- Know-how transfer
- Molecular dynamics of excited states
- Porting of the Car-Parrinello Projector Augmented Wave Code (CP-PAW)

Concerning the first point, it is hard to write a summary but we like to mention, that we learned a great deal from Blöchl's lectures which took place on a regular basis. The next two sections cover the work done concerning excited states and the porting of the code.

Excited State Dynamics

We investigated metastable states in $Na_2[Fe(CN)_5(NO)]\cdot 2H_2O$, sodium nitroprusside. In the relevant part of the crystal structure 5 CN-groups and one NO-group are bound to a central iron atom. Two metastable states can be reached by irradiating the crystal with laser light of proper wave length at temperatures below 150 K. This allows to write, read and erase information by holographic techniques, opening the possibility of three-dimensional holographic storage materials.

The two states are linkage isomers characterized by a tilted and inverted NO-group, respectively. So the reaction coordinate can be mapped onto the Fe-N-O angle.

Within the PAW method it is possible to define fixed occupations of the electronic states. In this way one can calculate excited-state properties. Structure relaxation as well as energy-conserving finite temperature-dynamics can be performed. Such simulations have been done and questions concerning the excitation process have been answered.

Porting of the PAW-Code

The PAW-Code was developed by Peter Blöchl during his work at the IBM Research Laboratory in Rüschlikon. The fact that it was hardly possible to compile this code on any other architecture

posed a real problem to many users. Up to now, I know of only two places where the code runs on non-IBM architectures but these adaptations were not done on the most recent version.

Since our group has access to Intel/AMD based Beowolf clusters, I invested some time in porting the code. This section reports on parallel performance measurements and defines the minimum requirements for using PAW on a PC cluster.

This work would not have been possible without the intensive support of Peter Blöchl and Dieter Kvasnicka, whom we again want to thank for the many hours they spent helping.

First parallel test runs were done on a PC cluster of the AURORA Project[1]. At that time the GESCHER cluster consisted of eight dual-PII nodes connected with an 100 Mbit/s network, each node with 500 MB of memory. Figure 1 shows the network configuration of this cluster and figure 2 illustrates the parallel performance of the code.

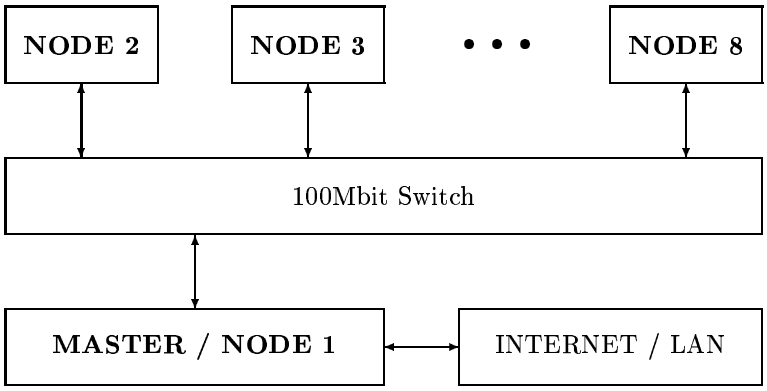

Figure 1: Network configuration of the GESCHER cluster.

A test on a local cluster of workstations – connected by a 10 Mbit/s network – confirmed our assumption, that 100 Mbit/s is the minimum requirement to efficiently run the PAW-Code in parallel (see also figure 2). I did not have the possibility to test the performance using a Myrinet communication so far. Now the code runs on Intel/AMD architectures using the Absoft[2]-compiler and on Alpha workstations (Compaq fort compiler). We have tried various other compilers but most of them do not yet support the full Fortran 90 standard. All necessary changes are implemented in the standard code and will be included in the next distribution[3].

Concerning the optimization of the numerical performance, we had to replace the highly efficient ESSL by optimized BLAS and FFT routines for the new architectures. After extensive benchmarking, we decided to use the ATLAS BLAS[4] which achieves around 1 gigaflop of floating point performance on an AMD Thunderbird 900 MHz doing a matrix-matrix multiplication and the FFTW[5] libraries. Interfaces for the library calls were created which allow to switch between various choices via preprocessor options.

[1] `http://www.vcpc.univie.ac.at/aurora/`; Special Research Program SFB F011 funded by the Austrian Science Fund.

[2] `http://www.absoft.com/`

[3] `Peter.Bloechl@tu-clausthal.de`

[4] `http://www.netlib.org/atlas`

[5] `http://www.fftw.org`

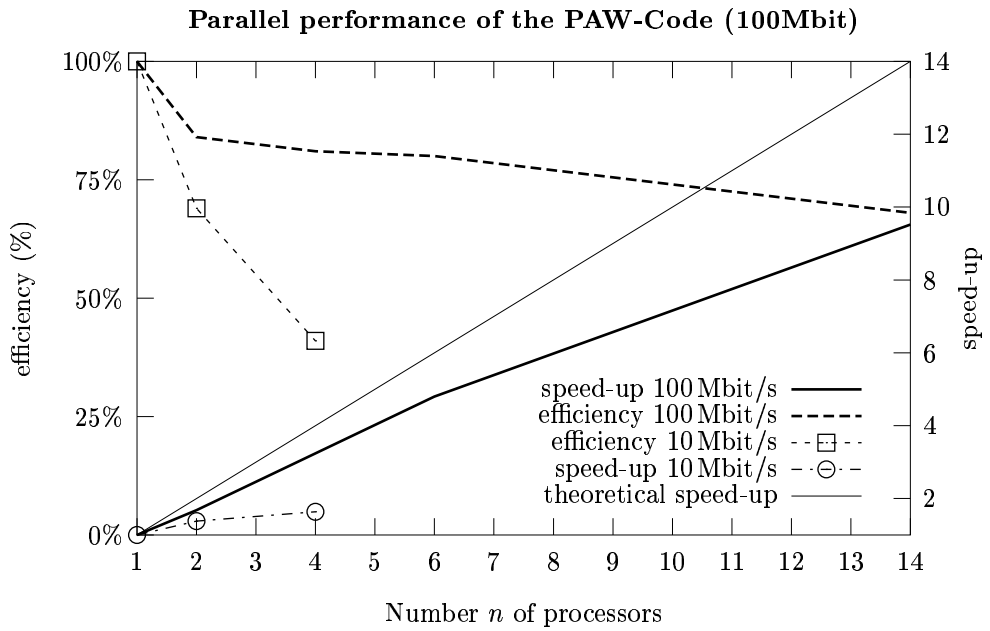

Figure 2: This performance graph was measured on the GESCHER Beowolf cluster at the University of Vienna and on local PII-PCs. A test system with 84 atoms per cell was used.

Acknowledgments We want to express our thanks to the ψ_k-Project for financial support as well as to K. Schwarz for making this visit possible. We very much appreciate, that we had the chance to go abroad – even as diploma students.

Clemens Först and Johannes Schimpl

6.3 Reports on Workshops/Conferences

6.3.1 Report on European Winter School

State of the art simulations in electronic structure and total energy for surface science

http://www-drfmc.cea.fr/SP2M/L_Sim/Congres/Corse_2001/cargese.html

Cargèse, February 19^{th}-March 3^{rd} 2001

This winter school was held in the "Institut d'Etudes Scientifiques" of Cargèse from the 19th of February to the 3rd of March 2001. It was organized by M. C. Desjonquères, D. Spanjaard and C. Barreteau. Five organisms gave a financial support: Centre National de la Recherche Scientifique (formation permanente), European Science Fundation (Ψ_k network), French Ministry of Education, Délégation Générale à l'Armement, Commissariat à l'Energie Atomique and Institut Français du Pétrole. This school has gathered together 40 participants coming from 16 different countries, mainly European, most of them were PhD students. The aim of this school was to synthetize the different methods of electronic structure and total energy calculations and define their specificity, their limitation, their field of application and their interest for simulation in surface physics. The lectures have been illustrated by many examples and several talks were devoted to experimental techniques (photoemission, scanning tunneling microscopy, magnetic dichroïsm etc..) the interpretation of which needs a good understanding of the electronic structure and the total energy.

The school was organized in two weeks of lectures presenting six domains. Each domain was covered by four or five lectures among which one fourth was experimental and three fourth theoretical. Each day was composed of 4 lectures of one hour and a half leaving time for discussion. Finally two poster sessions were organized allowing the participants to present their recent work.

PROGRAM

1) Electronic structure: methods of calculation.

David Vanderbilt

- Density Functional Theory (1H30)
- Pseudopotential and plane waves (1H30)
- Linear Response and molecular dynamics (1H30)

Erich Wimmer

- All Electron Methods (3H)

Cyrille Barreteau

- Tight Binding Methods (1H30)

2) Electronic structure: applications and experiments.

Peter Kratzer

- Theory of epitaxial film growth (1H30)
- Kinetics of epitaxial growth (1H30)

Enrique Garcia-Michel

- Quantum Wells (1H30)

Matti Lindroos

- Theory of Photoemission (1H30)

Maria Carmen Asensio

- Photoemission experiments (1H30)

Fernando Flores

- Theory of Scanning Tunneling Microscopy (1H30)

Sylvie Rousset

- Scanning Tunneling Microscopy experiments (1H30)

3) Empirical potentials and their applications.

Graeme Ackland

- General introduction (3H)

Guy Tréglia

- Kinetic Tight Binding Ising Model and its application to alloying at surfaces (1H30)

Pablo Jensen

- Understanding the growth of nanocluster films with simple models (1H30)

Joost Frenken

- Diffusion and phase transitions at surfaces (3H)

4) Surface magnetism.

Stefan Blügel

- Theory of surface magnetism (3H)

François Gautier

- Magnetism of metals: multilayers and magnetic dichroïsm (3H)

George Sawatzky

- Electronic structure of surfaces and interfaces of strongly correlated systems (3H)

5) Excitations at surfaces.

Paul Thiry

- General introduction to surface vibrations (1H30)

Paul Dumas

- Experimental observation of surface vibrations (1H30)

Giovanni Onida

- Theory of optical response of surfaces (1H30)

Volker Staemmler

- Surface electronic excitations (1H30)

6) Physisorption and Chemisorption.

Bjork Hammer

- Adsorption and Reactions at metal surfaces (3H)

David King

- Chemisorption experiments (3H)

Christophe Ramseyer

- Physisorption (1H30)

Hervé Toulhoat

- Ab-initio methods in chemisorption (1H30)

Original results and new fields of research

This meeting being a school, the aim of it was not to present the last results but to expose the different theoretical and experimental methods concerning the electronic structure and the total energy in surface science and the information that can be extracted from them. However, among the examples chosen to illustrate the lectures, some new fields of research can be identified.

The progress in *ab-initio* methods is obviously linked to the efficiency of computers. In addition substantial efforts are made to improve the algorithms (iterative algorithms, "order N" methods, or new pseudopotentials), to better describe electronic correlations and to calculate new physical quantities with the help of Linear Response Theory. Some developments in semi-empirical methods (like Tight-Binding) in order to improve their precision and to increase their efficiency have gained in interest because these methods allow to deal with large systems while keeping the quantum mechanics description.

Molecular dynamics using empirical potentials is still very active. It starts to be used in combi-

nation with *ab-initio* methods on larger size and time scales. The kinetic Monte-Carlo methods which are used to simulate growth and diffusion phenomena are in constant progress. The energy barriers needed in these simulations are derived either from *ab-initio* calculations or using empirical potentials.

The angle resolved photoemission remains the best technics for investigating the electronic structure of materials. Recent advances concern the determination of Fermi surfaces and the observation of electronic states in quantum wells (or dots).

Besides the well established methods to measure surface vibrations (HREELS or Helium scattering) the sum frequency generation spectroscopy is taking more and more importance since it allows the specific observation of interfaces or surfaces. The study of vibrations of adsorbed molecules by means of STM will certainly develop in the future and it starts to be coupled with *ab-initio* calculations.

The measure of magnetic dichroïsm is almost the only method that allows the determination of magnetic moments at the surface but its quantitative analysis remains difficult. Research in magnetism of thin films or multilayers are in rapid evolution in connection with the spin-electronics which might revolutionize the computer technology in the future.

Finally, in the domain of adsorption phenomena, the most recent advances include the study of complex molecules at surfaces by means of *ab-initio* calculations as well as the determination of (still relatively simple) reaction paths at surfaces. On the experimental point of view the measure of adsorption energies remains difficult but the femtocalorimetry is opening new perspectives.

Conclusion

We think that Cargèse winter school has reached its main objectives. It has contributed to give the PhD students a more global view of the field they are working on and provided them with the opportunity of discussing their results with high level scientists. Moreover it created bonds between young researchers of various European laboratories and new collaborations are likely to start in a near future.

List of Participants

Nr.	Name	e-mail
1.	BARRAL Maria Andrea	barral@df.uba.ar
2.	BAUD, Stéphanie	stephanie.baud@lpm.univ-fcomte.fr
3.	BEHLER, Jörg	behler@fhi-berlin.mpg.de
4.	BOUCHER Florent	Florent.Boucher@cnrs-imn.fr
5.	BRAZDOVA Veronika	vb@qc.ag-berlin.mpg.de
6.	BRENA Barbara	bab@physto.se
7.	CAPUTO Riccarda	r.caputodl@tin.it
8.	CHAKAROVA Svetla	frtsc@fy.chalmers.se
9.	DAPPE Yannick	ydappe@ipcms.u-strasbg.fr
10.	DESHPANDE Mrinalini Dilip	mdd@physics.unipune.ernet.in
11.	DUMONT Jacques	jacques.dumont@fundp.ac.be
12.	GAVAZA Mihai	mihai@osiris.univ-rennes1.fr
13.	GENESTE Grégory	geneste@cemes.fr
14.	GOTTSCHALCK Jakob	jakobg@ifa.au.dk
15.	IZQUIERDO Manuel	izquierdo@lure.u-psud.fr
16.	JACOBSON Niclas	nija@fy.chalmers.se
17.	JELINEK Pavel	jelinekp@fzu.cz
18.	JOBIC Stéphane	jobic@cnrs-imn.fr
19.	KUEHLERT Oliver	Oliver.Kuehlert@mpi-hd.mpg.de
20.	LAKARD Boris	b.lakard@libertysurf.fr
21.	LAZIC Predrag	plazic@thphys.irb.hr
22.	LEBEGUE Sebastien	lebegue@ipcms.u-strasbg.fr
23.	LEGUT Dominik	legut@ipm.cz
24.	MARINICA Dana-Codruta	dumitru@lcam.u-psud.fr
25.	MARINICA Mihai-Cosmin	cosmin.marinica@ppm.u-psud.fr
26.	MASCARAQUE Arantzazu	mascaraque@lure.u-psud.fr
27.	MENCHINI Carlo	menchini@mater.unimib.it
28.	MEYER Bernd	bemeyer@physics.rutgers.edu
29.	MINISINI Benoit	bminisini@ismans.univ-lemans.fr
30.	MOORE Lisa	L.Moore@qub.ac.uk
31.	MOTTET Christine	mottet@crmc2.univ-mrs.fr
32.	MURTAGH Conor	conor@duttfks1.tn.tudelft.nl
33.	NICOLAISEN Nanna	nanna@fys.ku.dk
34.	OFFERMANS Willy	w.k.offermans@tue.nl
35.	OLIVIER Stéphane	olivier@crmc2.univ-mrs.fr
36.	PRIEBE Andreas	apriebe@ix.urz.uni-heidelberg.de
37.	RASMUSSEN, Maria Dall	mdr@ifa.au.dk
38.	STEKOLNIKOV Andrey	andrey@ifto.physik.uni-jena.de
39.	TUMA Christian	ct@qc.ag-berlin.mpg.de
40.	WIAME Frédéric	frederic.wiame@fundp.ac.be

Organizers

Nr.	Name	e-mail
1.	BARRETEAU Cyrille	barreto@drfmc.ceng.cea.fr
2.	DESJONQUERES Marie Catherine	mcdjs@drecam.saclay.cea.fr
3.	SPANJAARD Daniel	spanjard@lps.u-psud.fr

List of Lecturers

Nr.	Name	e-mail
1.	ACKLAND Graeme	G.J.Ackland@ed.ac.uk
2.	ASENSIO Maria-Carmen	asensio@lure.u-psud.fr
3.	BARRETEAU Cyrille	barreto@drfmc.ceng.cea.fr
4.	BLUGEL Stefan	S.Bluegel@fz-juelich.de
5.	DUMAS Paul	pdumas@lure.u-psud.fr
6.	FLORES Fernando	fernando@uamca1.fmc.uam.es
7.	FRENKEN Joost	frenken@phys.leidenuniv.nl
8.	GARCIA-MICHEL Enrique	Enrique.Garcia.Michel@uam.es
9.	GAUTIER François	Jeannine.Wendling@ipcms.u-strasbg.fr
10.	HAMMER Bjork	hammer@ifa.au.dk
11.	JENSEN Pablo	Pablo.Jensen@dpm.univ-lyon1.fr
12.	KING David	eld1000@cam.ac.uk
13.	KRATZER Peter	kratzer@FHI-Berlin.mpg.de
14.	LINDROOS Matti	lindroos@alpha.cc.tut.fi
15.	ONIDA Giovanni	ONIDA@roma2.infn.it
16.	RAMSEYER Christophe	ramseyer@rs1.univ-fcomte.fr
17.	ROUSSET Sylvie	rousset@gps.jussieu.fr
18.	SAWATZKY George	G.A.Sawatzky@fys.rug.nl
19.	STAEMMLER Volker	staemm@mokat58.theochem.ruhr-uni-bochum.de
20.	THIRY Paul	paul.thiry@fundp.ac.be
21.	TOULHOAT Hervé	herve.toulhoat@ifp.fr
22.	TREGLIA Guy	treglia@crmc2.univ-mrs.fr
23.	VANDERBILT David	dhv@physics.rutgers.edu
24.	WIMMER Erich	ewimmer@materialsdesign.com

Abstracts

General introduction to density functional theory

David Vanderbilt
Rutgers University, USA

A general introduction will be given to density-functional theory (DFT). The lecture will begin with an explanation of the formal structure of DFT, with a focus on the Kohn-Sham theory, and then move on to describe the most commonly used local-density (LDA) and gradient-corrected (GGA) functionals. Some overview of the choices of implementation (basis set and loop structure) will be given. The talk will end with a discussion of of the limitations of DFT and a brief accound of current attempts to generate improved functionals or to go beyond DFT.

Pseudopotentials, plane waves

David Vanderbilt
Rutgers University, USA

The lecture will begin with a discussion of the formulation of DFT theory in a plane-wave basis, and of the advantages of adopting this choice of basis. A brief discussion of fast- Fourier-transform methods and of surface-slab and supercell techniques will be included. I will then review the theory of pseudopotentials, with a focus on norm-conserving semilocal potentials, norm-conserving Kleinman-Bylander potentials, and ultrasoft potentials.

Linear response theory and molecular dynamics

David Vanderbilt
Rutgers University, USA

The primary focus of this talk will be on the calculation of derivatives of the energy withing density-functional theory. The discussion will start with the Hellmann-Feynman force theorem, and an introduction will then be given to the linear-response theory (or more generally, the density-functional perturbation theory) for the computation of more general first and higher derivatives with respect to displacements, strains, electric fields, and chemical species. I will then review molecular-dynamics simulations, including in particular the Car-Parrinello fictitious-Lagrangian approach. The lecture will end with an example of molecular-dynamics simulations of premelting phenomena on the Al (110) surface.

All electron methods

Erich Wimmer
Materials Design, Le Mans, France

This lecture reviews the concepts of the most important all-electron electronic structure methods and their applications to problems in surface science. The following approaches are addressed: the full-potential linearized augmented plane wave (FLAPW) method [1], the linearized muffin-tin orbital (LMTO) method [2] and the related augmented spherical wave (ASW) approach [3] with its generalization to a full-potential implementation [4]. These methods, which were developed within the solid state physics community, are compared to localized orbital approaches using linear combination of atomic orbitals, which have evolved as tools in quantum chemistry. The advantages and as well as possible problems of various surface models, namely repeated slab geometry, thin film geometry, and finite cluster approaches are presented and discussed. Illustrative examples include surface charge densities, work functions, surface reconstructions, adsorption, surface reactions, and surface magnetism. The lecture also addresses the calculation of excited states (e.g. energy band gaps in semiconductors) using methods such as the screened exchange, which go beyond standard density functional theory. An outlook on remaining challenges and future developments conclude this lecture.

1. E. Wimmer, H. Krakauer, M. Weinert, and A. J. Freeman, Phys. Rev. B 24, 864 (1981) and references therein ; M. Weinert, J. Math. Phys. 22, 2433 (1981)

2. O. K. Andersen, Phys. Rev. B 12, 3060 (1975)

3. A. R. Williams, J. Kübler, and C. D. Gelatt, jr, Phys. Rev. B 19, 6094 (1979)

4. M. Methfessel, C. O. Rodriguez, and O. K. Andersen, Phys. Rev. B 40, 2009 (1989)

Tight Binding methods

Cyrille Barreteau
CEA Grenoble, France

The basic concepts of Tight-Binding will be presented: basis set, Hamiltonian expression, eigenvalue problem etc... I will introduce some important quantities like the Green operator, the density operator and the moments of a density of states, which have a rather transparent expression in the tight-binding formalism and can lead to interesting approximations in "real space" such as the recursion method, the Fermi-operator expansion or the moment expansion. I will also discuss on a very simple example ($1s$ TB on a simple cubic lattice) the main physical features that can be extracted from a tight-binding analysis of the electronic structure of surfaces. In this context the problem of self-consistency will be discussed. Finally the second part of the talk will be devoted to the total energy description in a tight-binding scheme. The link with more simple empirical potentials, and also with the DFT formalism will be made. I will end this course by a few illustrative examples.

From atomistic DFT studies to macroscopic properties:
I. Thermodynamics of Surfaces and Nanostructures

Peter Kratzer
Fritz-Haber-Institut der MPG, Berlin, Germany

In this lecture, equilibrium thermodynamics of crystal surfaces is reviewed, and examples are given how thermodynamic quantities can be extracted from density functional theory (DFT) calculations. The free surface energy as a key quantity for surface thermodynamics is introduced. The equilibrium between a crystal and its vapor is discussed. I describe the Wulff construction as a method for obtaining the equilibrium crystal shape. The importance of surface reconstructions is demonstrated for the example of the GaAs(001) surface. In experiments, one frequently encounters a situation close to equilibrium, but subject to constraints. This is demonstrated for the example of hetero-epitaxy: I discuss equilibrium between islands of InAs on GaAs subject to the constraints of a fixed island density. The lecture will stress methodological aspects: DFT calculations of thermodynamic quantities allow us to establish contact between the atomic structures at the surface and the macroscopic world of thin films, coatings, heterogeneous catalysis, etc., i.e. all those everyday's phenomena that occur at finite temperatures and pressures.

From atomistic DFT studies to macroscopic properties:
II. Kinetics of epitaxial growth

Peter Kratzer
Fritz-Haber-Institut der MPG, Berlin, Germany

This lecture gives an introduction to the various forms of epitaxy and their modeling. The theoretical treatment of open systems requires a wider basis than equilibrium thermodynamics. This is provided by kinetic equations at various levels of description (Master eq., Smoluchovski eq., mean-field rate equations), which contain the equilibrium as a limiting case. The additional physics brought into play by kinetic aspects is examplified by the difference between equilibrium shapes and growth shapes. Some basic concepts of kinetic theory are introduced, such as diffusion by hopping, and classical nucleation theory. I explain in detail the use of kinetic Monte Carlo (kMC) simulations for bridging the length and time scales between the atomic processes that can be investigated by DFT calculations, and the meso- or macroscopic phenomena, such as growth shapes and morphology. Recent applications of the kMC technique in conjunction with atomistic DFT calculations are discussed for homoepitaxy of metals and of compound semiconductor materials.

Understanding the growth of nanocluster films

Pablo Jensen
Université Claude Bernard, Lyon, France

We have investigated the growth of nanostructured films prepared by cluster deposition. Simulations of the first stages, the submonolayer regime, are reported for a wide variety of experimental situations (Ref 1). We want to help experimentalists, in analyzing their data, to determine which processes are important and to quantify them. For example, surprisingly high values for cluster diffusivity can be inferred from our models.

An important issue for future technological applications of cluster deposition is the relation between the size of the incident clusters and the size of the islands obtained on the substrate. What are the mechanisms leading to the shape relaxation of three dimensional crystallites? We will show (Ref 2) how Kinetic Monte-Carlo simulations can bridge the gap between the elementary process (a single atom diffusion step, typical time scale 10^{-12}s) and the total evolution time (up to years!), therefore helping to understand the relaxation mechanisms. We demonstrate that the usual phenomenological theories of equilibration, via atomic surface diffusion driven by curvature, are verified only at high temperatures. Below the roughening temperature, the relaxation is much slower, kinetics being governed by the nucleation of a critical germ on a facet. This leads to an it exponential dependence of the relaxation time on the crystallite size.

1. P. Jensen, Rev. Mod. Phys. **71**, 1695 (1999). Software for all these simulation programs is available on request from the author (jensen@dpm.univ-lyon1.fr).

2. N. Combe, P. Jensen and A. Pimpinelli, Phys. Rev. Lett **85**, 110 (2000)

Surface and interface vibrations

Paul Thiry
University of Namur, Belgium

The lecture starts with a reminder of the vibrational structure of an isolated molecule and of a crystal and how they can affect in first order, material dependent quantities such as dipole moment, polarisability, polarisation, susceptibility, dielectric constant, etc. Then we describe the characteristics of surface vibrations that arise as frustrated translations and/or rotations, Rayleigh waves or Fuchs-Kliewer modes. Starting from a classical and macroscopic point of view, using Maxwell equations and applying the relevant boundary conditions, we deduce the formula for the interaction of a moving electron with surface vibrations. The interaction of electromagnetic radiation with surface vibrations is then treated in the QM perturbation theory and matrix elements are obtained for IR and Raman spectroscopies. Selection rules are discussed. Finally we present a newly emerging non linear optical spectroscopy combining a tunable infrared laser with a fixed visible laser and detecting photons at the sum of the two frequencies (Sum Frequency Generation Spectroscopy).

Optical response of surfaces

Giovanni Onida
University of Roma , Italy

The lecture is a survey of some of the modern theoretical tools used to compute the optical response of surfaces. Methods, approximations and convergence problems are analyzed and described. In particular, we consider the GW method for the calculation of one-particle excitations (photoemission, inverse photoemission), and the Bethe-Salpeter equation (BSE) method to compute optical absorption and reflection spectra, all starting from standard, DFT-LDA calculations for the ground-state. Applications to GaAs(110), Si(100) and Ge(111) are shown, to give examples of calculations done at different levels of sophistication.

Adsorption and Reaction at metal surfaces

Bjørk Hammer
University of Aarhus, Denmark

The fundamental theory of adsorption at metal surfaces is presented in these lectures. First, the adsorption of atoms is considered in an effective medium theory (EMT) framework. This allows for a discussion of e.g. the physical origin of preferred adsorption sites and of the variation in adsorbate vibrational modes with the adsorption sites. Next, the adsorption of both atoms and molecules is presented from a density functional theory (DFT) viewpoint. Variations in chemisorption bond strength with type of metal surface, surface Miller index, surface defects, precoverage by adsorbates, bimetal overlayer composition, and surface strain are derived in the DFT and discussed on the basis of the Newns-Anderson method and the d-band model. Then reactions of adsorbates are considered and the trends in DFT based energy barriers for the dissociation of diatomic molecules are discussed as a function of surface structure, coverage, and composition. Finally, the lectures end with a critical assessment of the quality of DFT calculations in the context of surface reaction studies. The lecture notes are published as: B. Hammer and J. K. Norskov, Adv. Catal, 45, 71 (2000).

Adsorption Energetics and Bonding from Femtomole Calorimetry and from First Principles Theory

David King
University of Cambridge

The advent of an accurate, sensitive, single-crystal adsorption calorimeter (SCAC) in 1991 meant that, for the first time, a general tool was available for determining the energetics of surface processes, both reversible and irreversible, under well-defined conditions. This is partucularly valuable when the structure of the final state of system, adsorbate and substrate, is

well-characterized. Concurrently, first principles density functional theory (DFT) slab calculations were developped, particularly during the past six years, to the point where good comparisons can now be made with experimental results from the most reliable surface structure analyses. Results from the SCAC provide the most stringent benchmark currently available for these calculations: the total energy. Here we provide a review of the current state of the art in both experimental and theoretical studies of the energetics of adsorption and surface reactivity, including an exhaustive comparison of data for which experimental SCAC data and slab DFT results are available for the same systems. We demonstrate how the current understanding of chemical bonding and reactivity at surfaces has been transformed through the use of these technics.

Qingfeng Ge, Rickmer Kose and David King, Advances in Catalysis **45** (2000)

Scanning Tunneling Microscopy Theory

Fernando Flores
Universidad Autõnoma de Madrid, Spain

A review on the theory of the Scanning Tunneling Microscope has been presented. In a first step, tunneling currents have been discussed using an extended basis formalism : in this approach, Bardeen-tunneling theory has been introduced, and Tersoff-Hamann (TH) or Chen (C) approximations have also been critically analyzed. In a second step, tunneling currents have been discussed using a local basis formalism : in this approach, the tunneling currents are calculated using a LCAO-hamiltonian and a Keldish-Green function formalism. Finally, it has been discussed how to use state of art Density Functional theory to calculate STM-images .Typically, plane-waves or FLAPW codes yield very accurate electron local densities of states, from which STM-images are obtained using TH- or C-approximations. Alternatively, electron surface properties can also be obtained using a local orbital basis (SIESTA or FIREBALL codes): from these calculations, STM-images are obtained using a LCAO-method. The advantage of this approach is that the tip electronic structure can be much more easily incorporated in the calculations , yielding more accurate results .Several examples have been discussed : Al(111) , GaAs(110) , Fe(100) , W(110) ....

Scanning Tunneling Microscopy Experiments

Sylvie Rousset
Groupe de Physique des Solides, Paris, France

Since it was invented almost 20 years ago, scanning tunneling microscopy (STM) has been applied among a great variety of experiments and fields. The purpose of this course was to illustrate by a few key experiments the ability of this technics. After a brief summary of the principles of operation, experiments have been classified into two main domains: (i) surface structure and topography, and (ii) scanning tunneling spectroscopies (STS). STM has been very powerful by resolving surface structures from atomic structure towards mesoscopic order as it

was demonstrated on surface reconstructions, self-organization on crystal surfaces, and nucleation and epitaxial growth of various nanostructures. On the other hand not only topographic information is gained by STM but also spectroscopics. The local density of states of the sample is direcly measured. Surface states imaging on quantum corrals have lead to very spectacular imaging. More recently local inelastic electron tunneling spectroscopy was also performed by STS.

Surface electronic excitations

Volker Staemmler
University of Bochum, Germany

In this lecture, a short summary of theoretical methods for treating electronically excited states of oxide surfaces is given and the advantages of the different approaches are discussed: band structure methods, which explicitly take into account the 2D periodic structure of the surface and are suited for delocalized properties, and quantum chemical cluster methods, which are particularly suitable for local properties such as local excitations and adsorption processes. Experimental data and theoretical results are presented for several transition metal oxides, in particular NiO(100), CoO(100), MnO(100), and Cr_2O_3(111).

The electronic structure of surfaces and interfaces of strongly correlated systems

George Sawatzky
University of Gröningen, The Netherlands

In these lectures I will give a brief introduction to the electronic structure of strongly correlated systems concentrating mainly on transition metal oxides and emphasizing those points which will turn out to be important for the surface and interfaces. I will then demonstrate both with simple model calculations and with experimental electron spectroscopic studies that the parameters used in model Hamiltonians to describe the electronic structure of correlated systems can be dramatically modified at the surface and also at interfaces. This can lead to otherwise insulating materials having a metallic surface etc. I will also discuss some very recent LDA+U slab like calculations which again predict a strong reduction of the conductivity gap at the surface and the strong dependence on the kind of surface termination. Time permitting I will then discuss some ideas for the preparation of new materials with possible exotic properties using ultra thin epitaxial films.

General introduction to empirical potentials and their applications

Graeme Ackland
University of Edinburgh, U.K.

Atomistic computer simulations of condensed phase materials need the knowledge of the forces acting on each atom in any atomic configuration. Although this can be achieved with ab-initio methods of electronic structure calculations, the number of inequivalent atoms in the system is limited by the computer time and remains very small (of the order of one hundred). On the contrary, empirical potentials, in which the total energy has a simple functional form, allow to deal with very large systems. The various types of empirical potentials and their domain of application will be reviewed. Several examples will be given.

Theory of surface magnetism

Stefan Blügel
Institut fr̈ Festkörperforschung Jülich, Germany

The dimensionality and the coordination number are important parameters determining the magnetic properties. With the evolution of metallic systems from bulk over surfaces, ultrathin films, to linear chains and small atom aggregations the role of magnetism becomes increasingly more important. We begin the lecture with reminding the audience of the Stoner model and we will discuss the Stoner criterion with respect to the coordination number and the chemical trends. Then I will shortly review the magnetism of 3d, 4d, and 5d transition-metal monolayers on various noble-metal (100) substrates. Introducing the exchange interaction between neighboring atoms we will discuss the existence of different magnetic phases e.g. the p(1x1) ferromagnetic and c(2x2) antiferromagnetic structure (or more complicated ones if the time permits). Then we will move from the physics of two-dimensional magnets on noble metals to films on magnetic substrates such as 3d monolayers on Fe(100) and discuss the implications of the additional exchange interaction with the substrate. Finally repeating the monolayers to multilayers we will discuss the interlayer exchange coupling such as in Co/Cu/Co system.

Surface and interface magnetism in relation with ultrathin films, multilayers and nanostructures

François Gautier
IPCMS Strasbourg, France

The first part of these lectures has been devoted to an overview of the results of the surface and interface magnetism of transition metals in the itinerant magnetism framework. A detailed discussion of the magnetic anisotropy (including the exchange anisotropy) and an introduction to the magnetic dichroïsm have been presented. Then, the transport (GMR) and magnetic properties of some nanostructures have been discussed in relation with spin electronics.

Quantum wells

Enrique Garcia-Michel
Universidad Autonoma de Madrid, Spain

Quantum well state (QWS) are produced as the result of quantum confinement of electrons in small structures, for instance thin films. Films containing magnetic materials may exhibit spin polarized QWS, a topic of great interest because of their suitability for device applications. The basic physics behind QWS will be reviewed, together with their most relevant features for the applied and fundamental points of view.

Theory of Angle Resolved Photoemission Spectroscopy

Matti Lindroos
Tampere University, Finland

A short review of the theory of Angle Resolved Photoemission Spectroscopy is given. In addition to the standard Energy Distribution Curves a special attention is given to new Angle Scan Photoemission. Applications of the theory through calculations are given for High Tc superconductors and for more complicated three dimensional materials like copper.

Photoemission Experiments

Maria-Carmen Asensio
LURE Orsay, France and ICMM, CSIC Madrid, Spain

The most direct source of information on the electronic energy levels of atoms, molecules, and solids, is provided by different kinds of spectroscopic techniques. Among them, photoelectron spectroscopy (PES) is the most actively used to characterize a wide variety of materials such as magnetic thin films multilayers and high Tc superconductors. Taking into account that in Angle Resolved Photoemission (ARUPS), both the momentum parallel to the surface and the energy are rigorously conserved, studies of photoelectron angular dependence can be made in a diversity of ways.

In this presentation, some of the bases of the technique and its applications to metallic and metal/semiconductor interfaces, will be disclosed. Experimental Fermi Surfaces of magnetic interfaces such as thin films of Co and Fe on Cu(100) will be described as well as the evolution of the Fermi Surface of the following metal/semiconductor interfaces: Ag/Si(111), Pb/Ge(111) and Sn/Ge(111) [1,2,3]. Concerning the Fermi Surface of bulk new materials, our latest results for rare earth graphite intercalated compounds and Bi 2212 superconductor single crystals [4] will be discussed.

[1] A. Mascaraque et al., Phys. Rev. B 57, 14758(1998)

[2] J. Avila et al., Phys. Rev. Lett. 82, 442 (1999)

[3] A. Mascaraque et al., Phys. Rev. Lett. 82, 2524 (1999)

[4] N. Saini et al., Phys. Rev. Lett. 79, 3467 (1997)

6.4 ESF Workshop/Conference Announcements

6.4.1 Hands-on Workshop

FIRST ANNOUNCEMENT

The Nuts and Bolts of First-Principles Simulation

A one-week hands-on workshop in the theory and practise of first principles calculations using the new CASTEP code

6th-13th December 2001 at the University of Durham

(Exact programme to be confirmed)

Web page: http://cmt.dur.ac.uk/sjc/castep.html

Supported by:
ESF-STRUC Psi-k Programme

The CASTEP Developers' group

Molecular Simulations Inc

Overview:

This workshop is aimed at anyone who wants to learn how first-principles

simulation works and how to apply it. It is especially suitable for those just starting out in this research field such as students embarking on a Ph.D with a substantial first-principles element.

In the workshop you will use a completely new F90 version of CASTEP written from scratch to a radical modular design. For academics the workshop package includes a copy of the code to take away and use in your own research.

Highlights:

* Intensive training for a flying start in first-principles simulation
* Balanced programme of lectures, practical sessions and seminars
* Improve knowledge and skills particular to your research
* Learn how to use the new F90 CASTEP
* Talk to leading exponents and CASTEP developers
* Academic code distribution included in the workshop package
* Social programme

The code:

The CASTEP Developers' Group has rewritten CASTEP from scratch in FORTRAN 90. The design is highly modular and makes extensive use of many object-oriented ideas. The code has superb clarity and simplicity, making developments far more rapid and reliable. None of this compromises performance, which thanks to extensive algorithmic development and careful design, comfortably exceeds any previous benchmarks. CASTEP has been designed for a long and bright future.

The workshop:

The workshop schedule is divided between lectures and practical sessions.

The lectures will present all the background theory required for first principles calculations using CASTEP including density functional theory, implementation details, applications, case studies and research highlights.

The practical sessions will focus on building up your CASTEP skills, from the basics through to full-scale research calculations. A suite of 100 PC's running MSI's Materials Studio interface will ensure that everyone can explore at his or her own pace.

Interested?

Thanks to generous support from the ESF through the Psi-k network we shall be able to offer many places for young researchers at very low cost. Participation will be limited to 100. To register your interest at this stage, send an e-mail to Stewart Clark (s.j.clark@durham.ac.uk) with "CASTEP workshop" as the subject.

Organisers:

Philip Lindan (Kent)
Stewart Clark (Durham)
Walter Temmerman (Daresbury)

7 General Workshop/Conference Announcements

7.1 13th Workshop on Recent Developments in Electronic Structure Algorithms

June 15 - June 18, 2001
Princeton University
Princeton, New Jersey
`http://www.princeton.edu/~es2001`

The Thirteenth Annual Workshop on Recent Developments in Electronic Structure Algorithms (ES2001) will be held at Princeton University in Princeton, New Jersey from June 15 to June 18, 2001. To find out detailed information on this year's workshop, please visit our website:

`http://www.princeton.edu/~es2001`

The registration fee includes dormitory lodging, a banquet and all other meals, and participation in the activities of the workshop. Local participants may choose to register at a reduced rate that does not include lodging. Travel expenses to the conference are not included. The registration fees are:

$230 – Regular fee
$170 – Student fee
$90 – Local participant fee (no lodging)

Everyone intending to attend should register for ES2001, following the instructions in

`http://www.princeton.edu/~es2001/Registration`

(this includes speakers, for which the registration fee is waived). We also encourage partecipants to present a poster on their current activities. The deadline for registration is May 20. Post-deadline registrations will incur a $50 administrative charge.

ES2001 promises to be a very exciting workshop, and we hope that you will be able to participate. If you have any questions or comments, feel free to contact the local organizing committee at es2001@princeton.edu.

Finally, we invite you to share this announcement with anyone that might be interested in attending ES2001. A conference page that can be printed and displayed is available at

`http://www.princeton.edu/~es2001/es2001.ps`

Roberto Car
Paolo Giannozzi
Nicola Marzari
Marcel Nooijen
Annabella Selloni

7.2 Conference of the SIMU ESF Programme

BRIDGING THE TIME-SCALE GAP
September 10 to 13, 2001
Konstanz, Germany
Registration Deadline: July 1 2001
CONFERENCE WEB-SITE http://konstanz.cecam.fr

The conference is organized in the beautiful historical city of Konstanz along its charming lake (Bodensee). It will focus on new simulation techniques as well as current applications for bridging the time-scale gap from microscopic, ab-initio levels towards the mesoscopic and macroscopic ones.

Organized within SIMU, an ESF-supported programme, it will be open to everybody interested in the subject.

The main **topics** of the conference will be: Protein Folding Modelling, Polymer Structure and Dynamics, Multiscale Modelling in Materials, Methodological Developments in MD and MC, Applications of Statistical Mechanics to Biological Systems, Complex Fluids, Mesoscopic Fluids, Lattice Models, Perspectives in ab-initio MD, and Quantum Simulations.

Invited Speakers

Ali Alavi (Cambridge), Mike Allen (Bristol), Wanda Andreoni (Zrich), Jean-Louis Barrat (Lyon), Kurt Binder (Mainz), Daniel Borgis (Paris), David Ceperley (Urbana), David Chandler (Berkeley), Giovanni Ciccotti (Roma), Fabrizio Cleri (ENEA, Roma), Alessandro Curioni (Zrich), Christoph Dellago (Rochester), Marjolein Dijkstra, Daan Frenkel (Amsterdam), Alain Fuchs (Paris), Alexander Grosberg (Minneapolis), Jean-Pierre Hansen (Cambridge), Jrg Hutter (Zrich), Hannes Jonsson (Seattle), Ray Kapral (Toronto), Martin Karplus (Strasbourg), Alexander Khokhlov (Moscow), Mike Klein (Philadelphia), Walter Kob (Montpellier), Kurt Kremer (Mainz), David Landau (Athens, USA), Dominique Levesque (Paris), Chris Lowe Hartmut Lwen (Dsseldorf), Martin Mser (Mainz), Carlo Pierleoni (Roma), Luciano Reatto (Milan), Eugene Shakhnovich (Harvard), Berend Smit (Amsterdam), Michiel Sprik (Cambridge), Sauro Succi (Roma), Doros Theodorou (Athens, Greece), Mark Tuckerman (New York), Nigel Wilding (Liverpool)

Donal MacKernan
SIMU & CECAM (CENTRE EUROPEEN DE CALCUL ATOMIQUE ET MOLECULAIRE)
Ecole Normale Superieure de Lyon,
46 Allee d'Italie, 69364 Lyon Cedex 07, France
00-33-04-72728632 (office)
00-33-04-72728636 (fax)
Email: dmack@cecam.fr

7.3 ACSIN-6 Conference

Atomically Controlled Surfaces, Interfaces and Nanostructures Conference

North Lake Tahoe, California

July 9-12, 2001

The ACSIN-6 conference will be held July 9-12 in North Lake Tahoe, California. ACSIN-6 is a conference for presenting new concepts, techniques and applications of atomically controlled processes at surfaces, interfaces and nanostructures. The primary topics of the conference will be surfaces, interfaces, adsorption and clusters on surfaces, self-organized nanostructures, nanostructure fabrication, atomic manipulation, artificial atomic design, atomic scale devices and electronics, magnetism and optics, clusters, nanotubes and organics, atomic scale experimental techniques, and atomic scale theoretical approaches. There will be a limited number of parallel sessions.

Please find a list of invited speakers on our web site http://acsin.org/invited

Also, please note the following DEADLINES:

1. ABSTRACT SUBMISSION: MAY 8 http://www.acsin.org/abstracts
2. NOTIFICATIONS OF ABSTRACT ACCEPTANCE: MAY 15
3. EARLY REGISTRATION: MAY 22 http://www.acsin.org/registration
4. GROUP RATES FOR NORTHSTAR HOTEL (CONF. SITE): MAY 22
5. GROUP RATES FOR TAHOE BILTMORE HOTEL: JUNE 8
6. NOMINATIONS FOR ACSIN PRIZES: MAY 8
   http://www.acsin.org/prizes

Shirley Chiang, UC Davis, Co-chair
Giulia Galli, LLNL, Co-chair
Louis Terminello, LLNL, Co-chair

XI WORKSHOP ON COMPUTATIONAL MATERIALS SCIENCE

17 - 23 September 2001
Sofitel Timi Ama, Villasimius (CA), Sardinia, Italy

web page: http://www.dsf.unica.it/CMS2001
e-mail: workshop@dsf.unica.it

with the sponsorship of
European Commission-Community Research
High-Level Scientific Conferences

under the patronage of UNESCO

organized by: The Physics Department, Università di Cagliari, and the Cagliari Research Unit of Istituto Nazionale per la Fisica della Materia

An international workshop on computational techniques and applications to materials science

Attention, deadlines are changed !

See TENTATIVE INVITED SPEAKERS and INFO below.

FORMAT: About 20 invited lectures plus TALK (∼12) and POSTER contributed session.

VENUE: Sofitel Timi Ama at Villasimius (CA), an attractive sea resort on the south-eastern coast of Sardinia, providing comforts and an informal atmosphere.

CONTACT: For scientific and logistic queries: workshop@dsf.unica.it

CONTRIBUTIONS AND PROCEEDINGS:

Contributions in poster format are invited. ALL contributions (after refereeing) will be published probably in a special issue of the journal Computational Materials Science. Deadline for abstract

submission: June 30, 2001. Contact V. Fiorentini at +39 070 6754912 or P. Ruggerone at +39 070 6754847 or at workshop@dsf.unica.it for further details. Camera ready manuscripts will be due at the Workshop, LaTeX templates can be downloaded from the Workshop homepage: http://www.dsf.unica.it/CMS2001

INVITED SPEAKERS

E. Arrigoni ((Wuerzburg, Germany)
H. Brune (Lausanne, Switzerland)
B. Chiaia (Turin, Italy)
A.J. Freeman (Evanston, USA)
D. Helbing (Dresden, Germany)
J. Majewski (Munich, Germany)
A. Maritan (Triest, Italy)
F. Mauri (Paris, France) (*)
B. Persson (Juelich, Germany) (*)
U. Roethlisberger (Zurich, Switzerland)
A. Rubio (Valladolid, Spain)
A. Ruini (Modena, Italy)
J. Soler (Madrid, Spain)
A. Tramontano (IRBM, Italy)
A. Zunger (NREL, USA)

(*) not yet confirmed

REGISTRATION

The REGISTRATION form can be sent directly from the Workshop homepage

http://www.dsf.unica.it/CMS2001).

The deadline is June 20, 2001.

The registration should be accompanied by payment receipt of the CONFERENCE FEE (by FAX: ++39-070-510171). The fee includes full-board lodging at Hotel Sofitel Timi Ama from 17/9 afternoon to 23/9 lunch, coffee breaks, refreshments, social trip (or banquet), and amounts to

Double or triple room lodging It.Lire 1400000 (~US$ 670)/person Single room lodging It.Lire 1600000 (~US$ 760)/person.

PAYMENT should be effected by bank money transfer on the bank account # 22698 of Comitato Organizzatore di Attività di Fisica Computazionale, at Banco di Sardegna, Sede di Cagliari, Codice ABI 1015/7 - CAB 04800.

No fee is requested from the invited speakers.

The Organizing Committee is able to offer support (from 50% up to 100% of the conference fees

plus travel costs in some cases) to a limited number (∼50) of young scientists, preferrably PhD students. The deadline for the request of financial support is June 1, 2001. The committee will comunicate its decision on June 15, 2001.

Series Chairman : prof. A. Baldereschi - EPFL Lausanne

Workshop Chairman : prof. F. Meloni - INFM and Università di Cagliari

Scientific Secretariat: dr. V. Fiorentini - dr. P. Ruggerone INFM and Università di Cagliari

8 General Job Announcements

Postdoctoral Associateship
Carnegie Institution of Washington, Washington D.C.

A postdoctoral associateship is available for a creative independent researcher at the Carnegie Institution of Washington, Washington D.C. to study ferroelectric solid solutions using first-principles methods. This research is to understand high electromechanical coupling piezoelectrics such as PMN-PT and PZN-PT, and to explore the role of polarization rotation (Fu and Cohen, Nature 403, 281, 2000; Noheda et al. PRL 86, 3891, 2001) in perovskite solid solutions.

Applicants should be adept at independent and collaborative research. Also important is the ability and inclination to write up research for publication in a timely way and to present results at scientific meetings. Facility with FORTRAN is essential and with MPI is highly desirable. Applicants should send a vita, bibliography, and 3 letters of reference to cohen@gl.ciw.edu.

Please send applications by email or fax to (626)564-0715, or to the following address:

Ronald Cohen
Visiting Professor of Materials Science and Geophysics
California Institute of Technology
1200 E. California Blvd.
Mail Stop 252-21
Pasadena CA 91125

or

Ronald Cohen
Geophysical Laboratory, Carnegie Institution of Washington
5251 Broad Branch Rd., N.W.
Washington, D.C. 20015
http://www.gl.ciw.edu/ cohen/

Academic Staff Position ("BAT-IIa") for up to 5 years ("Wissenschaftliche/r Mitarbeiter/in zur Forschung für max. 5 Jahre")

Humboldt University Berlin
Institute of Chemistry

The quantum chemistry group at Humboldt University Berlin (Institute of Chemistry) invites applications for an academic staff position for up to 5 years in the area of application and development of first-principle computational chemistry/physics methods. It includes research on structure and reactivity of solid catalysts (oxidic materials) in collaboration with experimental groups. We offer a stimulating scientific environment, excellent computing facilities and a competitive salary with the benefits of a regular position. Applicants are expected to have a PhD in computational physics/chemistry/crystallography or equivalent qualifications and experience with computer codes for first-principle/ab initio simulations. The position is immediately available, but applications for later start dates are also welcome. Applications including a detailed resume with three academic references and a list of publications should be send to:

Joachim Sauer
Humboldt-Universitaet zu Berlin
Institut fuer Chemie
Sitz: Jaegerstrasse 10-11
D-10117 Berlin
Germany
FAX: +49-30-20192 302
E-mail: js@qc.ag-berlin.mpg.de

Postdoctoral Position to work on Nanotubes

Dpto. Fisica de Materiales

San Sebastian, SPAIN

Candidates are invited to apply for a post-doctoral position to work on the growth mechanism, electronic, optical, structural and transport properties of carbon and composite-nanotubes with particular emphasis on theoretical calculations of interest for: STM microsopy, nanodevices, chemical activity, mechanical behavior, optical response. In addition, the group is flexible and open to promising new research directions within the general topic of nanotubes. The techniques to be used range from semiempirical potentials to acurate ab-initio methods. Knowledge of molecular dynamics and electronic structure calculations is desirable.

The project is included in a new EU-funded project (COMELCAN) continuation of a previous Training and Mobility Research TMR) Network on "Nanotubes for Microstructure Technology" (NAMITECH). A very close collaboration with the experimental partners of the network (groups in France, Germany, Belgium and Ireland) is guaranteed. Please see the web page of the Network for further details (NAMITECH), including a monthly published Newsletter.

The objetives of the new COMELCAN program are:

i) To have a clear and consistent understanding of the growth mechanism of nanotubes.

ii) Development of composited systems.

iii) The understanding and control of the correlation between mechanical (bending, torsion, extension, contraction, etc.) and electronic properties (electronic structure, electrical conductivity, Hall effect, magnetoresistance) of single-wall nanotubes.

iv) Technological applications.

Applications should include a curriculum vitae, highlighting the main contributions, and a complete list of publications with an indication of those which the applicant selects as the most relevant for the application. reference letters will be given proper consideration. Accepted formats are paper, ascii/LaTeX/postscript/pdf email attachment, or a web address for html, LaTeX, ps, or pdf versions of the above. xxx or PR-online links are ok for the publication. Web links are the preferred format for all materials Applications should be sent to Dr. Angel Rubio (see below).

NOTE: The applicant must comply with the RTN rules for network employment of young scientists: The applicant should hold a Ph.D. degree or equivalent in Physics or Chemistry, be younger than 35, and should have some experience in computational Condensed Matter Theory.

Only nationals of Member States or Associated States of the EU (excluding Spain) and states from the former Easter countries are eligible for the position.

Dr. Angel Rubio
Dpto. Fisica de Materiales, Facultad de Quimicas
Universidad del Pais Vasco UPV/EHU and
Donostia International Physics Center (DIPC)
Apdo. 1072, 20018 San Sebastian/Donostia. SPAIN
Phone : +34-943015400
Fax : +34-943015600
Mail : arubio@sc.ehu.es

http://www.fam.cie.uva.es/~arubio

5-YEAR RESEARCH POSITION

"Ab initio simulation of materials and surfaces"

Autonomous University of Madrid

The Ab initio Simulation Group at the Condensed Matter Physics Department of the Autonomous University of Madrid is offering a five-year research position to be covered by an outstanding young researcher in the field of ab initio electronic structure calculations and simulations of materials. The group is one of the main developers of the SIESTA code for order-N DFT calculations of large systems (http://www.uam.es/siesta).

The position is part of a new program of contracts called Ramon y Cajal, started this year by the Spanish Ministry of Science and Technology (www.mcyt.es). The salary and research status are similar to those of a Profesor Titular (Associate Professor). They can lead independent projects and ask for government grants.

Interested candidates may send a CV and suggested reference persons to

Jose M. Soler
Dep. Fisica de la Materia Condensada, C-3
Universidad Autonoma de Madrid
E-28049 Madrid, Spain
Tel: 34-91-397-5155
Fax: 34-91-397-3961
Email: jose.soler@uam.es

9 Abstracts

Broken-Bond Rule for the Surface Energies of Noble Metals

I. Galanakis, G. Bihlmayer, V. Bellini, N. Papanikolaou, R. Zeller, S. Blügel, and P. H. Dederichs

Institut für Festkörperforschung, Forschungszentrum Jülich, D-52425 Jülich, Germany

Abstract

Using two different full-potential *ab initio* techniques we introduce a simple, universal rule based on the number of broken first-neighbor bonds to determine the surface energies of the three noble metals Cu, Ag and Au. When a bond is broken, the rearrangement of the electronic charge for these metals does not lead to a change of the remaining bonds. Thus the energy needed to break a bond is independent of the surface orientation. This novel finding can lead to the development of simple models to describe the energetics of a surface like step and kink formation, crystal growth, alloy formation, equilibrium shape of mesoscopic crystallites and surface faceting.

Submitted to Phys. Rev. Lett.
Contact person: Iosif Galanakis (i.galanakis@fz-juelich.de).
Reprints available on request or can be downloaded from:
http://xxx.lanl.gov with absract number cond-mat/010520

The elastic constants of $MgSiO_3$ perovskite at pressures and temperatures of the Earth's mantle

Artem R. Oganov, John P. Brodholt, G. David Price
Crystallography and Mineral Physics Unit, Department of Geological Sciences, University College London, Gower Street, London WC1E 6BT, U.K.

Abstract

Convection in the Earth's mantle is fundamentally responsible for plate tectonics, and the associated continental drift, earthquakes, and volcanism. The convective temperature anomalies, associated with the ascending hot and descending cold streams, can be obtained from seismic tomography, provided elastic properties of the mantle minerals are known as a function of temperature at mantle pressures (up to 1.36 Mbar). Such information cannot currently be given by experiments. Circumventing this experimentally formidable task, we perform ab initio molecular dynamics (AIMD) simulations of elastic and seismological properties of $MgSiO_3$ perovskite, the major mineral of the lower mantle (LM), at relevant thermodynamic conditions. We believe that these are the first true finite-temperature AIMD simulations of elastic constants to be performed for any material. Our results imply that the LM is either significantly anelastic or compositionally heterogeneous on the large scale. The temperature contrast between the cold slabs and hot plumes was found to be about 800 K at 1,000 km, increasing to 1,500 K at 2,000 km and, possibly, over 2,000 K at the core-mantle boundary.

(To appear in Nature, 2001)
Contact person: A.Oganov (a.oganov@ucl.ac.uk)

Theoretical investigation of metastable Al_2SiO_5 polymorphs

Artem R. Oganov, G. David Price, and John P. Brodholt
Crystallography and Mineral Physics Unit, Department of Geological Sciences, University College London, Gower Street, London WC1E 6BT, U.K.

Abstract

Using theoretical simulations based on density functional theory within the generalised gradient approximation, we predict a series of metastable phase transitions occurring in low-pressure Al_2SiO_5 polymorphs (andalusite and sillimanite); similar results were obtained using semiclassical interatomic potentials within the ionic shell model. Soft lattice modes as well as related structural changes are analysed. For sillimanite, we predict an isosymmetric phase transition at ca 35 GPa; an incommensurately modulated form of sillimanite can also be obtained at low temperatures and high pressures. The high-pressure isosymmetric phase contains five-coordinated Si and Al atoms. The origin of the fivefold coordination is discussed in detail. Andalusite was found to transform directly into an amorphous phase at ca 50 GPa. Our study provides insight into the nature of metastable modifications of crystal structures, and the ways in which they are formed. Present results indicate the existence of a critical bonding distance, above which interatomic interactions cannot be considered as bonding. The critical distance for the Si-O bond is 2.25 Å.

(To appear in Acta Crystallographica A, 2001)
Contact person: A.Oganov (a.oganov@ucl.ac.uk)

Localization of 3d Electrons in thin Mn and Mn-oxide films by Resonant Photoemission

M.C. Richter[(1)], P. Bencok[(1)], R. Brochier[(1)], V. Ilakovac[(1)], O. Heckmann[(1)],
G. Paolucci[(2)], A. Goldoni[(2)], R. Larciprete[(2)], J.-J. Gallet[(3)],
F. Chevrier[(3)], G. van der Laan[(4)], K. Hricovini[(1,3)]

[(1)] *LPMS, Universite de Cergy-Pontoise, Neuville Oise, 95 031 Cergy-Pontoise, France*

[(2)] *Sincrotrone Trieste, 34012 Basovizza, Trieste, Italy*

[(3)] *LURE, Centre Universitaire Paris-Sud, 91 898 Orsay, France*

[(4)] *Daresbury Laboratory, Warrington WA4 4AD, United Kingdom*

Abstract

Abstract - We have applied the tool of resonant photoemission at the L_3 absorption edge to thin Mn layers deposited on Cu(100). This allows us to study the transition from atomic to solid state phase by following the $3d$ band formation through the localization of a photon-excited electron in the influence of a $2p$ core hole. We have observed for the first time localized behavior for one of the transitions of the Mn $2p3p3d$ decay above L_3 absorption threshold for coverages smaller than 0.5 mono-layers. We show that the auto-ionization time of the $2p$ core hole intermediate state is comparable to the time of localization of the photon excited $3d$ electron in the influence of the $2p$ core hole in the case of the highest binding energy transition of the $2p3p3d$ decay.

(Accepted for Phys. Rev. B)

Contact person: G.VanDerLaan@dl.ac.uk

Non-reciprocal x-ray linear dichroism

G. van der Laan
Daresbury Laboratory, Warrington WA4 4AD, UK

Abstract

Recently, a new optical effect was observed by J. Goulon *et al.*, Phys. Rev. Lett. **85**, 4385 (2000) using linearly polarized synchrotron radiation. The authors have correctly analysed the effect using the matematical framework of Buckingham and Barron. A brief review is given with the underlying simplicity discussed from a symmetry point of view.

(Published in J. Synchrotron Rad. 8, 1059 - 1060 (2001))
Contact person: G.VanDerLaan@dl.ac.uk

Core-level magnetic circular dichroism as a probe for electron-correlation effects

Gerrit van der Laan
Magnetic Spectroscopy Group, Daresbury Laboratory,
Warrington WA4 4AD, UK

Abstract

We show how the spectral structure of the magnetic circular dichroism (MCD) in core-level spectroscopy can be analysed using angular momentum algebra. The results are supported by full-multiplet calculations in intermediate coupling, which for localized materials are in very good agreement with the experimental results. To demonstrate the general applicability we analyse a wide variety of systems. For didactical reasons we start off with the photoemission from an l shell and the spin-orbit split core j levels using a one-particle model, followed by the more realistic examples of rare earths $4f$ photoemission from an incompletely filled shell and $N_{4,5}$ x-ray absorption as the intermediate state in resonant photoemission. This gives a clear indication of the restrictions imposed by the one-particle model. We show that even for itinerant metals, such as nickel and iron, the $2p$ photoemission spectra can not be explained using a one-particle model. Recent experimental results for the Ni $2p$ photoemission of nickel metal show that inter-configurational mixing has to be taken into account in order to understand the detailed structure of the MCD. Apart from its invaluable use to quantify the ground-state spin and orbital magnetic moments, MCD therefore also provides a powerful tool to study - in an element-specific way - the electron-correlation effects arising in a large variety of materials.

(Published in J. Electron Spectrosc. Relat. Phenomen. **117 - 118**, 89 - 101 (2001).)
Contact person: G.VanDerLaan@dl.ac.uk

Oxygen-driven magnetization reorientation in Fe(001) bilayer. A tight-binding study

Štěpán Pick
J. Heyrovský Institute of Physical Chemistry,
Academy of Sciences of the Czech Republic, Dolejškova 3,
CZ-182 23 Prague 8, Czech Republic
Hugues Dreyssé
Institut de Physique et Chimie des Matériaux de Strasbourg,
UMR CNRS 46, 23 rue du Loess, Boîte Postale 20 CR,
F-67037 Strasbourg, France

Abstract

The experiment [J. Chen et al., Phys. Rev. B **45**, 3636 (1992)] finds destabilization of the perpendicular magnetization in a Fe(001) bilayer on Ag(001) substrate that is driven by even small amount of adsorbed oxygen. Here, we present a semi-empirical tight-binding model investigating the phenomenon. We consider the p(3×3) and (1×1) oxygen overlayers to study the low and high coverage cases, respectively. The geometry we employ is based on existing models from the literature of the Fe surface expansion in (1×1)O/Fe(001). The (1×1) leads to a destabilization of the perpendicular magnetization. For the p(3×3) structure we have indication of the reorientation transition if the model with a large (23%) local expansion of the bilayer in the vicinity of the adsorption site is supposed.

Published in Phys. Rev. B **63** 2001, 205427

Ab initio Relativistic Spin-Polarised Theory of Angle-Resolved Photoemission

M. Woods[1], A. Ernst[2,3], P. Strange[1], W. M. Temmerman[2]

[1] *Physics Department, Keele University, Keele, Staffordshire, ST5 5BG, U.K.*

[2] *Daresbury Laboratory, Daresbury, Warrington, WA4 4AD, Cheshire, U.K.*

[3] *Max Planck Institut für Mikrostrukturphysik, Halle, Germany*

Abstract

An *ab-initio* real-space fully-relativistic spin- and angle-resolved photoemission theory has been developed. The method is based on density functional theory and implemented using multiple-scattering theory with a Green's function calculated using a real-space cluster method. An efficient computer code has been developed to calculate the spectra. Interpretation of the results exhibits the signatures of relativity in the photoemission spectra, and describes what photoemission can tell us about relativistic effects in the band structure. We illustrate our theory and code by presenting results for transition metal surfaces.

(Submitted to J. Phys. CM)

Contact person: Paul Strange (p.strange@phys.keele.ac.uk)

First principles relativistic theory of photoemission from magnetic surfaces

M. Woods[a], P. Strange[a], A. Ernst[b,c] and W. M. Temmerman[b]
[a] *Department of Physics, Keele University, Staffordshire, ST5 5BG, UK*
[b] *Daresbury Laboratory, Daresbury, Warrington WA4 4AD, UK*
[c] *Max-Planck-Institut fur Mikrostukturphysik, Weinberg 2, D-06120 Halle, Germany*

Abstract

A first principles theory of spin- and angle-resolved photoemission has been developed. The theory is based on density functional theory and is fully relativistic. It is implemented using multiple scattering theory with a Green's function calculated using a real space cluster method. No lattice symmetry or periodicity is assumed and therefore our approach can be applied to low-dimensional systems. We illustrate the theory with a calculation of the photoemission spectra from Ni(100) and interpret the result in terms of the band structure. The effect of the polarisation of the photon on the spectra is emphasised.

(Accepted for publication: Journal of Magnetism and Magnetic Materials)
Contact person: Paul Strange (p.strange@phys.keele.ac.uk)

Relativistic theory of magnetic x-ray scattering

E. Arola and P. Strange
Physics Department, Keele University, Keele, Staffordshire ST5 5BG, UK

Abstract

We present a description of a first principles formalism for the scattering of circularly polarised x-rays within the framework of relativistic density functional theory (DFT). The scattering amplitudes are calculated using standard time-dependent perturbation theory to second order in the electron-photon interaction vertex. An implementation of the theory based on relativistic spin-polarised multiple scattering theory is discussed. This method is relatively easy to implement, but has a limited range of applicability. We suggest that an implementation using the self-interaction corrections to DFT may make the theory applicable to rare earth materials where many of the key experiments have been performed. The theory is illustrated with appropriate examples.

(Accepted for publication: Applied Physics Letters)
Contact person: Paul Strange (p.strange@phys.keele.ac.uk)

Static overscreening and nonlinear response in the Hubbard model

Erik Koch
Max-Planck Institut für Festkörperforschung,
Heisenbergstraße 1, 70569 Stuttgart, Germany

Abstract

We investigate the static charge response for the Hubbard model. Using the Slave-Boson method in the saddle-point approximation we calculate the charge susceptibility. We find that RPA works quite well close to half-filling, breaking, of course, down close to the Mott transition. Away from half filling RPA is much less reliable: Already for very small values of the Hubbard interaction U, the linear response becomes much more efficient than RPA, eventually leading to overscreening already beyond quite moderate values of U. To understand this behavior we give a simple argument, which implies that the response to an external perturbation at large U should actually be strongly non-linear. This prediction is confirmed by the results of exact diagonalization.

(submitted to: Phys. Rev. B)
Latex-file available from E. Koch: `E.Koch@fkf.mpg.de`

Anisotropic spin-orbit coupling and magnetocrystalline anisotropy in vicinal Co films

Sarnjeet S. Dhesi
European Synchrotron Radiation Facility, BP 220, F-3804 Grenoble, France
Gerrit van der Laan and Esther Dudzik
Magnetic Spectroscopy Group, Daresbury Laboratory, Warrington WA4 4AD, UK

Abstract

The anisotropy of the spin-orbit interaction, $\langle \lambda_a \rangle$, in vicinal Co films has been measured using x-ray magnetic linear dichroism (XMLD). A linear increase in $\langle \lambda_a \rangle$ with Co step density is found using a new sum rule and represents the first experimental confirmation that XMLD probes the magnetocrystalline anisotropy energy (MAE). X-ray magnetic circular dichroism is used to confirm that the XMLD arises from changes in the local step-edge electronic structure. The XMLD sum rule gives a larger MAE compared to macroscopic values and is discussed with respect to other local probes of the MAE.

(Accepted for publication in the Physical Review Letters)
Contact person: G.VanDerLaan@dl.ac.uk

A Kinetic Monte Carlo Investigation of Island Nucleation and Growth in Thin-Film Epitaxy in the Presence of Substrate-Mediated Interactions

Kristen A. Fichthorn,[1] Michael L. Merrick,[1] and Matthias Scheffler[2]
[1]*Department of Chemical Engineering, The Pennsylvania State University, University Park, PA 16802, USA*
[2]*Fritz-Haber-Institut der Max-Planck-Gesellschaft, Faradayweg 4–6, 14195 Berlin-Dahlem, Germany*

Abstract

Island nucleation and growth during thin-film epitaxy is typically described using mean-field rate equations, which can be solved to predict the density of stable islands as a function of the deposition rate and the diffusivity of an isolated adatom. Recent theoretical and experimental studies indicate that medium- and long-range interactions between adatoms may change the simple picture that nucleation theory provides, because the presence of these interactions invalidates some of its assumptions. In this work, we investigate the ramifications of medium-range, substrate-mediated interactions for aspects of island nucleation and growth. The interactions are quantified for Ag on a strained Ag(111) substrate using density-functional theory calculations. We discuss our incorporation of these interactions into a kinetic Monte Carlo model to study thin-film epitaxy. The simulated thin-film growth is compared to predictions by standard nucleation theory. We discuss features of island nucleation and growth that are actuated by the presence of medium-range interactions.

(submitted to: Appl. Phys. A)
Contact person: Matthias Scheffler (scheffler@fhi-berlin.mpg.de)

On the Nature of RuS_2 HDS Active Sites: Insight from ab-initio Theory

M. E. Grillo
Fritz-Haber-Institut der Max-Planck-Gesellschaft, Faradayweg 4–6, 14195 Berlin-Dahlem, Germany
P. Sautet
Institut de Recherches sur la Catalyse, 2 Av. A. Einstein, 69626 Villeurbanne Cedex, France and Laboratoire de Chimie Theorique, Ecole Normale Superieure de Lyon, 69364 Lyon Cedex 07, France

Abstract

The adsorption of thiophene over different hydrogenated $RuS_2(111)$ defect-surface terminations has been studied using *ab-initio* density functional theory. The highest adsorption energy is obtained for thiophene adsorbing with the molecular ring perpendicular to the surface plane (η^1-coordination) on a stoichiometric termination at a hydrogen coverage involving solely protonic SH species at the surface. However, as previously calculated for the (100) surface, this position do not seem to favor thiophene activation. The presence of surface hydrides (RuH) stabilizes the η^5-coordination through the enhanced hybridization to the thiophene C-S and C-C π-states respect to the η^1-position. The largest tendency to thiophene activation with respect to the αC-S bond breaking is obtained for a η^5-coordination on a reduced termination exposing coordinatively unsaturated Ru-atoms. In this equilibrium geometry, the thiophene ring is centered over a hydride specie (RuH) over the sulfur vacancy. Participation of hydridic surface species in the activation process is analyzed in terms of the relative position of the density of H-s-states for both types of hydrogens at the surface. The mechanisms governing the activation are discussed based on the change of the thiophene electronic structure over interaction with the model active-surfaces.

(submitted to: Journal of Molecular Catalysis A: Chemical)
Contact person: Maria E. Grillo (grillo@fhi-berlin.mpg.de)

First-principles studies of kinetics in epitaxial growth of III-V semiconductors

P. Kratzer, E. Penev and M. Scheffler
Fritz-Haber-Institut der Max-Planck-Gesellschaft, Faradayweg 4–6,
14195 Berlin-Dahlem, Germany

Abstract

We demonstrate how first-principles calculations using density-functional theory (DFT) can be applied to gain insight into the molecular processes that rule the physics of materials processing. Specifically, we study the molecular beam epitaxy (MBE) of arsenic compound semiconductors. For homoepitaxy of GaAs on GaAs(001), a growth model is presented that builds on results of DFT calculations for molecular processes on the $\beta 2$-reconstructed GaAs(001) surface, including adsorption, desorption, surface diffusion and nucleation. Kinetic Monte Carlo simulations on the basis of the calculated energetics enable us to model MBE growth of GaAs from beams of Ga and As_2 in atomistic detail. The simulations show that island nucleation is controlled by the reaction of As_2 molecules with Ga adatoms on the surface. The analysis reveals that the scaling laws of standard nucleation theory for the island density as a function of growth temperature are not applicable to GaAs epitaxy. We also discuss heteroepitaxy of InAs on GaAs(001), and report first-principles DFT calculations for In diffusion on the strained GaAs substrate. In particular we address the effect of heteroepitaxial strain on the growth kinetics of coherently strained InAs islands. The strain field around an island is found to cause a slowing-down of material transport from the substrate towards the island and thus helps to achieve more homogeneous island sizes.

(submitted to: Appl. Phys. A)
Contact person: Peter Kratzer (kratzer@fhi-berlin.mpg.de)

Surface Core-Level Shifts at an oxygen-rich Ru Surface: O/Ru(0001) vs. RuO_2(110)

Karsten Reuter and Matthias Scheffler
Fritz-Haber-Institut der Max-Planck-Gesellschaft, Faradayweg 4–6,
14195 Berlin-Dahlem, Germany

Abstract

We present density-functional theory calculations of Ru $3d$ and O $1s$ surface core-level shifts (SCLSs) at an oxygen-rich Ru(0001) surface, namely for the O(1×1)/Ru(0001) chemisorption phase and for two surface terminations of fully oxidized RuO_2(110). Including final-state effects, the computed SCLSs can be employed for the analysis of experimental X-ray photoelectron spectroscopy (XPS) data enabling a detailed study of the oxidation behaviour of the Ru(0001) surface. We show that certain peaks can be used as a fingerprint for the existence of the various phases and propose that the long disputed satellite peak in RuO_2(110) XPS data originates from a hitherto unaccounted surface termination.

(submitted to: Surf. Sci.)
Contact person: Karsten Reuter (reuter@fhi-berlin.mpg.de)

First-principles study of hyperfine fields in a Cd impurity in the Fe/Ag(100) interface

C. O. Rodriguez,[1] M. V. Ganduglia-Pirovano,[2] E. L. Peltzer y Blancá,[1] and M. Petersen[2]

[1] *IFLYSIB, Grupo de Física del Sólido, C.C. 565, La Plata 1900, Argentina*

[2] *Fritz-Haber-Institut der Max-Planck-Gesellschaft, Faradayweg 4–6, 14195 Berlin-Dahlem, Germany*

Abstract

Monolayer resolved hyperfine fields (HFFs) at the Fe/Ag(100) interface have recently been determined using ^{111}In probe atoms, which decay to ^{111}Cd, in perturbed $\gamma\gamma$ angular-correlation spectroscopy (PAC). Isolated radioactive probe atoms in PAC allow to sense the presence of HFFs at the Fe and induced HFFs at the Ag layers but, poses a complementary physical problem to that of the HFFs at the host Fe/Ag system: that of an impurity within the layers. Using density-functional theory (DFT) within the generalized gradient approximation (GGA) and a supercell approach, we investigate this problem. Similarly as experimentalists insert the probe atom on a layer by layer growth, preparing samples with radioactive probe atoms either in the Fe/Ag interface, or in the second (from the interface) Ag layer, or embedded within the bulk Fe, our supercell methodology can simulate each of these systems. The theoretical approach has the advantage of having the capability of distinguishing between two different cases at the interface: Cd in the Fe or Ag side. This allows us to make a clear assignment of the measured HFFs. We discuss: i) the relation of the HFF in the Cd probe with that of the original host atom, ii) the precision of state of the art DFT-GGA calculations to obtain quantitative predictions of HFFs in very complex systems such as interfaces and the effect of lattice relaxations (interlayer spacings, lateral displacements). The importance of including spin-orbit (SO) coupling and the influence of additionally considering orbital polarization (OP) are assessed.

(submitted to: Phys. Rev. B)

Contact person: M. Veronica Ganduglia-Pirovano (pirovano@fhi-berlin.mpg.de)

Indium incorporation and surface segregation during InGaN growth by molecular beam epitaxy

Huajie Chen, R. M. Feenstra
Department of Physics, Carnegie Mellon University, Pittsburgh, Pennsylvania 15213, USA
J. E. Northrup
Xerox Palo Alto Research Center, 3333 Coyote Hill Road, Palo Alto, California 94304, USA
J. Neugebauer
Fritz-Haber-Institut der Max-Planck-Gesellschaft, Faradayweg 4–6, 14195 Berlin-Dahlem, Germany
D. W. Greve
Department of Electrical and Computer Engineering, Carnegie Mellon University, Pittsburgh, Pennsylvania 15213, USA

Abstract

InGaN alloys with (0001) or (000-1) polarities are grown by plasma-assisted molecular beam epitaxy. Scanning tunneling microscopy images, interpreted using first-principles theoretical calculations, show that there is strong indium surface segregation on InGaN for both (0001) and (000-1) polarities. The dependence on growth temperature and group III/V ratio of indium incorporation in InGaN is reported, and a model based on indium surface segregation is proposed to explain the observations.

(submitted to: Mat. Res. Soc. Proc.)
Contact person: Jörg Neugebauer (neugebauer@fhi-berlin.mpg.de)

Stability, diffusion, and complex formation of beryllium in wurtzite GaN

Sukit Limpijumnong, Chris G. Van de Walle
Xerox PARC, Palo Alto, CA 94304, USA
J. Neugebauer
Fritz-Haber-Institut der Max-Planck-Gesellschaft, Faradayweg 4–6, 14195 Berlin-Dahlem, Germany

Abstract

We have studied the properties of Be dopants in GaN using first principles calculations. Substitutional Be on a Ga site acts as an acceptor, but interstitial Be poses a potential problem because of its low formation energy and donor character. We study the diffusion of interstitial Be and find it to be highly anisotropic. We also study the formation of complexes between substitutional and interstitial Be, and between substitutional Be and hydrogen. We have calculated the Be-H vibrational modes to aid in experimental identification of such complexes.

(submitted to: Mat. Res. Soc. Proc.)
Contact person: Jörg Neugebauer (neugebauer@fhi-berlin.mpg.de)

First-principles studies of beryllium doping of GaN

Chris G. Van de Walle, Sukit Limpijumnong
Xerox PARC, Palo Alto, CA 94304, USA
J. Neugebauer
Fritz-Haber-Institut der Max-Planck-Gesellschaft, Faradayweg 4–6, 14195 Berlin-Dahlem, Germany

Abstract

The structural and electronic properties of beryllium substitutional acceptors and interstitial donors in GaN are investigated using first-principles calculations based on pseudopotentials and density functional theory. In p-type GaN, Be interstitials, which act as donors, have formation energies comparable to substitutional Be on the Ga site, which is an acceptor. In thermodynamic equilibrium, incorporation of Be interstitials will therefore result in severe compensation. To investigate the kinetics of Be interstitial incorporation and outdiffusion we have explored the total-energy surface. The diffusivity of Be interstitials is highly anisotropic, with a migration barrier in planes perpendicular to the c-axis of 1.2 eV, while the barrier for motion along the c-axis is 2.9 eV. We have also studied complex formation between interstitial donors and substitutional acceptors, and between hydrogen and substitutional beryllium. The results for wurtzite GaN are compared with those for the zincblende phase. Consequences for p-type doping using Be acceptors are discussed.

(submitted to: Phys. Rev. B)
Contact person: Jörg Neugebauer (neugebauer@fhi-berlin.mpg.de)

Modeling of Structural and Elastic Properties of $In_{1-x}Ga_xN$ Alloys

Frank Grosse
HRL Laboratories, 3011 Malibu Canyon Road, Malibu, CA 90265, USA
J. Neugebauer
Fritz-Haber-Institut der Max-Planck-Gesellschaft, Faradayweg 4–6, 14195 Berlin-Dahlem, Germany

Abstract

$In_{1-x}Ga_xN$ alloys are investigated by combining density-functional theory (DFT) calculations and an extended valence force field model (VFF). Based on a large number of ordered $In_{1-x}Ga_xN$ supercells we determined the accuracy of various valence force field models with respect to *ab initio* DFT calculations. To get the correct energy difference between the stable wurtzite and the metastable zincblende phase the inclusion of the ion-ion-interaction within the VFF model was necessary. As a direct consequence the inequivalent bonds of the wurtzite structure including the non-ideal c/a ratio and internal u parameter are described correctly. The wurtzite phase is found to be stable against the zincblende phase for all concentrations.

(submitted to: MRS Symposia Proc.)
Contact person: Jörg Neugebauer (neugebauer@fhi-berlin.mpg.de)

Magnetic $4d$ monoatomic rows on Ag vicinal surfaces

V. Bellini, N. Papanikolaou, R. Zeller and P. H. Dederichs
Institut für Festkörperforschung, Forschungszentrum Jülich, D-52425 Jülich, Germany

Abstract

The magnetic properties of $4d$ monoatomic rows on Ag substrates have been studied by *ab initio* calculations using the Screened Korringa-Kohn-Rostoker (SKKR) Green's Functions method within Density Functional Theory (DFT) in its Local Spin Density approximation (LSDA). The rows were placed at step edge (step decoration) and on terrace positions of different vicinal Ag surfaces, i.e. *fcc* (711), *fcc* (410) and *fcc* (221). The results for the magnetic moments are explained in terms of the different coordination number of the row atoms and the different hybridization between the rather extended $4d$ orbitals of the row atoms and the *sp*-like valence electrons of the Ag substrates. For the *fcc* (711) vicinal surface, we explore the possibility of antiferromagnetic coupling between the atoms in each row and discuss, by means of total energy calculations, the stability of the antiferromagnetic solutions with respect to the ferromagnetic ones.

(Accepted for publication in Phys. Rev. B)
Manuscripts available from: N.Papanikolaou@fz-juelich.de

10 Book Announcement

Performance Optimization of Numerically Intensive Codes

Stefan Goedecker

Département de recherche fondamentale sur la matière condensée,

SP2M/NM, CEA-Grenoble, 38054 Grenoble cedex 9, France

The increase of the speed of computers has been following Moore's law for many years now and therefore the present day computers are many times faster than just a few years ago. Because of this development the computing and simulation capabilities have already become rather impressive making this discipline the third pillar of today's scientific investigations, next to such traditional pillars as theory and experiment. Nevertheless, as any practitioner in the field knows, there exists an insatiable demand for even more computational power. For many computational problems that we would like to solve the CPU time is really the only limiting factor. For these reasons it is of utmost importance to get the best possible performance from the hardware that is at our disposal nowadays. Obtaining a large fraction of the theoretical peak speed of the hardware can not be taken for granted. As a matter of fact many computational scientists do not even know how close their program gets to the possible peak speed of their computer. Measuring the speed of their program frequently reveals that it runs at less than 10 percent of this peak speed. Obtaining a significantly higher fraction of the peak speed requires more than Fortran or C programming knowledge.

Our new optimization book (**S. Goedecker, A. Hoisie: "Performance Optimization of numerically intensive codes", SIAM publishing company, Philadelphia, USA 2001 (ISBN 0-89871-484-2), http://www.siam.org/catalog/mcc12/se12.htm**)

aims at providing any computational scientist with exactly the knowledge necessary to write efficient programs that will run at the highest possible speed. It starts with a chapter on basic notions of computer architecture. Since our intended audience is not computer scientists we restrict ourselves to the minimum information necessary for optimization purposes and we present the material in a way that is accessible to a physicist, chemist, biologist or engineer. Before describing optimization techniques we still first introduce different timing and performance monitoring techniques. The optimization part is then subdivided into the optimization of floating point operations and the optimization of memory access. We mainly concentrate on the most popular RISC type architectures, but also treat briefly vector machines. The memory

access optimization is the most important point on RISC architectures. Apparently small modifications can lead to amazingly large changes in performance. The most elementary example is a matrix copy. Due to better cache use the loop order

```
        do j=1,n
        do i=1,n
10      a(i,j)=b(i,j)
```

is more than 10 times faster for large matrices compared to the inverse loop order

```
        do i=1,n
        do j=1,n
10      a(i,j)=b(i,j) .
```

After this part on serial optimization a chapter on optimization techniques for parallel machines follows. The book ends with several case studies that were taken mainly from electronic structure codes such as full and sparse matrix vector multiplications, wavelet transforms, Fast Fourier transforms, loops from a Configuration Interaction program and multigrid algorithms. These examples demonstrate that it is not unusual to speed up a program by a factor of 5 by these techniques even when starting from a reasonable version of the program. In most cases the optimization involves modifications in the data structures. Since changing data structures in an existing code can be cumbersome, we recommend to give a lot of thought to the layout of the data structures at the earliest possible stage of program development. Optimization should so to say start before writing a program.

In addition to presenting various optimization techniques the book also critically examines the strong and weak points of commercial hard- and software. Thus, the knowledge contained in this book will also be helpful, for example, in making decisions when buying computer hardware. Concerning software, one pervasive theme of the book is to point out what the possibilities and limits of optimizing compilers are.

In conclusion, we hope that this book, by bridging a gap between the computer science and numerical mathematics literature, will contribute to educating the computational science community about these frequently neglected issues that are important for the scientific progress in our field.

11 SCIENTIFIC HIGHLIGHT OF THE MONTH

Third-generation MTOs

O. K. Andersen, T. Saha-Dasgupta, S. Ezhov, L. Tsetseris, O. Jepsen,
R.W. Tank, C. Arcangeli, and G. Krier
Max-Planck Institute für Festkörperforschung, D-70569, Stuttgart, Germany

Abstract

The 3rd-generation muffin-tin orbital formalism is reviewed and illustrated by applications to tetrahedrally coordinated semiconductors and high-temperature superconductors.

Introduction

Muffin-tin orbitals (MTOs) have been used for a long time in *ab initio* calculations of the electronic structure of condensed matter. Over the years, several MTO-based methods have been developed. The ultimate aim is to find a generally applicable electronic-structure method which is *intelligible, fast,* and *accurate.* Our recent progress in that direction will be reported in the present Highlight.

In order to be *intelligible* an electronic-structure method should, in our opinion, employ a *minimal* and *flexible* basis of *short-ranged* orbitals. As an example, the method should be able to describe the valence electrons in *sp*-bonded materials using merely four short-ranged *s*- and *p*-orbitals per atom and, for insulating phases, using merely *occupied* orbitals such as bond orbitals. Another example is materials with strong electronic correlations. For such materials, one must first construct a realistic Hamiltonian, and this requires an accurate single-particle basis which can be partitioned into correlated and non-correlated orbitals, without introducing too many of the former. A flexible basis of short-ranged orbitals is thus asked for. The method should, in other words, enable the user to construct a first-principles, solvable Hamiltonian for the problem at hand.

Now, a small basis of short-ranged orbitals is a prerequisite for a method to be *fast,* but it may be a hindrance for the *accuracy,* because the orbitals of a smaller basis are in general more complicated than those of a larger basis.

Most other *ab initio* methods, such as plane-wave pseudopotential, LAPW, PAW, and LCAO methods, aim at *simulation,* and are therefore primarily *accurate* and *robust.* But they are neither fast nor intelligible in the above-mentioned sense, because they employ basis sets with about hundred functions per atom. *Understanding* is therefore attempted *after* the calculation, by means of projections onto *e.g.* charge densities, electron-localization functions (ELFs), partial waves, Wannier functions in case of insulators, a.s.o.

In this Highlight we start by explaining broadly what 3rd-generation MTOs are and, by the examples of diamond-structured Si and the CuBr - Ge series, demonstrate that they are intelligible and accurate.

Next, we sketch the formalism, which is essentially the multiple-scattering formalism of Korringa, Kohn, and Rostoker (KKR) [1] with the following three extensions: (1) Exact *screening* transformations are introduced to reduce the spatial range and the energy dependence -or the dimension- of the structure matrix. (2) The formalism is proved to hold for *overlapping* MT potentials, to leading order in the potential-overlap. (3) Energy-independent MTO basis sets are derived which span the solutions $\Psi_i(\mathbf{r})$ with energies ε_i of Schrödinger's equation to within errors proportional to $(\varepsilon_i-\epsilon_0)(\varepsilon_i-\epsilon_1)..(\varepsilon_i-\epsilon_N)$, where $\epsilon_0,\epsilon_1,...,\epsilon_N$ is a chosen energy mesh. By virtue of the variational principle, the errors of the energies ε_i are then proportional to $(\varepsilon_i-\epsilon_0)^2(\varepsilon_i-\epsilon_1)^2..(\varepsilon_i-\epsilon_N)^2$. To work with a discrete energy mesh and divided, finite differences is far more flexible and accurate than working with a condensed mesh and energy derivatives, as was the case for the linear (N=1) MTO (LMTO) methods of the 1st- and 2nd-generation. Moreover, in those methods the partial waves inside the MT-spheres were treated to linear order, but the wave function in the interstitial was treated merely to zeroth order. For the MTOs of the 3rd-generation, the MT-spheres and the interstitial regions are treated on the same footing like in the KKR method, because only in that case is there an elegant and efficient way of treating downfolding and overlapping MT-potentials. This, however, causes the expansion energies ϵ_n to be *global* parameters, independent of the *Rl*-channel, and that is why we often need to go beyond *linear* methods. Descriptions of how we expand the charge density locally in screened spherical waves and of how the overlapping MT-potential, which defines the MTO basis set, is derived from the full potential, lie outside the scope of the present Highlight, but we refer to previous [2, 3, 4, 5] and coming [6] publications. Moreover, our production code for those parts of the new method is still under construction [7]. The overlapping-potential feature of the present formalism has been taken up also by Vitos et al. [8] in Green-function calculations for closely-packed alloys with the usual cell-projection technique for the charge density.

In the final section we demonstrate how 3rd-generation MTOs have been used to discover the material-dependent trend in the band structures of the hole-doped high-temperature superconductors and its correlation with the maximum T_c [9].

Most readers would presumably look at merely the first and the last sections, skipping the heavy middle part about the formalism. For the rare person who might want to know more, we refer to the original papers [2, 3, 4, 5, 10].

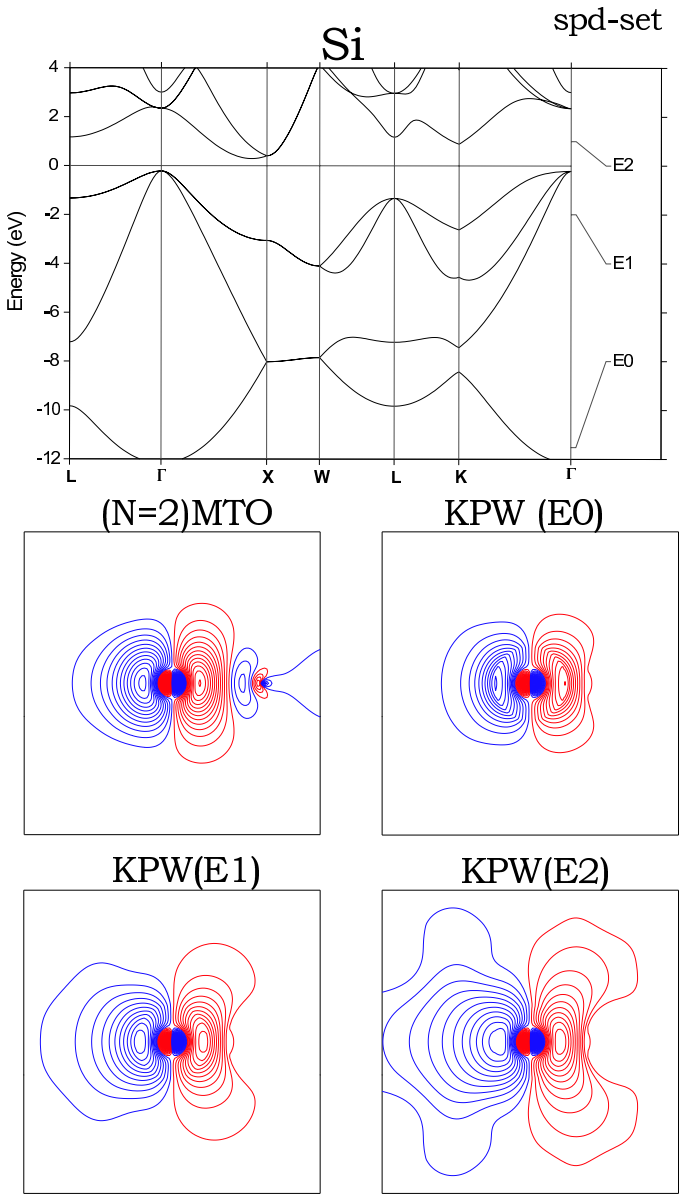

Figure 1: Band structure of Si calculated with the Si *spd*-QMTO basis set corresponding to the energy mesh shown on the right-hand side. The contour plots show the Si p orbital pointing in the [111]-direction between two nearest neighbors in the $(1\bar{1}0)$-plane. Shown are the kinked partial waves (KPWs) at the three energies and the QMTO. The KPWs are normalized to one, times a cubic harmonics, at the central hard sphere [see Eqs. (14 and (21)]. The contours are the same in all plots. See text.

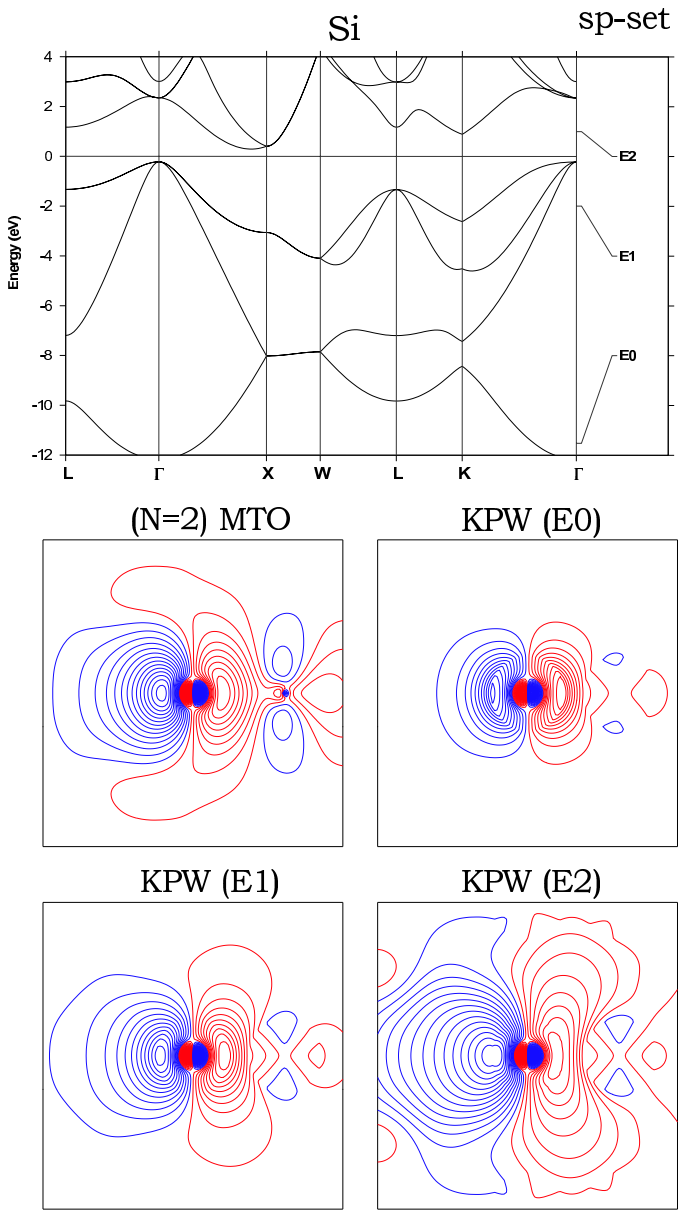

Figure 2: Same as Fig.1, but for the Si *sp*-set.

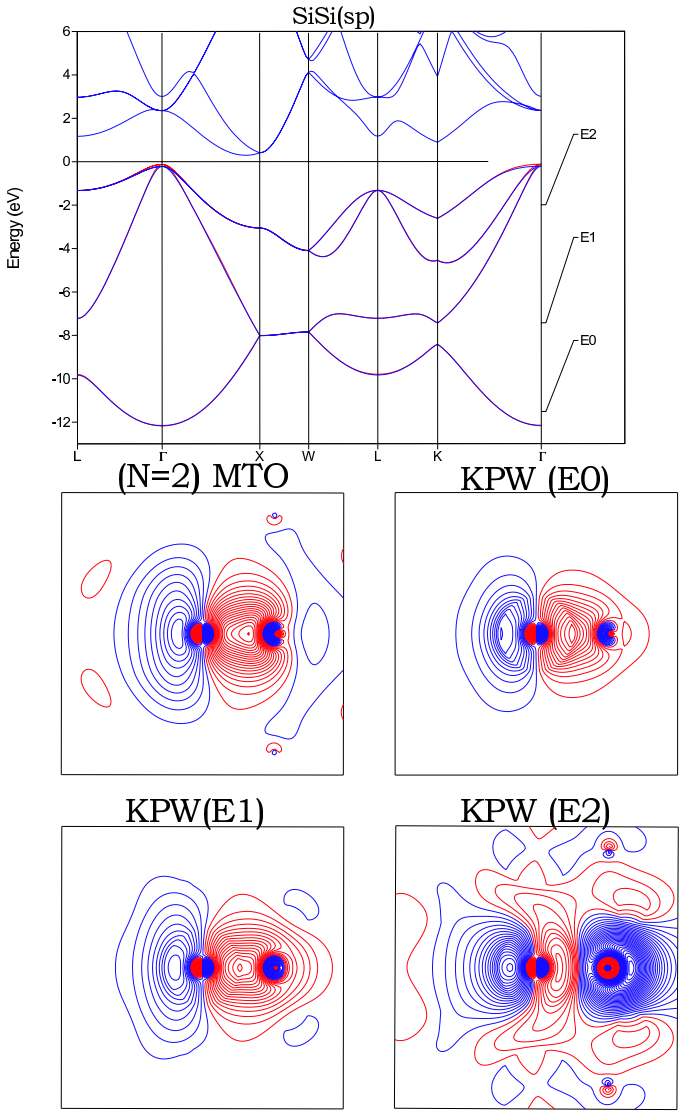

Figure 3: Same as Figs. 1-2, but for the Si(sp)Si-set with sp-QMTOs on merely every second Si atom, the one seen to the left in the figure. The red valence bands are obtained with this 'ionic' $Si^{4-}Si^{4+}$ basis. The blue, stippled bands are the ones from Fig. 1.

Illustrations for tetrahedrally-bonded semiconductors

At the top of Fig. 1 we show the LDA energy bands $\varepsilon_i(\mathbf{k})$ of Si in the diamond structure, calculated with the basis set of Si-centered s-, p-, and d-MTOs (9 orbitals/atom) for the energy mesh ϵ_0, ϵ_1, ϵ_2 indicated on the right-hand side. These bands have meV-accuracy for the MT-potential used for their construction, which in the present case was the standard all-electron, Si_2E_2 atomic-spheres potential. With three energy points, the MTOs are of order N=2, that is, they are *quadratic* MTOs, so-called QMTOs.

The p-QMTO pointing along [111], from one Si to its nearest neighbor, is shown in the $(1\bar{1}0)$-plane by the first contour plot. This orbital is localized and smooth with a few wiggles at the nearest neighbor. The remaining three contour plots show the major constituents of this p_{111}-QMTO: The p_{111}-*kinked partial wave* (KPW) at the central site for the three energies. In

general, the NMTOs for the energy mesh $\epsilon_0, ..., \epsilon_N$ are superpositions:

$$\chi^{(N)}_{R'L'}(\mathbf{r}) = \sum_{n=0}^{N} \sum_{RL \in A} \phi_{RL}(\epsilon_n, \mathbf{r})\; L^{(N)}_{nRL,R'L'}\,, \tag{1}$$

of the kinked partial waves, $\phi_{RL}(\varepsilon, \mathbf{r})$, at the $N+1$ points of the energy mesh. In the present case, the L=lm-summation is over the s-, p-, and d-KPWs, and the R-summation is over the Si sites, that is, over mainly the nearest neighbors, as a comparison between the contour plots of the QMTO and the KPWs should reveal. These RL-values, for which we have MTOs in the basis set, we call the *active* (A) ones.

A KPW is basically a *partial wave with a tail* joined continuously to it with a *kink* at a central, so-called hard sphere of radius a_R. This kink is seen in the contour plots, and most clearly for the lowest energy, ϵ_0. As usual, the partial wave $\varphi_{Rl}(\varepsilon, r_R)\, Y_L(\hat{\mathbf{r}}_R)$, where $r_R \equiv |\mathbf{r} - \mathbf{R}|$ and $\hat{\mathbf{r}}_R \equiv \widehat{\mathbf{r} - \mathbf{R}}$, is a product of a spherical (or cubic) harmonic and a regular solution with energy ε of the radial Schrödinger equation,

$$-\left[r\varphi_{Rl}(\varepsilon, r)\right]'' = \left[\varepsilon - v_R(r) - l(l+1)/r^2\right] r\varphi_{Rl}(\varepsilon, r)\,, \tag{2}$$

for the potential $v_R(r)$ of the MT-well at $\mathbf{R}$. The tail of the kinked partial wave is a so-called *screened spherical wave* (SSW), $\psi_{RL}(\varepsilon, \mathbf{r})$, which is essentially the solution with energy ε of the wave equation in the interstitial between the hard spheres, $-\Delta\psi(\varepsilon, \mathbf{r}) = \varepsilon\psi(\varepsilon, \mathbf{r})$, satisfying the boundary condition that, independent of the energy, $\psi_{RL}(\varepsilon, \mathbf{r})$ go to $Y_L(\hat{\mathbf{r}}_R)$ at the central hard sphere and to *zero* (with a kink) at all other hard spheres. It is this latter confinement, easily recognized in the KPW contour plots, particularly at the highest energy ϵ_2, which makes the KPW localized, when the energy is not too high. At the same time, it makes the KPW have pure L-character at the central sphere only, because outside it is influenced by the hard spheres centered at the neighbors. The default value of the hard-sphere radii is 90 per cent of the covalent, atomic, or ionic radius, whichever is appropriate.

The kinked partial wave thus has a kink, not only at its own, but also at the neighboring hard spheres, inside which it essentially vanishes. 'Essentially' because the above-mentioned boundary condition only applies to the active components of the spherical-harmonics expansions of the SSW on the hard spheres. For the *passive* components, in the present case the Si f- and higher components, as well as all components on empty (E) spheres, the SSW equals the corresponding partial-wave solution of Schrödinger's equation throughout the MT-sphere. The small bump seen in the lowest contour along the [111]-direction is caused by the slight f-character on the nearest neighbor.

In the valence and lowest conduction bands of Si there are only s- and p-, but no d-electrons. We should therefore be able to use a basis with only Si s- and p-MTOs, that is, with only 4 orbitals per atom. In the language used above, we thus let the Si s- and p-partial waves remain active, while the Si d-waves are included among the passive ones, *i.e.* those 'folded down' into the SSW-tails of the active KPWs. The results for the bands and the p_{111}-QMTO are shown in Fig. 2. These bands are indistinguishable from those obtained with the Si *spd*-set, on the scale of the figure, although between the energies of the mesh, the bands obtained with the *sp*-set do lie slightly above those obtained with the *spd*-set. However, by making the mesh denser (increasing N), the accuracy can be increased arbitrarily. The KPW of the *sp*-set is seen to

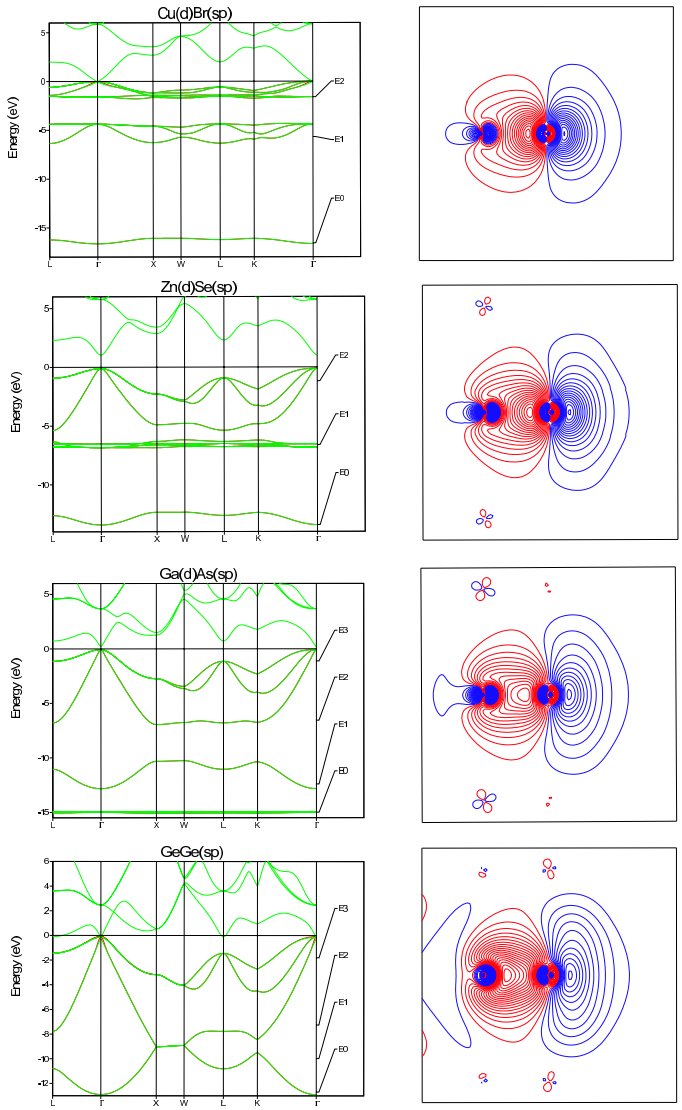

Figure 4: Valence bands (red) of the series CuBr – Ge, calculated with the ionic basis sets where the *sp*-MTOs are on the anion and, except for Ge, the *d*-MTOs are on the cation. The contour plots show the p_{111}-MTO on the anion (the atom to the right). From top to bottom, the ionicity decreases and the covalency increases.

have d-character on the nearest Si neighbor, and the QMTO and the KPW, particularly the one at the highest energy, are seen to be somewhat less localized than those for the spd-set.

It is even possible to construct an arbitrarily accurate MTO-basis which spans merely the *occupied* orbitals, that is, which spans the valence band with a basis of merely 2 orbitals per atom. An advantage of this is that the sum of the one-electron energies might be calculated in real space, without diagonalization, as the trace of the Hamiltonian, using the MTO orthonormalization procedure described in Sect. 5 of Ref. [5]. This is a method where the amount of computation increases merely linearly with the size of the system (or cell), a so-called *order*-N *method* (Here, N refers to the number of atoms in the system, not the order N of the MTOs). For covalent semiconductors like Si it is customary to take the valence-band orbitals as the bond-orbitals, which are the bonding linear combinations of the directed sp^3-hybrids of orthonormal MTOs. It is, however, far simpler and more general, *e.g.* not limited to elemental semiconductors and tetrahedral structures, to take the valence-band orbitals as the s- and p-MTOs on *every second* Si atom, all partial waves on the nearest neighbors being downfolded. This corresponds to an *ionic* description, $Si^{4-}Si^{4+}$. As Fig. 3 shows, this QMTO-set describes merely the valence band and it does so surprisingly well, considering the fact that the two silicons are treated differently so that the degeneracy along the XW-line is slightly broken. The error between the energy points is proportional to $[\varepsilon_i(\mathbf{k}) - \epsilon_0][\varepsilon_i(\mathbf{k}) - \epsilon_1][\varepsilon_i(\mathbf{k}) - \epsilon_2]$, like for the basis with 4 orbitals per atom shown in Fig. 2 because we used QMTOs in both cases, but the prefactors are larger for the smaller basis. This comes from the longer range and the concomitant stronger energy dependence of the KPWs as the number of active channels decreases. However, by making the mesh finer, the errors can be made arbitrarily small. In the present case, the basis with 2 *cubic* MTOs (CMTOs) per atom turns out to yield energies with about the same accuracy as the basis with 4 QMTOs per atom. After orthonormalization of this ionic valence-band set, the sum of the one-electron energies may be calculated as the trace of the Hamiltonian. The directed sp^3-hybrids formed from these orbitals actually look like bond orbitals. Since the ionic Si(sp)Si-set gives the occupied states in diamond-structured Si with arbitrary accuracy, the same procedure with the sp-orbitals placed exclusively on the *anion* (but with the d-orbitals on the cation), will of course work for any IV-IV, III-V, II-VI, and I-VII semiconductor and insulator. This is illustrated in Fig. 4. Such *ionic* MTO *basis sets* which 'automatically' span the occupied, and no further, states of any non-metal could make density-functional molecular-dynamics calculations highly efficient for such systems.

As an example of a minimal set spanning all states in a *wide* energy range, we show in Fig. 5 for GaAs the LDA valence and conduction bands, 18 of which fall in the 35 eV-range displayed. The dotted bands were calculated variationally using a basis of Ga spd- and As $spdf$-QMTOs. The good accuracy obtained with this basis of merely 25 orbitals per cell demonstrates the power of the NMTO method. Note that *no* principal quantum numbers were needed, even for this large energy range which includes the Ga $3d$ semi-core band at -15 eV. This NMTO representation should be useful for computing excited-state properties, *e.g.* with the GW method [11]. For calculating x-ray dichroism spectra of magnetic materials, a relativistic spin-polarized version of the NMTO method has been developed [12].

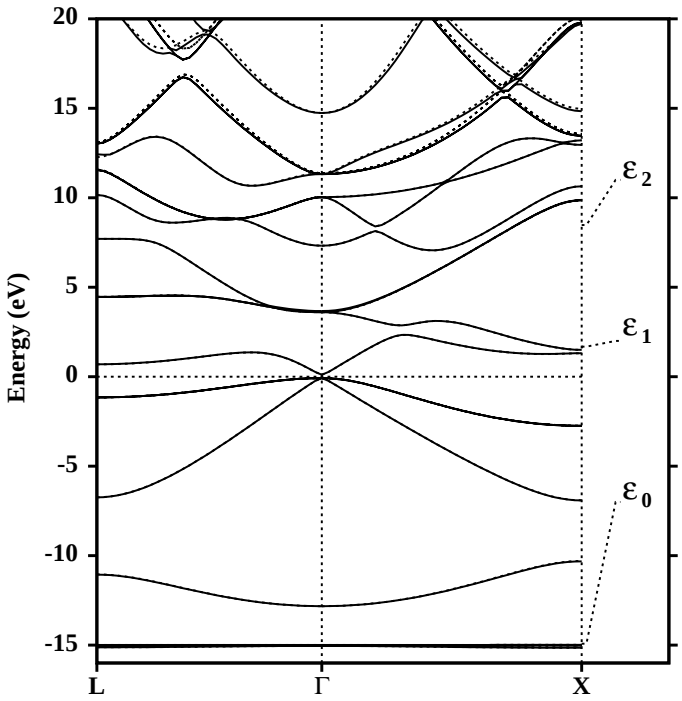

Figure 5: Band structure of GaAs over a wide energy range, calculated with the QMTO method and the energy mesh indicated on the right-hand side (dashed), compared with the exact result (solid).

Formalism

In this section we review the formalism behind the illustrations in Figs. 1-5. We first consider the tail-functions, the screened spherical waves.

Screened spherical waves (SSWs)

The screened spherical wave at site R' and with angular momentum L' at the own hard sphere is a linear combination of *bare* spherical waves:

$$n^{\alpha}_{R'L'}(\varepsilon,\mathbf{r}) = \sum_{RL\in A} n_l(\kappa r_R)\, Y_L(\hat{\mathbf{r}}_R)\; X^{\alpha}_{RL,R'L'}(\varepsilon) \equiv \sum_{RL\in A} n^0_{RL}(\varepsilon,\mathbf{r})\; X^{\alpha}_{RL,R'L'}(\varepsilon)\,, \qquad (3)$$

whose radial parts we have here written as spherical Neumann functions, rather than decaying Hankel functions, because we want to keep the notation of scattering theory although the energies ($\kappa^2 \equiv \varepsilon$) of the valence band are mostly negative when we use overlapping MT-spheres. The screening transformation $X^{\alpha}(\varepsilon)$ is determined by the hard-sphere boundary condition and the superscripts α refer to the choice of hard spheres, as well as the normalization as will later become evident. Finally, we have written n^{α} instead of ψ^{α}, because in (3) we have not yet truncated the active components and augmented the passive ones. In order to determine $X^{\alpha}(\varepsilon)$ in such a way that $n^{\alpha}(\varepsilon,\mathbf{r})$ fits the boundary conditions, we need to expand $n^{\alpha}_{R'L'}(\varepsilon,\mathbf{r})$ in spherical-harmonics around all sites. For this, we have the well-known expansion:

$$n_l(\kappa r_R)\, Y_L(\hat{\mathbf{r}}_R) = \sum_{\bar{L}} j_{\bar{l}}(\kappa r_{\bar{R}})\, Y_{\bar{L}}(\hat{\mathbf{r}}_{\bar{R}})\; \kappa^{-1} B^0_{\bar{R}\bar{L},RL}(\varepsilon)\,, \qquad (4)$$

of the *bare* spherical wave at site R in spherical harmonics around another site $\bar{R}$. The expansion coefficients are spherical Bessel functions times

$$\kappa^{-1} B^0_{\bar{R}\bar{L},RL}(\varepsilon) \equiv \sum_{l'} 4\pi\, i^{-l+\bar{l}-l'} C_{L\bar{L}l'}\, n_{l'}(\kappa\,|\mathbf{R}-\bar{\mathbf{R}}|)\; Y^*_{l'(\bar{m}-m)}\left(\widehat{\mathbf{R}-\bar{\mathbf{R}}}\right), \tag{5}$$

where $B^0_{\bar{R}\bar{L},RL}(\varepsilon)$ are the bare KKR structure constants as they are usually defined, albeit in real space. $C_{L\bar{L}l'} \equiv \int Y_L(\hat{\mathbf{r}})\, Y^*_{\bar{L}}(\hat{\mathbf{r}})\, Y_{l'(\bar{m}-m)}(\hat{\mathbf{r}})\, d\hat{\mathbf{r}}$ are the Gaunt coefficients. We now define an on-site block as zero, $B^0_{R\bar{L},RL}(\varepsilon) \equiv 0$, and name $B^0(\varepsilon)$ the bare *structure matrix,* which is Hermitian. It is convenient to write the expansion (4) of the *bare* spherical waves, for any R' and $\bar{R}$ including R'=$\bar{R}$, symbolically as:

$$n^0(\varepsilon,\mathbf{r}) = j(\varepsilon,\mathbf{r})\,\kappa^{-1} B^0(\varepsilon) + n(\varepsilon,\mathbf{r}) \tag{6}$$

where capitals denote matrices (*e.g.* B^0), and lower case letters denote vectors (*e.g.* $j(\varepsilon,\mathbf{r})$) or diagonal matrices (*e.g.* $\kappa^{-1}\tan\alpha(\varepsilon)$), specifically numbers (*e.g.* κ). The spherical-harmonics expansions for the *screened* spherical wave, we write in the analogous way:

$$n^\alpha(\varepsilon,\mathbf{r}) = j^\alpha(\varepsilon,\mathbf{r})\,\kappa^{-1} B^\alpha(\varepsilon) + n(\varepsilon,\mathbf{r}), \tag{7}$$

where $j^\alpha(\varepsilon,\mathbf{r}) \equiv j^\alpha_{RL}(\varepsilon,r)\, Y_L(\hat{\mathbf{r}})$ and the radial function is that linear combination,

$$j^\alpha_{RL}(\varepsilon,r) \equiv j_l(\kappa r) - n_l(\kappa r)\tan\alpha_{RL}(\varepsilon), \tag{8}$$

which satisfies the partial boundary condition: For any active component this is that $j^\alpha_{RL}(\varepsilon,r)$ should vanish at the hard sphere so that we can substitute that radial component of $n^\alpha(\varepsilon,\mathbf{r})$ continuously inside the hard sphere by zero. For any passive component this is that $j^\alpha_{RL}(\varepsilon,r)$ should match (have the same radial logarithmic derivative as) the radial Schrödinger solution, $\varphi_{Rl}(\varepsilon,r)$ given by (2), so that we can substitute that radial component of $n^\alpha(\varepsilon,\mathbf{r})$ continuously and differentiably by $\varphi_{Rl}(\varepsilon,r)$. With these substitutions, $n^\alpha_{RL}(\varepsilon,\mathbf{r})$ becomes the SSW, *i.e.,* we might write: $\psi^\alpha_{RL}(\varepsilon,\mathbf{r}) \equiv \tilde{n}^\alpha_{RL}(\varepsilon,\mathbf{r})$ with the tilde denoting the substitutions. In conclusion, $\alpha_{RL}(\varepsilon)$ is the hard-sphere phase-shift for RL active (A) and the real, potential-dependent phase-shift for RL passive (P):

$$\alpha_{RL}(\varepsilon) = \begin{cases} \arctan\{j_l(\kappa a_R)/n_l(\kappa a_R)\} & \text{for} \quad RL \in A \\ \eta_{Rl}(\varepsilon) & \text{for} \quad RL \in P \end{cases}. \tag{9}$$

Due to the presence of the centrifugal potential in the radial Schrödinger equation (2), we have: $\lim_{l\to\infty}\eta_l(\varepsilon) = 0$, and this ensures that the L-dimension of the matrices dealt with in the multiple-scattering formalism is finite, *i.e.* $\max l \sim 3$. The passive partial waves with non-zero phase-shifts we call *intermediate* (I).

The subscript RL, rather than Rl, on α and $j^\alpha(\varepsilon,r)$ takes into consideration that downfolding can be m-dependent, *e.g.* for the cuprates to be considered in the following section the conduction-band orbital is Cu $d_{x^2-y^2}$ with all other partial waves downfolded.

We finally need to express the *screening transformation,* $X^\alpha(\varepsilon)$, and the *screened structure matrix,* $B^\alpha(\varepsilon)$, in terms of the bare structure matrix given analytically by (5). We thus expand

each term of the linear combination (3) in spherical-harmonics using (6), and compare with (7) using (8):

$$n^{\alpha}(\varepsilon,\mathbf{r}) = \left\{ \begin{array}{lcl} n^{0}(\varepsilon,\mathbf{r})\, X^{\alpha}(\varepsilon) & = & j(\varepsilon,\mathbf{r})\,\kappa^{-1}B^{0}(\varepsilon)\, X^{\alpha}(\varepsilon) \;+\; n(\varepsilon,\mathbf{r})\, X^{\alpha}(\varepsilon) \\ j^{\alpha}(\varepsilon,\mathbf{r})\,\kappa^{-1}B^{\alpha}(\varepsilon) + n(\varepsilon,\mathbf{r}) & = & j(\varepsilon,\mathbf{r})\,\kappa^{-1}B^{\alpha}(\varepsilon) + n(\varepsilon,\mathbf{r})\left[1-\kappa^{-1}\tan\alpha(\varepsilon)\, B^{\alpha}(\varepsilon)\right] \end{array} \right.$$

As a result:

$$X^{\alpha}(\varepsilon) \;=\; 1-\kappa^{-1}\tan\alpha(\varepsilon)\, B^{\alpha}(\varepsilon)\,, \quad \text{where} \quad B^{\alpha}(\varepsilon)^{-1} \;=\; B^{0}(\varepsilon)^{-1} + \kappa^{-1}\tan\alpha(\varepsilon)\,, \qquad (10)$$

or equivalently:

$$B^{\alpha}(\varepsilon) \;=\; \kappa\cot\alpha(\varepsilon) \;-\; \kappa\cot\alpha(\varepsilon)\left[\kappa\cot\alpha(\varepsilon) + B^{0}(\varepsilon)\right]^{-1}\kappa\cot\alpha(\varepsilon)\,. \qquad (11)$$

Note that B^{α} in contrast to B^{0} has on-site elements. The screened structure matrix (11) completely specifies the set of SSWs. Whereas the bare structure matrix (5) is long ranged and strongly energy-dependent, the hard-sphere confinement makes the screened structure matrix localized in real space and weakly energy-dependent. We generate $B^{\alpha}_{RL,R'L'}(\varepsilon)$ by matrix inversion for clusters in real space (R), and the L-dimension limited by $\max l$.

In fact, for charge-selfconsistent NMTO calculations it is more efficient to compute, once for a given structure, a *strongly* screened structure matrix $B^{\beta}(\varepsilon)$ defined by having *hard-sphere* phase-shifts not only for the active, but also for the intermediate channels, that is:

$$\beta_{RL}(\varepsilon) = \arctan\left\{j_{l}(\kappa a_{R})/n_{l}(\kappa a_{R})\right\} \quad \text{for} \quad l \leq \max l, \quad \textit{i.e.,}\ \text{for}\ RL \in A+I. \qquad (12)$$

The strongly screened scattered waves are basically *cellular functions,* as may be seen from the front-page picture of Ref. [2]. In case we deal with a crystal with lattice translations $\mathbf{T}$, the strongly screened structure matrix is Block-summed to

$$B^{\beta}_{RL,R'L'}(\varepsilon,\mathbf{k}) = \sum_{T}\exp(i\mathbf{k}\cdot\mathbf{T})\, B^{\beta}_{(\mathbf{R}+\mathbf{T})L,R'L'}(\varepsilon)\,.$$

Finally, the downfolded structure matrix $B^{\alpha}(\varepsilon)$, whose active block (A) will be used for solving Schrödinger's equation [see (19), (20), and (56)], is calculated in each iteration by partitioning:

$$B^{\alpha}_{AA}(\varepsilon) = B^{\beta}_{AA}(\varepsilon) - B^{\beta}_{AI}(\varepsilon)\left[\kappa\cot\eta_{I}(\varepsilon) + B^{\beta}_{II}(\varepsilon)\right]^{-1} B^{\beta}_{IA}(\varepsilon)\,. \qquad (13)$$

It may be noted that although screening (3) is a linear transformation of the set of $n^{\alpha}(\varepsilon,\mathbf{r})$-functions, it is *not* a linear transformation of the set of $\psi^{\alpha}(\varepsilon,\mathbf{r})$-functions due to their augmentation. This was not the case in the 2nd-generation formalism. Downfolding is a special case of a screening transformation; it turns out to be a linear transformation followed by truncation of the inactive channels.

Kinked partial waves (KPWs) and the screened KKR equations

We now come to specify the KPW which has the SSW as its tail and first return to the Si *sp*-set illustrated in Fig. 2. We cut the p_{111}-KPW along the [111]-line from the central Si atom through its nearest neighbor and half-way into the back-bond void. The result is shown by

the solid curve in Fig. 6 for an energy ε between ϵ_0 and ϵ_1. The kinks at the central and the nearest-neighbor a-spheres are clearly seen, and so is the downfolded d-character at the nearest neighbor. In fact, the KPW shown in Fig. 6 was not constructed from the Si_2E_2 potential used in Fig. 2, although it is indistinguishable from it on the scale of the figure, but from a potential $\sum_R v_R(r_R)$ where the spherically symmetric potential-wells $v_R(r)$ are centered exclusively on the atoms (no empty spheres) and have ranges s_R (=MT-radii) so large that the central MT-sphere in the present case reaches 3/4 the distance to the nearest-neighbor site. The overlap, defined as $\omega_{12} \equiv [(s_1 + s_2) / |\mathbf{R}_1 - \mathbf{R}_2|] - 1$, is thus 50 per cent. In Fig. 6 the extent of the *central* MT-well is indicated by s. This kind of potential, where the MT-spheres can be as fat as van der Waals spheres, we call an *overlapping* MT-potential.

In order to construct the KPW in Fig. 6, we integrate the radial Schrödinger equation (2) numerically from the origin all the way to s, obtaining the partial wave $\varphi_l(\varepsilon, r) Y_L(\hat{\mathbf{r}})$ shown by the dot-dashed curve. From here, we continue the integration *smoothly backwards* from s to a over the *flat* potential $[v(r) \equiv 0]$, obtaining the phase-shifted partial wave $\varphi_l^o(\varepsilon, r) Y_L(\hat{\mathbf{r}})$ shown by the dotted curve. $\varphi_l(\varepsilon, r)$ and $\varphi_l^o(\varepsilon, r)$ match in value and slope at s, but their curvatures, which are given by the radial Schrödinger equation (2), differ because $v(r)$ goes discontinuously to zero at s, *i.e.,* $v(s)$ is finite. At the central a-sphere, $\varphi_l^o(\varepsilon, r) Y_L(\hat{\mathbf{r}})$ is joined *continuously* but with a kink to the SSW, $\psi_{RL}^{\alpha}(\varepsilon, \mathbf{r})$, shown by the dashed curve. In terms of these contributions, the KPW shown by the solid curve is

$$\phi_{RL}^{\alpha}(\varepsilon, \mathbf{r}) \equiv [\varphi_{Rl}^{\alpha}(\varepsilon, r_R) - \varphi_{Rl}^{o\,\alpha}(\varepsilon, r_R)] Y_L(\hat{\mathbf{r}}_R) + \psi_{RL}^{\alpha}(\varepsilon, \mathbf{r}), \tag{14}$$

where $\varphi(r)$ is truncated for $r > s$ and $\varphi^o(r)$ is truncated for $r < a$ and $r > s$. The first term goes quadratically to zero at the MT-sphere:

$$\varphi_l(\varepsilon, r) - \varphi_l^o(\varepsilon, r) = \frac{1}{2}(s - r)^2 v(s) \varphi_l(\varepsilon, s) + o\left((s - r)^2\right), \tag{15}$$

and is therefore often called a *tongue.* The subscript α on φ and φ^o in (14) merely labels a normalization, which is such that the KPW is continuous. This implies that $\psi_{RL}^{\alpha}(\varepsilon, \mathbf{r})$ and $\varphi_l^o(\varepsilon, r) Y_L(\hat{\mathbf{r}})$ take the same value at the own sphere. The value of the former is $n_l(\kappa a_R) Y_L(\hat{\mathbf{r}}_R)$, according to (7) and the fact that $j_{RL}^{\alpha}(\varepsilon, a_R) \equiv 0$. As a consequence:

$$\varphi_{Rl}^{o\,\alpha}(\varepsilon, r) = \frac{n_l(\kappa a_R)}{j_{Rl}^{\eta}(\kappa a_R)} j_{Rl}^{\eta}(\kappa r) = \frac{j_l(\kappa r) - n_l(\kappa r) \tan \eta_{Rl}(\varepsilon)}{\tan \alpha_{RL}(\varepsilon) - \tan \eta_{Rl}(\varepsilon)} = n_l(\kappa r) - \cot \eta_{RL}^{\alpha}(\varepsilon) j_{RL}^{\alpha}(\varepsilon, r), \tag{16}$$

where we have used the definition (8) of j^{η} and j^{α}, and we have defined $\eta^{\alpha}(\varepsilon)$ as the phase shift with respect to the hard-sphere background:

$$\tan \eta_{RL}^{\alpha}(\varepsilon) \equiv \tan \eta_{Rl}(\varepsilon) - \tan \alpha_{RL}(\varepsilon). \tag{17}$$

We may finally use (7) to obtain the spherical-harmonics expansions of the KPW, valid at, and somewhat outside the hard spheres:

$$\begin{aligned} \phi^{\alpha}(\varepsilon, \mathbf{r}) &= \varphi^{\alpha}(\varepsilon, \mathbf{r}) - \varphi^{o\,\alpha}(\varepsilon, \mathbf{r}) + j^{\alpha}(\varepsilon, \mathbf{r}) \kappa^{-1} B^{\alpha}(\varepsilon) + n(\varepsilon, \mathbf{r}) \\ &= \varphi^{\alpha}(\varepsilon, \mathbf{r}) + j^{\alpha}(\varepsilon, \mathbf{r}) \kappa^{-1} [\kappa \cot \eta^{\alpha}(\varepsilon) + B^{\alpha}(\varepsilon)] \\ &\equiv \varphi^{\alpha}(\varepsilon, \mathbf{r}) + j^{\alpha}(\varepsilon, \mathbf{r}) \kappa^{-1} K^{\alpha}(\varepsilon). \end{aligned} \tag{18}$$

Here, we have used (16) and have defined a *screened KKR matrix,* with the elements

$$K^{\alpha}_{RL,R'L'}(\varepsilon) \;=\; \kappa\cot\eta^{\alpha}_{RL}(\varepsilon)\;\delta_{RR'}\delta_{LL'} \;+\; B^{\alpha}_{RL,R'L'}(\varepsilon)\,. \tag{19}$$

This, or its inverse, the so-called *scattering-path operator* $K^{\alpha}(\varepsilon)^{-1} \equiv G^{\alpha}(\varepsilon)$, is the central quantity of multiple-scattering and MTO theory. Comparison of (19) with (11) shows that, apart from additive and multiplicative normalizations, the screened structure matrix is the scattering-path operator for the repulsive potential specified by the phase-shifts (9).

From the expansions (18), it is intuitively clear, and the details will be discussed below in connection with Eq. (24), that any linear combination $\sum_{RL\in A}\phi^{\alpha}_{RL}(\varepsilon_i,\mathbf{r})\,c^{\alpha}_{RL,i}$ of KPWs, with the property that

$$\sum_{RL\in A} K^{\alpha}_{R'L',RL}(\varepsilon_i)\;c^{\alpha}_{RL,i} \;=\; 0, \quad \text{for all active } R'L', \tag{20}$$

is a solution $\Psi_i(\mathbf{r})$ with energy ε_i of Schrödinger's equation because the eigenvector $c^{\alpha}_{RL,i}$ leaves behind the partial-wave expansions $\sum_{RL}\varphi^{\alpha}_{RL}(\varepsilon_i,\mathbf{r})\,c^{\alpha}_{RL,i}$, which are solutions by construction. The linear, homogeneous equations (20) are the *screened KKR equations*, and the energy ε_i is determined by the condition that these equations have a proper solution, *i.e.* that $\det K^{\alpha}(\varepsilon_i) = 0$.

In order to get rid of the spurious $\sqrt{\varepsilon}$-dependences and to obtain a Hamiltonian formalism [see Eq. (29)], it is convenient to *renormalize* the SSW to have value $Y_L(\hat{\mathbf{r}})$ at its own hard sphere and, hence, to renormalize $\varphi^{o\,\alpha}_{Rl}(\varepsilon,r_R)$ to be unity for $r_R = a_R$, and to renormalize the partial wave and the KPW accordingly. Denoting these renormalized functions by the superscript a, which refers to hard-sphere radii rather than to hard-sphere phase-shifts α, we thus have:

$$\psi^{a}_{RL}(\varepsilon,\mathbf{r}) \equiv \frac{\psi^{\alpha}_{RL}(\varepsilon,\mathbf{r})}{n_l(\kappa a_{RL})}, \qquad \varphi^{o\,a}_{Rl}(\varepsilon,a_{RL}) \equiv 1, \quad \text{and} \quad \phi^{a}_{RL}(\varepsilon,\mathbf{r}) \equiv \frac{\phi^{\alpha}_{RL}(\varepsilon,\mathbf{r})}{n_l(\kappa a_{RL})}. \tag{21}$$

These are the normalizations used in all figures. The KKR matrix is renormalized to what we call the *kink matrix:*

$$K^{a}_{RL,R'L'}(\varepsilon) \;\equiv\; \frac{-K^{\alpha}_{RL,R'L'}(\varepsilon)}{\kappa n_l(\kappa a_R)\;\kappa n_{l'}(\kappa a_{R'})}, \tag{22}$$

which obviously remains Hermitian. The expansion (18), the Wronskian relation $j^{\alpha}(\varepsilon,a)' = -1/a^2\kappa n(\kappa a)$ with $' \equiv \partial/\partial r$, and the renormalizations (21) and (22) show that $K^{a}_{RL,R'L'}(\varepsilon)$ is the kink of $\phi_{R'L'}(\varepsilon,\mathbf{r})$ at the a_R-sphere, projected onto $Y_L(\hat{r}_R)/a_R^2$. The inverse of the kink matrix we call the *Green matrix:*

$$G^{a}(\varepsilon) \equiv K^{a}(\varepsilon)^{-1}\,. \tag{23}$$

In the following we shall always use this a-normalization, and since from now on we shall seldom change the screening, we usually drop the superscript a.

Due to its kinks, an individual KPW is not a solution of Schrödinger's equation, but any *smooth* linear combination of KPWs *is*. For coefficients $c_{RL,i}$ such that the kink in Fig. 6 between $\varphi^{o}_{R'l'}(\varepsilon_i,r_{R'})\,Y_{L'}(\hat{\mathbf{r}}_{R'})$ and $\psi_{R'L'}(\varepsilon_i,\mathbf{r})$ on the central sphere (R') is cancelled by the sum of the kinks from the tails of the KPWs on the neighbors, that is, for a solution of the kink-cancellation equations (20) (using a-normalization), we have:

$$\varphi^{o}_{R'l'}(\varepsilon_i,r_{R'})\,c_{R'L',i} = \mathcal{P}_{R'L'}\sum_{RL\in A}\psi_{RL}(\varepsilon_i,\mathbf{r})\,c_{RL,i}, \tag{24}$$

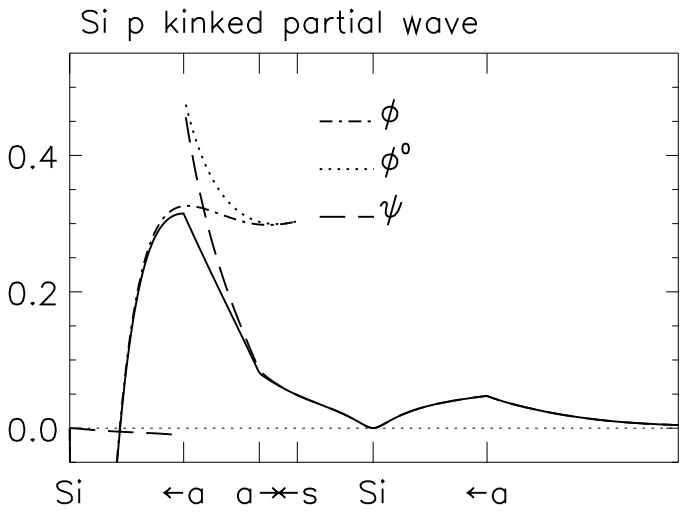

Figure 6: Si p_{111}-KPW for the Si sp-set and its constituents φY, $\varphi^o Y$, and ψ. The MT-potential used no empty spheres. s denotes the range of the central well. The a's indicate the hard spheres at the central and the nearest-neighbor sites.

where $\mathcal{P}_{R'L'}$ projects onto an active $Y_{L'}\left(\hat{r}_{R'}\right)$. This equation holds because both the left and the right-hand sides are solutions of the radial wave equation with the same value and slope at $a_{R'}$ and, hence, they are identical. With (24) satisfied, the KPW-definition (14) yields

$$\sum_{RL\in A}\phi_{RL}\left(\varepsilon_i,\mathbf{r}\right)c_{RL,i} \;=\; \sum_{l'=0}^{\infty}\sum_{m'=-l}^{l}\varphi_{R'l'}\left(\varepsilon_i,r_{R'}\right)Y_{L'}\left(\hat{\mathbf{r}}_{R'}\right)c_{R'L',i} + \sum_{R(\neq R')L\in A}\left[\varphi_{Rl}\left(\varepsilon_i,r_R\right)-\varphi^o_{Rl}\left(\varepsilon_i,r_R\right)\right]Y_L\left(\hat{\mathbf{r}}_R\right)c_{RL,i}, \tag{25}$$

for $\mathbf{r}$ inside a sphere, centered at $\mathbf{R}'$ and passing through the center of the nearest neighbor. In (25) the first term is a solution of Schrödinger's equation by construction and the l'-sum is infinite because the partial-wave expansions of the SSWs at the neighboring sites include passive as well as active partial waves. In the second term, $\varphi-\varphi^o$ vanishes outside its own MT-sphere, and this second term therefore vanishes outside all MT-spheres different from the central one. If the MT-spheres do not overlap, (25) therefore solves Schrödinger's equation exactly. If the potential-well from a neighboring site (R) *overlaps* the central site (R'), then the $\varphi_{RL}-\varphi^\circ_{RL}$ tongues (15) stick into the MT-sphere at R' and cause an error. To find its size, we operate with the Hamiltonian for the overlapping MT-potential,

$$\mathcal{H} \;\equiv\; -\nabla^2 \;+\; \sum_{R'}v_{R'}\left(r_{R'}\right)\;, \tag{26}$$

on the smooth function

$$\Psi_i\left(\mathbf{r}\right) \;\equiv\; \sum_{RL\in A}\phi_{RL}\left(\varepsilon_i,\mathbf{r}_R\right)c_{RL,i}, \tag{27}$$

of which (25) is the expansion around site R', and obtain:

$$\left(\mathcal{H}-\varepsilon_i\right)\Psi_i\left(\mathbf{r}\right) \;=\; \sum_{R'}v_{R'}\left(r_{R'}\right)\sum_{R(\neq R')L\in A}\left[\varphi_{Rl}\left(\varepsilon_i,r_R\right)-\varphi^\circ_{Rl}\left(\varepsilon_i,r_R\right)\right]Y_L\left(\hat{\mathbf{r}}_R\right)c_{RL,i} \tag{28}$$

$$\sim\; \frac{1}{2}\sum_{RR'}^{pairs}v_{R'}\left(s_{R'}\right)\left[\left(s_{R'}-r_{R'}\right)^2+\left(s_R-r_R\right)^2\right]v_R\left(s_R\right)\Psi_i\left(\mathbf{r}\right).$$

This shows that the smooth linear combination (27) of KPWs, given by the solution of the KKR equations (20), solves Schrödinger's equation for the *superposition* of MT-wells to within an error which is of *second order in the potential overlap* [13, 3]. If needed, the kinetic-energy error (28) can be corrected for, and the simplest correction is to use merely:

$$\Delta\varepsilon_i \approx \langle \Psi_i \left| \mathcal{H} - \varepsilon_i \right| \Psi_i \rangle \sim \frac{1}{2} \sum_{RR' \in pairs} v_{R'}\left(s_{R'}\right) \left[\left(s_{R'} - r_{R'}\right)^2 + \left(s_R - r_R\right)^2 \right] v_R\left(s_R\right) \rho_{R'R,i} \,,$$

to correct the KKR energy ε_i. Here, $\rho_{R'R,i}$ is the probability that state i is inside the overlap of the MT-spheres at sites R and R'.

Since the kink matrix (22) specifies the kinks of the KPW-set, it also specifies how the MT-Hamiltonian operates on the set of kinked partial waves, specifically:

$$\left(\mathcal{H} - \varepsilon\right) \phi_{R'L'}\left(\varepsilon, \mathbf{r}\right) = - \sum_{RL \in A} \delta\left(r_R - a_R\right) Y_L\left(\hat{\mathbf{r}}_R\right) K_{RL,R'L'}\left(\varepsilon\right) . \tag{29}$$

The overlap-integral between two KPWs may be obtained by use of Green's second theorem and the result is simply:

$$\begin{aligned} \left\langle \phi_{R'L'}\left(\varepsilon'\right) \mid \phi_{RL}\left(\varepsilon\right) \right\rangle \;&=\; \left\langle \psi_{R'L'}\left(\varepsilon'\right) \mid \psi_{RL}\left(\varepsilon\right) \right\rangle \;+ \\ &\delta_{R'R}\delta_{L'L} \left(\int_0^{s_R} \varphi_{RL}\left(\varepsilon', r\right) \varphi_{RL}\left(\varepsilon, r\right) r^2 dr - \int_{a_R}^{s_R} \varphi^o_{RL}\left(\varepsilon', r\right) \varphi^o_{RL}\left(\varepsilon, r\right) r^2 dr \right) \\ = \quad \frac{K_{R'L',RL}\left(\varepsilon'\right) - K_{R'L',RL}\left(\varepsilon\right)}{\varepsilon' - \varepsilon} \quad &\longrightarrow \dot{K}_{R'L',RL}\left(\varepsilon\right) \quad \text{if} \quad \varepsilon' \to \varepsilon. \end{aligned} \tag{30}$$

Here, $\dot{} \equiv \partial/\partial\varepsilon$ and the diagonal part of the integral has been calculated the '3-fold way' indicated in Fig. 6. This means that all cross-terms between products of ψ, φ, and φ°-functions, and between φ or φ°-functions on different sites are neglected. For solutions of the KKR equations, this gives the correct result due to the cancellation discussed in connection with expression (24). The KKR eigen(column)vector c_i should be normalized according to: $1 = c_i^\dagger \dot{K}\left(\varepsilon_i\right) c_i$ in order that $\langle \Psi_i \mid \Psi_i \rangle = 1$.

An accurate approximation for the *charge density,* which is consistent with the 3-fold way and, hence, with the normalization has the following *simple* form:

$$\rho\left(\mathbf{r}\right) \equiv \sum_{RR'} \sum_{LL'} \int^{\varepsilon_F} \phi_{RL}\left(\varepsilon, \mathbf{r}_R\right) \; N_{RL,R'L'}\left(\varepsilon\right) \; \phi_{R'L'}\left(\varepsilon, \mathbf{r}_{R'}\right)^* d\varepsilon = \rho^\psi\left(\mathbf{r}\right) + \sum_R \left[\rho^\varphi_R\left(\mathbf{r}_R\right) - \rho^{\varphi^\circ}_R\left(\mathbf{r}_R\right) \right] \tag{31}$$

where the global contribution is:

$$\rho^\psi\left(\mathbf{r}\right) \equiv \sum_{RR'} \sum_{LL'} \int^{\varepsilon_F} \psi_{RL}\left(\varepsilon, \mathbf{r}_R\right) \; N_{RL,R'L'}\left(\varepsilon\right) \; \psi_{R'L'}\left(\varepsilon, \mathbf{r}_{R'}\right)^* d\varepsilon \tag{32}$$

and the local contributions, $\rho^\varphi_R\left(\mathbf{r}_R\right) - \rho^{\varphi^\circ}_R\left(\mathbf{r}_R\right)$, which vanish quadratically at their respective MT-sphere, are:

$$\begin{aligned} \rho^\varphi_R\left(\mathbf{r}\right) \;&=\; \sum_{LL'} Y_L\left(\hat{\mathbf{r}}\right) Y^*_{L'}\left(\hat{\mathbf{r}}\right) \int^{\varepsilon_F} \varphi_{Rl}\left(\varepsilon, r\right) \; N_{RL,RL'}\left(\varepsilon\right) \; \varphi_{Rl'}\left(\varepsilon, r\right) d\varepsilon \\ \rho^{\varphi^\circ}_R\left(\mathbf{r}\right) \;&=\; \sum_{LL'} Y_L\left(\hat{\mathbf{r}}\right) Y^*_{L'}\left(\hat{\mathbf{r}}\right) \int^{\varepsilon_F} \varphi^\circ_{Rl}\left(\varepsilon, r\right) \; N_{RL,RL'}\left(\varepsilon\right) \; \varphi^\circ_{Rl'}\left(\varepsilon, r\right) d\varepsilon \,. \end{aligned} \tag{33}$$

The common density-of-states matrix in these equations is:

$$N_{RL,R'L'}(\varepsilon) = \sum_{i\in occ} c_{RL,i}\delta(\varepsilon-\varepsilon_i)\, c^*_{R'L',i} = \frac{1}{\pi}\mathrm{Im}G_{RL,R'L'}(\varepsilon+i\delta)\,. \tag{34}$$

We will evaluate the charge density locally, that is: pick a site R and find $\rho(\mathbf{r})$ in its neighborhood. For that purpose, we 'blow up' from the downfolded a-representation specified by (9) to the strongly screened b-representation specified by (12). We thus need

$$G^b_{AA}(\varepsilon) = K^a_{AA}(\varepsilon)^{-1} = G^a_{AA}(\varepsilon) \equiv G^a(\varepsilon) \quad \text{and} \quad G^b_{IA}(\varepsilon) = -K^b_{II}(\varepsilon)^{-1} K^b_{IA}(\varepsilon)\, G^b_{AA}(\varepsilon)\,. \tag{35}$$

The P-part of $G^a(\varepsilon)$ vanishes because the P-part of $K^a(\varepsilon)$ is diagonal with diverging elements. Note that the product $K^b_{II}(\varepsilon)^{-1} K^b_{IA}(\varepsilon)$ was used already for the downfolding (13).

Muffin-tin orbitals (MTOs) and their Hamiltonian and overlap matrices

Since computation of the kink-matrix is expensive, it is not efficient to find a one-electron energy from: $\det K(\varepsilon_i) = 0$, and then solve the linear equations for the corresponding $c_{RL,i}$. Rather, we shall construct an energy- and state-independent basis set of Nth-order MTOs, so-called NMTOs (1), with the property that it spans any wave function $\Psi_i(\mathbf{r})$ with energy ε_i in the neighborhood of $N+1$ chosen energies, $\epsilon_0, ..., \epsilon_N$, to within an error proportional to $(\varepsilon_i-\epsilon_0)...(\varepsilon_i-\epsilon_N)$. Solution of the generalized eigenvalue problem,

$$\sum_{RL\in A} \left\langle \chi^{(N)}_{R'L'} \left| \mathcal{H}-\varepsilon_i \right| \chi^{(N)}_{RL} \right\rangle b_{RL,i} \;=\; 0, \quad \text{for all active } R'L', \tag{36}$$

then yields energies with errors proportional to $(\varepsilon_i-\epsilon_0)^2...(\varepsilon_i-\epsilon_N)^2$ by virtue of the variational principle. This procedure has the added bonus that perturbations to the overlapping MT-Hamiltonian $\mathcal{H}$ are easily included.

It can be proved [5] that the error of the wave functions introduced by using the 3-fold way is proportional to $(r_R-a_R)^{2N+1}(\varepsilon_i-\epsilon_0)...(\varepsilon_i-\epsilon_N)$. The 3-fold way is therefore a consistent approximation, not only in the KKR, but also in the NMTO method.

MTOs with $N=0$

We have seen that all wave functions with $\varepsilon_i=\epsilon_0$ may be expressed as $\sum_{RL}\phi_{RL}(\epsilon_0,\mathbf{r})\,c_{RL,i}$. Therefore, the MTOs with $N=0$ are simply the KPWs at the chosen energy: $\chi^{(0)}_{RL}(\mathbf{r}) = \phi_{RL}(\epsilon_0,\mathbf{r})$. In the basis of these, the Hamiltonian and overlap matrices are given by respectively:

$$\left\langle \chi^{(0)} \left| \mathcal{H}-\epsilon_0 \right| \chi^{(0)} \right\rangle = -K(\epsilon_0) \quad \text{and} \quad \left\langle \chi^{(0)} \mid \chi^{(0)} \right\rangle = \dot{K}(\epsilon_0)\,, \tag{37}$$

as may easily be found from Eq. (29) and the normalization chosen. Since neglect of the off-diagonal elements of the overlap matrix, normalized to have diagonal elements 1, only causes errors in the energy bands of second order,

$$\tilde{K}_{RL,R'L'}(\epsilon_0) \;\equiv\; -\dot{K}_{RL,RL}(\epsilon_0)^{-\frac{1}{2}}\, K_{RL,R'L'}(\epsilon_0)\, \dot{K}_{R'L',R'L'}(\epsilon_0)^{-\frac{1}{2}} \tag{38}$$

is a *first-order, two-centre, tight-binding Hamiltonian.*

MTOs with $N > 0$

By an equation of the usual type:

$$(\mathcal{H} - \varepsilon)\, \gamma_{RL}(\varepsilon, \mathbf{r}) = -\delta(r_R - a_R)\, Y_L(\hat{\mathbf{r}}_R)\,, \tag{39}$$

we define a *contracted Green function,* $\gamma_{RL}(\varepsilon, \mathbf{r})$, which has one of its spatial variables confined to the a-spheres, *i.e.* $\mathbf{r}' \rightarrow RL$. Considered a function of $\mathbf{r}$, this contracted Green function is a (possibly delocalized, impurity-) solution with energy ε of Schrödinger's equation, except at its own sphere and for its own angular momentum where it has a kink of size unity. This kink becomes negligible when ε is close to a one-electron energy because the Green function has a pole there. Comparison of Eq. (39) with Eq. (29) now shows that

$$\gamma(\varepsilon, \mathbf{r}) = \phi(\varepsilon, \mathbf{r})\, G(\varepsilon)\,. \tag{40}$$

The contracted Green function is thus factorized into a matrix, $G(\varepsilon)$, which has the full energy dependence, and a vector of functions, $\phi(\varepsilon, \mathbf{r})$, which has the full spatial dependence and a weak energy dependence [14]. We now want to factorize the $\mathbf{r}$ and ε-dependences completely and, hence, to approximate $\phi(\varepsilon, \mathbf{r})\, G(\varepsilon)$ by $\chi^{(N)}(\mathbf{r})\, G(\varepsilon)$:

We note that subtracting from the contracted Green function a function $\omega^{(N)}(\varepsilon, \mathbf{r})$ which is analytical in energy,

$$\phi(\varepsilon, \mathbf{r})\, G(\varepsilon) \;-\; \omega^{(N)}(\varepsilon, \mathbf{r}) \;\equiv\; \chi^{(N)}(\varepsilon, \mathbf{r})\, G(\varepsilon)\,, \tag{41}$$

produces an equally good Green function, in the sense that both yield the same Schrödinger-equation solutions. If we can therefore determine the vector $\omega^{(N)}(\varepsilon, \mathbf{r})$ of analytical functions in such a way that each $\chi^{(N)}_{RL}(\varepsilon, \mathbf{r})$ takes the *same* value, $\chi^{(N)}_{RL}(\mathbf{r})$, at *all* energies, $\epsilon_0, ..., \epsilon_N$, then

$$\chi^{(N)}_{RL}(\varepsilon, \mathbf{r}) \;=\; \chi^{(N)}_{RL}(\mathbf{r}) \;+\; O\left((\varepsilon - \epsilon_0) ... (\varepsilon - \epsilon_N)\right),$$

and hence, $\chi^{(N)}(\mathbf{r})$ is the set of NMTOs!

At this stage we need to remember that the divided differences of a function $f(\varepsilon)$ on an energy mesh are given by a table of the form:

$$\begin{array}{lll}
\epsilon_0 & f(\epsilon_0) \equiv f_0 & \\
 & & \frac{f_0 - f_1}{\epsilon_0 - \epsilon_1} \equiv \frac{\Delta f}{\Delta[01]} \\
\epsilon_1 & f(\epsilon_1) \equiv f_1 & \qquad\qquad \frac{\frac{\Delta f}{\Delta[01]} - \frac{\Delta f}{\Delta[12]}}{\epsilon_0 - \epsilon_2} \equiv \frac{\Delta^2 f}{\Delta[012]}\,, \\
 & & \frac{f_1 - f_2}{\epsilon_1 - \epsilon_2} \equiv \frac{\Delta f}{\Delta[12]} \\
\epsilon_2 & f(\epsilon_2) \equiv f_2 &
\end{array}$$

and that if the mesh condenses onto the energy ϵ_ν,

$$\frac{\Delta^N f}{\Delta[0...N]} \quad \rightarrow \quad \frac{1}{N!}\, \overset{(N)}{f}(\epsilon_\nu)\,. \tag{42}$$

Now, since

$$\chi^{(N)}(\epsilon_0, \mathbf{r}) \;=\; \chi^{(N)}(\epsilon_1, \mathbf{r}) \;=\; ... \;=\; \chi^{(N)}(\epsilon_N, \mathbf{r})\,,$$

the Nth divided difference of $\chi^{(N)}(\varepsilon,\mathbf{r})\,G(\varepsilon)$ equals $\chi^{(N)}(\mathbf{r})$ times the Nth divided difference of $G(\varepsilon)$. Moreover, if we let $\omega^{(N)}(\varepsilon,\mathbf{r})$ be a polynomial in energy of (N-1)st degree, its Nth divided difference on the mesh will vanish. Taking the Nth divided difference of (41), therefore leads to the following solution for the NMTO set:

$$\chi^{(N)}(\mathbf{r})\,\frac{\Delta^N G}{\Delta[0...N]} \;=\; \frac{\Delta^N \gamma(\mathbf{r})}{\Delta[0...N]} \;=\; \frac{\Delta^N \phi(\mathbf{r})\,G}{\Delta[0...N]}. \tag{43}$$

In order to obtain the explicit expression for the matrix weights in (1), we need to take the Nth divided difference of the product $\phi(\varepsilon,\mathbf{r})\,G(\varepsilon)$. For this purpose we recall the *Lagrange* expression

$$f^{(N)}(\varepsilon)=\sum_{n=0}^{N} f(\epsilon_n)\; l_n^{(N)}(\varepsilon), \quad \text{with} \quad l_n^{(N)}(\varepsilon)\equiv \prod_{m=0,\neq n}^{N}\frac{\varepsilon-\epsilon_m}{\epsilon_n-\epsilon_m}, \tag{44}$$

for the Nth degree polynomial $f^{(N)}(\varepsilon)$ which passes through the $N+1$ mesh points. Differentiating this polynomial N times yields the desired expression for the Nth divided difference:

$$\frac{\Delta^N f}{\Delta[0...N]} \;=\; \frac{1}{N!}\frac{d^N f^{(N)}(\varepsilon)}{d\varepsilon^N} \;=\; \sum_{n=0}^{N} f(\epsilon_n)\,\frac{d^N l_n^{(N)}(\varepsilon)}{d\varepsilon^N} \;=\; \sum_{n=0}^{N}\frac{f(\epsilon_n)}{\prod_{m=0,\neq n}^{N}(\epsilon_n-\epsilon_m)}. \tag{45}$$

This shows, by the way, that the Nth divided difference depends on the $N+1$ energies to which it refers, but not on their order. By use of (45) we obtain the desired expression:

$$L_n^{(N)} \;=\; \frac{G(\epsilon_n)}{\prod_{m=0,\neq n}^{N}(\epsilon_n-\epsilon_m)}\left[\frac{\Delta^N G}{\Delta[0...N]}\right]^{-1}, \tag{46}$$

in terms of the values of the Green matrix on the energy mesh. From (46) we immediately see that $\sum_{n=0}^{N} L_n^{(N)}=1$, which ensures that $\chi_{RL}^{(N)}(\mathbf{r})\sim\phi_{RL}(\varepsilon,\mathbf{r})$ in case the KPW-set varies little over the mesh. We also realize that the NMTO-set (1) may be interpreted as Lagrange interpolation of the energy-dependence of the KPW-set, with the weights being energy-independent matrices, $L_n^{(N)}$, rather than Nth-degree scalar polynomials, $l_n^{(N)}(\varepsilon)$. Finally, we emphasize that the size of the NMTO basis is independent of N, but as N increases each basis function may become more and more complicated.

We now work out the effect of the Hamiltonian on the NMTO set. It follows from (43) that NMTOs with $N>0$ are smooth, because the kinks of the functions $\gamma(\varepsilon,\mathbf{r})$ are equal to unity and thereby independent of energy. Since the NMTOs with $N>0$ are smooth, the contributions from the delta-function on the right-hand side of (39) for the contracted Green function will cancel in the end, and the effect of operating on (41) is therefore effectively:

$$\mathcal{H}\chi^{(N)}(\varepsilon,\mathbf{r})\,G(\varepsilon) \;=\; \mathcal{H}\gamma(\varepsilon,\mathbf{r})-\mathcal{H}\omega^{(N)}(\varepsilon,\mathbf{r}) \;=\; \varepsilon\gamma(\varepsilon,\mathbf{r})-\mathcal{H}\omega^{(N)}(\varepsilon,\mathbf{r}).$$

Taking again the Nth divided differences for the mesh on which $\chi^{(N)}(\varepsilon,\mathbf{r})$ is constant, yields:

$$\mathcal{H}\chi^{(N)}(\mathbf{r})\,\frac{\Delta^N G}{\Delta[0...N]} \;=\; \mathcal{H}\frac{\Delta^N \gamma(\mathbf{r})}{\Delta[0...N]} \;=\; \frac{\Delta^N \varepsilon\gamma(\mathbf{r})}{\Delta[0...N]}. \tag{47}$$

Before we continue with the evaluation of the NMTO Hamiltonian and overlap matrices to be used in the generalized eigenvalue problem (36), we derive a few illuminating relations:

Using again Eq. (45) and picking for instance the last mesh point, we obtain:

$$\frac{\Delta^N(\varepsilon-\epsilon_N)f}{\Delta[0...N]} = \sum_{n=0}^{N}\frac{(\epsilon_n-\epsilon_N)f(\epsilon_n)}{\prod_{m=0,\neq n}^{N}(\epsilon_n-\epsilon_m)} = \sum_{n=0}^{N-1}\frac{(\epsilon_n-\epsilon_N)f(\epsilon_n)}{\prod_{m=0,\neq n}^{N}(\epsilon_n-\epsilon_m)} = \sum_{n=0}^{N-1}\frac{f(\epsilon_n)}{\prod_{m=0,\neq n}^{N-1}(\epsilon_n-\epsilon_m)}$$
$$= \frac{\Delta^{N-1}f}{\Delta[0..N-1]}.$$

As a consequence:

$$(\mathcal{H}-\epsilon_N)\chi^{(N)}(\mathbf{r})\frac{\Delta^N G}{\Delta[0...N]} = (\mathcal{H}-\epsilon_N)\frac{\Delta^N\gamma(\mathbf{r})}{\Delta[0...N]} = \frac{\Delta^{N-1}\gamma(\mathbf{r})}{\Delta[0..N-1]}. \tag{48}$$

Solving for the NMTOs (43) yields:

$$(\mathcal{H}-\epsilon_N)\chi^{(N)}(\mathbf{r}) = \chi^{(N-1)}(\mathbf{r})\left(E^{(N)}-\epsilon_N\right), \tag{49}$$

where $\chi^{(N-1)}(\mathbf{r})$ is the energy-independent MTO of order $N-1$, obtained by *not* using the *last* point, and where

$$E^{(N)} \equiv \epsilon_N + \frac{\Delta^{N-1}G}{\Delta[0..N-1]}\left[\frac{\Delta^N G}{\Delta[0...N]}\right]^{-1} = \frac{\Delta^N\varepsilon G}{\Delta[0...N]}\left[\frac{\Delta^N G}{\Delta[0...N]}\right]^{-1} = \sum_{n=0}^{N}\epsilon_n L_n^{(N)}, \tag{50}$$

is the *energy matrix* which, in contrast to $\chi^{(N-1)}(\mathbf{r})$ is independent of which mesh point is omitted. The first equation (50) shows how to compute $E^{(N)}$ and the last equation shows that $E^{(N)}$ is the energy *weighted* on the $0...N$-mesh by the Lagrange matrices (46).

Let us next consider a sequence of energy meshes, starting with the single-point mesh ϵ_0, then adding ϵ_1 in order to obtain the two-point mesh ϵ_0, ϵ_1, then adding ϵ_2 obtaining the three-point mesh ϵ_0, ϵ_1, ϵ_2, a.s.o. Associated with these meshes we obtain a sequence of NMTO sets: the KPW-set $\chi^{(0)}(\mathbf{r})$, the LMTO-set $\chi^{(1)}(\mathbf{r})$, the QMTO-set $\chi^{(2)}(\mathbf{r})$, a.s.o. Working *downwards*, we thus always *delete* the point with the *highest* index. Equation (49) now shows that with respect to the *order* of the NMTO-set, $\mathcal{H}-\epsilon_N$ may be viewed as a *step-down* operator and $E^{(N)}-\epsilon_N$ as the corresponding *transfer matrix*. In this sequence we may include the case N=0 provided that we define: $E^{(0)}-\epsilon_0 \equiv -K(\epsilon_0)$ and $\chi^{(-1)}(\mathbf{r}) \equiv \delta(\mathbf{r})$. Hence, $N+1$ successive step-down operations on the NMTO-set yield:

$$(\mathcal{H}-\epsilon_0)...(\mathcal{H}-\epsilon_N)\,\chi^{(N)}(\mathbf{r}) = \delta(\mathbf{r})\left(E^{(0)}-\epsilon_0\right)...\left(E^{(N)}-\epsilon_N\right).$$

This, first of all tells us that one has to operate N times with ∇^2, that is with ∇^{2N}, before getting to the non-smoothness of an NMTO, and secondly, that the higher the N, the more spread out the NMTO.

By taking matrix elements of (49), the transfer matrix may be expressed as:

$$E^{(N)}-\epsilon_N = \left\langle\chi^{(N)} \mid \chi^{(N-1)}\right\rangle^{-1}\left\langle\chi^{(N)}\left|\mathcal{H}-\epsilon_N\right|\chi^{(N)}\right\rangle. \tag{51}$$

This holds also for N=0, provided that we take the value of $\chi^{(0)}(\mathbf{r})$ at its screening sphere to be $\varphi^{\circ\,a}(\varepsilon,a)=1$ [as is also dictated by the 3-fold way (30)] so that $\left\langle\chi^{(0)} \mid \chi^{(-1)}\right\rangle = 1$. The form (51) shows that the transfer matrices with $N \geq 1$ are *not* Hermitian but short ranged, as one may realize by recursion starting from N=0. Finally, it should be remembered that the NMTOs

considered sofar have particular normalizations (which are *not:* $\left\langle \chi^{(N)} \mid \chi^{(N)} \right\rangle = 1$), and so do the transfer matrices.

Instead of using the Lagrange form (45) to factorize the NMTO (43), one may use the step-down property (49) to obtain:

$$\chi^{(N)}(\mathbf{r}) \;=\; \phi(\epsilon_N, \mathbf{r}) + \frac{\Delta\phi(\mathbf{r})}{\Delta[N-1,N]}\left(E^{(N)} - \epsilon_N\right) + ... + \frac{\Delta^N\phi(\mathbf{r})}{\Delta[0...N]}\left(E^{(1)} - \epsilon_1\right)..\left(E^{(N)} - \epsilon_N\right), \tag{52}$$

since from (29) and (48)

$$(\mathcal{H} - \epsilon_N)\,\phi(\epsilon_N, \mathbf{r}) = -\delta_{N,0}\delta(\mathbf{r})\,K(\epsilon_0) \quad \text{and} \quad (\mathcal{H} - \epsilon_N)\,\frac{\Delta^{N-M}\phi(\mathbf{r})}{\Delta[M...N]} = \frac{\Delta^{N-M-1}\phi(\mathbf{r})}{\Delta[M..N-1]}.$$

Expression (52) for the NMTO-set is the matrix equivalent -or the quantized form- of *Newton's* expression,

$$f^{(N)}(\varepsilon) \;=\; f(\epsilon_N) + \frac{\Delta f}{\Delta[N-1,N]}(\varepsilon - \epsilon_N) + ... + \frac{\Delta^N f}{\Delta[0...N]}(\varepsilon - \epsilon_1)..(\varepsilon - \epsilon_N), \tag{53}$$

for the Nth-degree polynomial (44) passing through the $N+1$ mesh points. In this case, $f(\epsilon_n) = \phi_{RL}(\epsilon_n, \mathbf{r})$. The Newton form (52) expresses the NMTO as a kinked partial wave at the same site and with the same angular momentum, plus a smoothing cloud of energy-derivative functions centered at all sites and with all angular momenta. This is clearly illustrated in Figs. 1-3. For a condensed mesh and using (42), the Newton expression (52) for the NMTO-set obviously reduces to the matrix-equivalent of the *Taylor* series for the energy-dependence of $\phi_{RL}(\varepsilon, \mathbf{r})$.

To calculate the NMTO *Hamiltonian* and *overlap matrices* we use expression (43) for the NMTO-set and therefore first need to evaluate the Hamiltonian and overlap matrices for the Nth divided difference of the contracted Green function (40). Since according to (48), operation with the Hamiltonian on this Nth divided difference yields the (N-1)st divided difference, we need expressions for $\left\langle \Delta^N\gamma/\Delta[0...N] \mid \Delta^N\gamma/\Delta[0...N] \right\rangle$ and $\left\langle \Delta^N\gamma/\Delta[0...N] \mid \Delta^{N-1}\gamma/\Delta[0..N-1] \right\rangle$. Pre and post-multiplication of the KPW overlap matrix (30) with the appropriate Green matrices yield

$$\langle \gamma(\varepsilon') \mid \gamma(\varepsilon) \rangle \;=\; -\frac{G(\varepsilon') - G(\varepsilon)}{\varepsilon' - \varepsilon} \quad \longrightarrow\; -\dot{G}(\varepsilon) \;=\; G(\varepsilon)\,\dot{K}(\varepsilon)\,G(\varepsilon) \quad \text{if } \varepsilon' \to \varepsilon,$$

and taking then the Nth divided difference with respect to ε' and the Mth divided difference with respect to ε gives:

$$\left\langle \frac{\Delta^N\gamma}{\Delta[0...N]} \mid \frac{\Delta^M\gamma}{\Delta[0..M]} \right\rangle \;=\; -\sum_{n'=0}^{N}\sum_{n=0}^{M} \frac{\Delta G/\Delta[n'n]}{\prod_{m'=0,\neq n'}^{N}(\varepsilon_{n'} - \varepsilon_{m'})\prod_{m=0,\neq n}^{M}(\varepsilon_n - \varepsilon_m)}.$$

It can be shown that this double-sum is simply the $(N+M+1)$st *Hermite divided difference* $\Delta^{M+N+1}G/\Delta[[0..M]\,N]$ of the Green matrix [5]. $\Delta^{M+N+1}G/\Delta[[0..M]\,N]$ is defined as the $(M+N+1)$st derivative of that polynomial of degree $M+N+1$ which takes the values $G(\epsilon_0), ..., G(\epsilon_N)$ at the $N+1$ mesh points and the energy-derivative values $\dot{G}(\epsilon_0), .., \dot{G}(\epsilon_M)$ at the first $M+1$ points. The single-sum expressions for the relevant cases $M = N-1$ and $M = N$ are respectively

$$\frac{\Delta^{2N}G}{\Delta[[0..N-1]\,N]} \;=\; \sum_{n=0}^{N-1} \frac{\dot{G}(\epsilon_n) - G(\epsilon_n)\left(\sum_{n'=0,\neq n}^{N-1}\frac{2}{\epsilon_n - \epsilon_{n'}} + \frac{1}{\epsilon_n - \epsilon_N}\right)}{(\epsilon_n - \epsilon_N)\prod_{m=0,\neq n}^{N-1}(\epsilon_n - \epsilon_m)^2} + \frac{G(\epsilon_N)}{\prod_{m=0}^{N-1}(\epsilon_N - \epsilon_m)^2} \tag{54}$$

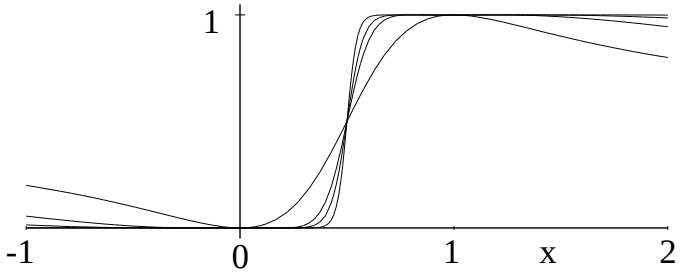

Figure 7: Variational energy-estimates for a two-level model ($\varepsilon_j = 0, 1$) using single NMTOs with $N = 0, 1, 2$, and 4 as functions of the position x of the center of the energy mesh. For $N > 0$, the mesh is: $\epsilon_n = x - 0.2 + 0.4n/N$.

and

$$\frac{\Delta^{2N+1} G}{\Delta\left[[0...N]\right]} = \sum_{n=0}^{N} \frac{\dot{G}\left(\epsilon_n\right) - G\left(\epsilon_n\right) \sum_{n'=0,\neq n}^{N} \frac{2}{\epsilon_n - \epsilon_{n'}}}{\prod_{m=0,\neq n}^{N} \left(\epsilon_n - \epsilon_m\right)^2}. \tag{55}$$

For the overlap and Hamiltonian matrices we thus obtain the most important result [15]:

$$\begin{aligned} \left\langle \frac{\Delta^N \gamma}{\Delta\left[0..N\right]} \left| \mathcal{H} - \varepsilon \right| \frac{\Delta^N \gamma}{\Delta\left[0..N\right]} \right\rangle &= \frac{\Delta^N G}{\Delta\left[0..N\right]} \left\langle \chi^{(N)} \left| \mathcal{H} - \varepsilon \right| \chi^{(N)} \right\rangle \frac{\Delta^N G}{\Delta\left[0..N\right]} \\ &= \frac{-\Delta^{2N} G}{\Delta\left[[0.N-1]\,N\right]} - \left(\varepsilon - \epsilon_N\right) \frac{-\Delta^{2N+1} G}{\Delta\left[[0..N]\right]} \end{aligned} \tag{56}$$

This expression for the NMTO Hamiltonian and overlap matrices is not only simple and beautiful, but it also offers sweet coding and speedy computation. We realize that in the formalism of the 3rd-generation MTO, all relevant quantities are expressed in terms of *one* matrix, $G\left(\varepsilon\right) = \left\langle \chi^{(0)} \left| \varepsilon - \mathcal{H} \right| \chi^{(0)} \right\rangle^{-1} = K\left(\varepsilon\right)^{-1}$. We have thus derived orbital sets exclusively from multiple-scattering theory for MT-potentials.

At first glance on (56), it seems strange that the eigenvalues ε_i appear as 'ratios' of energy derivatives of Hermite interpolations of the Green matrix, which has poles inside the mesh. One might have felt more comfortable about interpolating the kink matrix. To develop some feeling for expression (56), let us first consider the simplest possible 1×1 Green matrix, $G\left(\varepsilon\right) = \sum_j \left(\varepsilon - \varepsilon_j\right)^{-1}$, which is that of a single, normalized kinked partial wave with principal quantum numbers j. The variational energy relatively to ϵ_N can easily be worked out as [5]:

$$\frac{\Delta^{2N} G / \Delta\left[[0..N-1]\,N\right]}{\Delta^{2N+1} G / \Delta\left[[0...N]\right]} = \frac{\sum_j \left(\varepsilon_i - \epsilon_N\right)^{-1} \prod_{n=0}^{N-1} \left(\varepsilon_j - \epsilon_n\right)^{-2}}{\sum_j \prod_{n=0}^{N} \left(\varepsilon_j - \epsilon_n\right)^{-2}}$$

and the deviation from the exact result, $\varepsilon_i - \epsilon_N$, is therefore, to leading order, $\sum_{j\neq i} \left(\varepsilon_j - \epsilon_N\right) \times \prod_{n=0}^{N} \left(\varepsilon_i - \epsilon_n\right)^2 / \left(\varepsilon_j - \epsilon_n\right)^2$. This is in accord with the opening statement of this section, that the energies have errors proportional to $\left(\varepsilon_i - \epsilon_0\right)^2 ... \left(\varepsilon_i - \epsilon_N\right)^2$. Fig. 7 shows how for the two-level system, $G\left(\varepsilon\right) = \frac{1}{\varepsilon} + \frac{1}{\varepsilon - 1}$, this variational energy switches between the exact eigenvalues 0 and 1 as the centre x of the mesh sweeps from –1 to +2. The various curves refer to $N = 0, 1, 2$, and 4. For $N > 0$, we used meshes of total width 0.4. We see that the switching curves sharpen up as N increases, and that good results are obtained already with $N = 1$, the so-called chord-LMTO.

As another example, let us work out the expressions for the LMTO Hamiltonian and overlap matrices in terms of the kink matrix which, according to (37), is essentially the first-order

two-centre Hamiltonian. The results obtained from (54)-(56) are:

$$\begin{aligned}\left\langle \chi^{(1)} \left| \mathcal{H} - \varepsilon_1 \right| \chi^{(1)} \right\rangle &= -\left[\frac{\Delta G}{\Delta\left[01\right]}\right]^{-1} \frac{\Delta^2 G}{\Delta\left[\left[0\right]1\right]} \left[\frac{\Delta G}{\Delta\left[01\right]}\right]^{-1} \\ &= \left(\epsilon_0 - \epsilon_1\right)\left(G_0 - G_0\right)^{-1}\left(-\dot{G}_0 + \Delta G/\Delta\left[01\right]\right)\left(G_0 - G_1\right)^{-1} \\ &\rightarrow \quad -\dot{G}^{-1}\frac{\ddot{G}}{2!}\dot{G}^{-1} \;=\; -K + K\dot{K}^{-1}\frac{\ddot{K}}{2!}\dot{K}^{-1}K,\end{aligned}$$

with $G_n \equiv G\left(\epsilon_n\right)$, and

$$\begin{aligned}\left\langle \chi^{(1)} \mid \chi^{(1)} \right\rangle &= -\left[\frac{\Delta G}{\Delta\left[01\right]}\right]^{-1} \frac{\Delta^3 G}{\Delta\left[\left[01\right]\right]} \left[\frac{\Delta G}{\Delta\left[01\right]}\right]^{-1} \\ &= \left(G_0 - G_1\right)^{-1}\left(-\dot{G}_0 + 2\Delta G/\Delta\left[01\right] - \dot{G}_1\right)\left(G_0 - G_1\right)^{-1} \\ &\rightarrow \quad -\dot{G}^{-1}\frac{\dddot{G}}{3!}\dot{G}^{-1} \;=\; \dot{K} - K\dot{K}^{-1}\frac{\ddot{K}}{2!} - \frac{\ddot{K}}{2!}\dot{K}^{-1}K + K\dot{K}^{-1}\frac{\dddot{K}}{3!}\dot{K}^{-1}K.\end{aligned}$$

The results for a condensed mesh in terms of the kink matrix and its first three energy derivatives may be recognized as almost identical to those of the 2nd-generation LMTO-ASA method. To get exactly to this LMTO-ASA form, one needs to transform to the nearly orthonormal LMTO set: $\hat{\chi}^{(1)}\left(\mathbf{r}\right) \equiv \chi^{(1)}\left(\mathbf{r}\right)\dot{K}^{-1/2}$, which corresponds to Löwdin orthonormalization of the 0th-order set. However, the present formalism does not require the ASA, but it holds to leading order for overlapping MT-potentials and can be generalized to an arbitrary energy mesh. This is a most crucial improvement.

For a crystal and in the **k**-representation, one may use $\Delta^N\gamma\left(\mathbf{k},\mathbf{r}\right)/\Delta\left[0...N\right]$ as basis-set, so that inversion of $\Delta^N G/\Delta\left[0..N\right]$ is avoided. In this case, we solve the generalized eigenvalue problem

$$\left(-\frac{\Delta^{2N}G^{\alpha}\left(\mathbf{k}\right)}{\Delta\left[\left[0..N-1\right]N\right]} + \left(\varepsilon_j\left(\mathbf{k}\right) - \epsilon_N\right)\frac{\Delta^{2N+1}G^{a}\left(\mathbf{k}\right)}{\Delta\left[\left[0...N\right]\right]}\right) g_j^a\left(\mathbf{k}\right) \;=\; 0,$$

in the downfolded representation (of size A) and normalize the eigenvectors according to:

$$g_j^{a\dagger}\left(\mathbf{k}\right)\left(-\Delta^{2N+1}G^{a}\left(\mathbf{k}\right)/\Delta\left[\left[0...N\right]\right]\right) g_j^a\left(\mathbf{k}\right) = 1.$$

The wave function in the strongly localized representation (of size $B \geq A$) is then:

$$\begin{aligned}\Psi_j\left(\mathbf{k},\mathbf{r}\right) &= \sum_{RL\in A}\frac{\Delta^N\gamma\left(\mathbf{k},\mathbf{r}\right)_{RL}}{\Delta\left[0..N\right]} g^a_{RL,j}\left(\mathbf{k}\right) \\ &= \sum_{RL\in B}\sum_{T}\sum_{n=0}^{N}\phi^b_{RL}\left(\epsilon_n,\mathbf{r}-\mathbf{T}\right)\, e^{i\mathbf{k}\cdot\mathbf{T}}\sum_{R'L'\in A}\frac{G^b_{RL,R'L'}\left(\epsilon_n,\mathbf{k}\right)}{\prod_{m=0,\neq n}^{N}\left(\epsilon_n-\epsilon_m\right)} g^a_{R'L',j}\left(\mathbf{k}\right) \\ &\equiv \sum_{RL\in B}\sum_{T}\sum_{n=0}^{N}\phi^b_{RL}\left(\epsilon_n,\mathbf{r}-\mathbf{T}\right)\, e^{i\mathbf{k}\cdot\mathbf{T}}\, c^b_{nRL,j}\left(\mathbf{k}\right),\end{aligned}$$

because it may be shown that downfolding merely *truncates* the contracted Green function $\gamma\left(\varepsilon,\mathbf{r}\right)$, but leaves it otherwise unchanged. In this expression, we have been explicit about the summations and have defined an eigenvector $c^b_{nRL,j}\left(\mathbf{k}\right)$. In terms of this, the localized form of the charge density becomes

$$\begin{aligned}\rho\left(\mathbf{r}\right) &= \sum_{RL,R'L'\in B}\sum_{T}\sum_{n,n'=0}^{N}\phi^b_{RL}\left(\epsilon_n,\mathbf{r}-\mathbf{T}\right)\, N^b_{n(\mathbf{R}+\mathbf{T})L,n'R'L'}\,\phi^b_{R'L'}\left(\epsilon_{n'},\mathbf{r}\right) \\ &= \rho^{\psi}\left(\mathbf{r}\right) + \sum_{R\in B}\left[\rho^{\varphi}_R\left(\mathbf{r}_R\right) - \rho^{\varphi^\circ}_R\left(\mathbf{r}_R\right)\right],\end{aligned}$$

where we use the forms analogous to those following (31), but with the density matrix

$$N^b_{n(\mathbf{R}+\mathbf{T})L,n'R'L'} = \sum_{\mathbf{k}j\in occ} e^{i\mathbf{k}\cdot\mathbf{T}} c^b_{nRL,j}\left(\mathbf{k}\right) c^{b\,*}_{n'R'L',j}\left(\mathbf{k}\right).$$

We finally remark that *energy-dependent, linear transformation*s of the kinked partial waves: $\hat{\phi}\left(\varepsilon,\mathbf{r}\right) = \phi\left(\varepsilon,\mathbf{r}\right)\hat{T}\left(\varepsilon\right)$ change the individual NMTOs, but not the Hilbert space spanned by them [5]. Transformation to a *nearly orthonormal* representation, defined by $\left\langle \hat{\chi}^{(N)} \mid \hat{\chi}^{(N-1)} \right\rangle = 1$, is simple because this does not require taking the square root of the overlap matrix. Moreover, in a nearly orthonormal representation, the transfer matrices are Hamiltonians, as Eq. (51) shows, and starting from such a representation, it is a simple matter to obtain a completely *orthonormal* one. This is all explained in Ref. [5].

Band structure trend in cuprates and correlation with $T_{c\,\max}$.

In this final section, we present an extended version of a recent paper [9], which demonstrates the use of the 3rd-generation MTO method to extract the materials-dependent trend relevant for high-temperature superconductivity. Other applications of this method to correlated electron systems include Refs. [16].

The mechanism of high-temperature superconductivity (HTSC) in the hole-doped cuprates remains a puzzle [17]. Many families with CuO_2-layers have been synthesized and all exhibit a phase diagram with T_c going through a maximum as a function of doping. The prevailing explanation is that at low doping, superconductivity is destroyed with rising temperature by the loss of phase coherence, and at high doping by pair-breaking [18]. For the *materials*-dependence of T_c at optimal doping, $T_{c\,\max}$, the only known but not understood systematics is that for materials with multiple CuO_2-layers, such as $HgBa_2Ca_{n-1}Cu_nO_{2n+2}$, $T_{c\,\max}$ increases with the number of layers n, until $n \sim 3$. There is little clue as to why for n fixed, $T_{c\,\max}$ depends strongly on the family, *e.g.* why for n=1, $T_{c\,\max}$ is 40 K for La_2CuO_4, 85 K for $Tl_2Ba_2CuO_6$, and 90 K for $HgBa_2CuO_4$, although the Neel temperatures are fairly similar. A wealth of structural data has been obtained, and correlations between structure and T_c have often been looked for as functions of doping, pressure, uniaxial strain, and family. However, the large number of structural and compositional parameters makes it difficult to find what besides doping controls the superconductivity. Insight was recently provided by Seo et al. [19] who grew ultrathin epitaxial $La_{1.9}Sr_{0.1}CuO_4$ films with varying degrees of strain and measured all relevant structural parameters and physical properties. For this single-layer material it was concluded that the distance between the charge reservoir and the CuO_2-plane is the key structural parameter determining the normal state and superconducting properties.

Most theories of HTSC are based on a Hubbard model with *one* Cu $d_{x^2-y^2}$-like orbital per CuO_2 unit. The one-electron part of this model is in the **k**-representation:

$$\varepsilon\left(\mathbf{k}\right) = -2t\left(\cos k_x + \cos k_y\right) + 4t'\cos k_x \cos k_y - 2t''\left(\cos 2k_x + \cos 2k_y\right) + \ldots, \qquad (57)$$

with t, t', t'', ... denoting the hopping integrals (≥ 0) on the square lattice (Fig. 8). First, only t was taken into account, but the consistent results of LDA band-structure calculations [20]

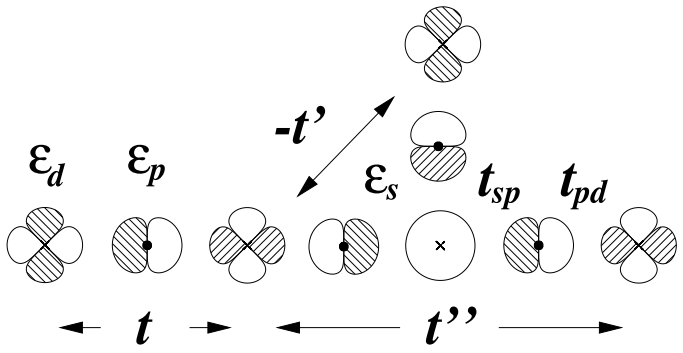

Figure 8: Relation between the one-orbital model $(t, t', t'', ...)$ and the nearest-neighbor four-orbital model [20] ($\varepsilon_d - \varepsilon_p \sim 1\,\mathrm{eV}$, $t_{pd} \sim 1.5\,\mathrm{eV}$, $\varepsilon_s - \varepsilon_p \sim 16 - 4\,\mathrm{eV}$, $t_{sp} \sim 2\,\mathrm{eV}$) .

and angle-resolved photoemission spectroscopy (for overdoped, stripe-free materials)[21], have led to the current usage of including also t', with $t'/t \sim 0.1$ for La_2CuO_4 and $t'/t \sim 0.3$ for $YBa_2Cu_3O_7$ and $Bi_2Sr_2CaCu_2O_8$, whereby the constant-energy contours of expression (57) become rounded squares oriented in respectively the [11]- and [10]-directions. It is conceivable that the materials-dependence enters the Hamiltonian primarily via its one-electron part (57), and that this dependence is captured by LDA calculations. But it needs to be filtered out:

The LDA band structure of the best known, and only stoichiometric optimally doped HTSC, $YBa_2Cu_3O_7$, is more complicated than what can be described with the t-t' model. Nevertheless, careful analysis has shown [20] that the *low*-energy *layer*-related features, which are the only generic ones, can be described by a *nearest*-neighbor, tight-binding model with *four* orbitals per layer (Fig. 8), Cu $3d_{x^2-y^2}$, O_a $2p_x$, O_b $2p_y$, and Cu $4s$, with the interlayer hopping proceeding via the diffuse Cu $4s$-orbital whose energy, ε_s, is several eV above the conduction band. Also the intralayer hoppings t', t'', ... beyond nearest neighbors in (57) proceed via Cu $4s$. The constant-energy contours, $\varepsilon_i(\mathbf{k}) = \varepsilon$, of the tight-binding model in Fig. 8 could be expressed simply as [20]:

$$1 - u - d(\varepsilon) + (1+u)\, p(\varepsilon) \;=\; \frac{v^2}{1 - u + s(\varepsilon)} \tag{58}$$

in terms of the coordinates $u \equiv \frac{1}{2}(\cos k_x + \cos k_y)$ and $v \equiv \frac{1}{2}(\cos k_x - \cos k_y)$, and the quadratic functions

$$d(\varepsilon) \equiv \frac{(\varepsilon - \varepsilon_d)(\varepsilon - \varepsilon_p)}{4t_{pd}^2} \quad \text{and} \quad s(\varepsilon) \equiv \frac{(\varepsilon_s - \varepsilon)(\varepsilon - \varepsilon_p)}{4t_{sp}^2},$$

which describe the coupling of $O_{a/b}\, p_{x/y}$ to respectively Cu $d_{x^2-y^2}$ and Cu s. The term proportional to $p(\varepsilon)$ in (58) describes the admixture of $O_{a/b}\, p_z$ orbitals for dimpled layers and actually extends the four-orbital model to a six-orbital one [20]. For ε near the middle of the conduction band, $d(\varepsilon)$, $s(\varepsilon)$, and $p(\varepsilon)$ are positive and the energy dependence of $d(\varepsilon)$ may be linearized ($\dot{d} > 0$), while that of $s(\varepsilon)$ and of $p(\varepsilon)$ may be neglected. $p = 0$ for flat layers and $p = s^2/(1+s)^2$ for extended saddlepoints. The bilayer bonding and antibonding subbands have ε_s-values split by $\mp t_{ss}^{\perp}$. Now, if ε_s were infinitely far above the conduction band, or t_{sp} were vanishingly small, the right-hand side of (58) would vanish, with the result that the constant-energy contours would depend only on u. The dispersion of the conduction band near the Fermi level would thus be that of the one-orbital model (57) with $t = (1-p)/4\dot{d}$ and $t' = t'' = 0$.

For realistic values of ε_s and t_{sp}, the conduction band attains Cu s-character proportional to v^2, thus vanishing along the nodal direction, $k_x = k_y$, and peaking at $(\pi, 0)$, where it is of order 10 per cent. The repulsion from the Cu s-band lowers the energy of the van Hove singularities and turns the constant-energy contours towards [10]-direction. This same v^2-dependence pertains to the interlayer splitting caused by $t_{ss}^{\perp}$ in a multilayer material. In order to go from (58) to (57),

$$\frac{1}{1-u+s} = \frac{2r}{1-2ru}, \quad \text{with} \quad r \equiv \frac{1/2}{1+s}, \tag{59}$$

was expanded in powers of $2ru$. This provided explicit expressions such as:

$$t = [1 - p + o(r)]/4\dot{d}, \qquad t' = [r + o(r)]/4\dot{d}, \qquad \text{and} \quad t'' = \frac{1}{2}t' + o(r),$$

for the hopping integrals of the one-orbital model in terms of the parameters of the four(six)-orbital model and the expansion energy $\sim \varepsilon_F$. Note that all intralayer hoppings beyond nearest neighbors are expressed in terms of the *range*-parameter r. Although one may think of r as t'/t, this holds only for flat layers and when $r < 0.2$. When $r > 0.2$, the series (57) must be carried beyond t''. Dimpling is seen not to influence the range of the intralayer hopping, but to reduce t through admixture of $O_{a/b}\, p_z$. In addition, it reduces t_{pd}.

We shall now generalize this analysis to all known families of HTSC materials using the 3rd-generation MTO method which allows us to construct *minimal basis sets* for the *low-energy part* of an LDA band structure with sufficient accuracy that we can extract the materials dependence. This dependence we find to be contained solely in ε_s, which is now the energy of the *axial* orbital, a hybrid between Cu s, Cu d_{3z^2-1}, apical-oxygen $O_c\, p_z$, and farther orbitals on *e.g.* La or Hg. The range, r, of the intralayer hopping is thus controlled by the structure and chemical composition *perpendicular* to the CuO_2-layers. It turns out that the materials with the larger r (lower ε_s) tend to be those with the higher observed values of $T_{c\,\max}$. In the materials with the highest $T_{c\,\max}$, the axial orbital is almost pure Cu $4s$.

It should be noted that r describes the *shape* of the non-interacting band in a 1 eV-range around the Fermi level, whose accurate position is unknown because we make no assumptions about the remaining terms of the Hamiltonian, inhomogeneities, stripes, a.s.o.

The top of Fig. 9 shows the LDA energy bands calculated for the simplest, idealized, infinite-layer cuprate, $CaCuO_2$. The red conduction band was obtained using a single Bloch-sum of the Cu $d_{x^2-y^2}$ (N=4)MTO, which is shown in the CuO_2-layer in the bottom part of the figure. All other channels were downfolded. We see the central Cu $3d_{x^2-y^2}$-orbital, surrounded by four O $2p$-orbitals anti-bonding to it. At the four next Cu sites there is substantial diffuse Cu $4s$-character bonding to O $2p$. This character is best recognized as a strengthening of the O $2p$ back-lobes followed by sharp truncation at the outermost node of the Cu $4s$ orbital. Having understood these general in-layer features, we now consider the real materials:

Fig. 10 shows the LDA bands for the single-layer La_2CuO_4 and $Tl_2Ba_2CuO_6$. Whereas the high-energy band structures are complicated and very different, the low-energy conduction bands shown by dashed lines contain the generic features. Most notably, the dispersion along ΓDZ is suppressed for $Tl_2Ba_2CuO_6$ relatively to La_2CuO_4, whereas the dispersion along ΓXZ is the same. This is the v^2-effect. The low-energy bands were calculated using the first-order tight-binding Hamiltonian (38) with a single Bloch sum of Cu $d_{x^2-y^2}$-KPWs, or (N=0)MTOs, with ϵ_0

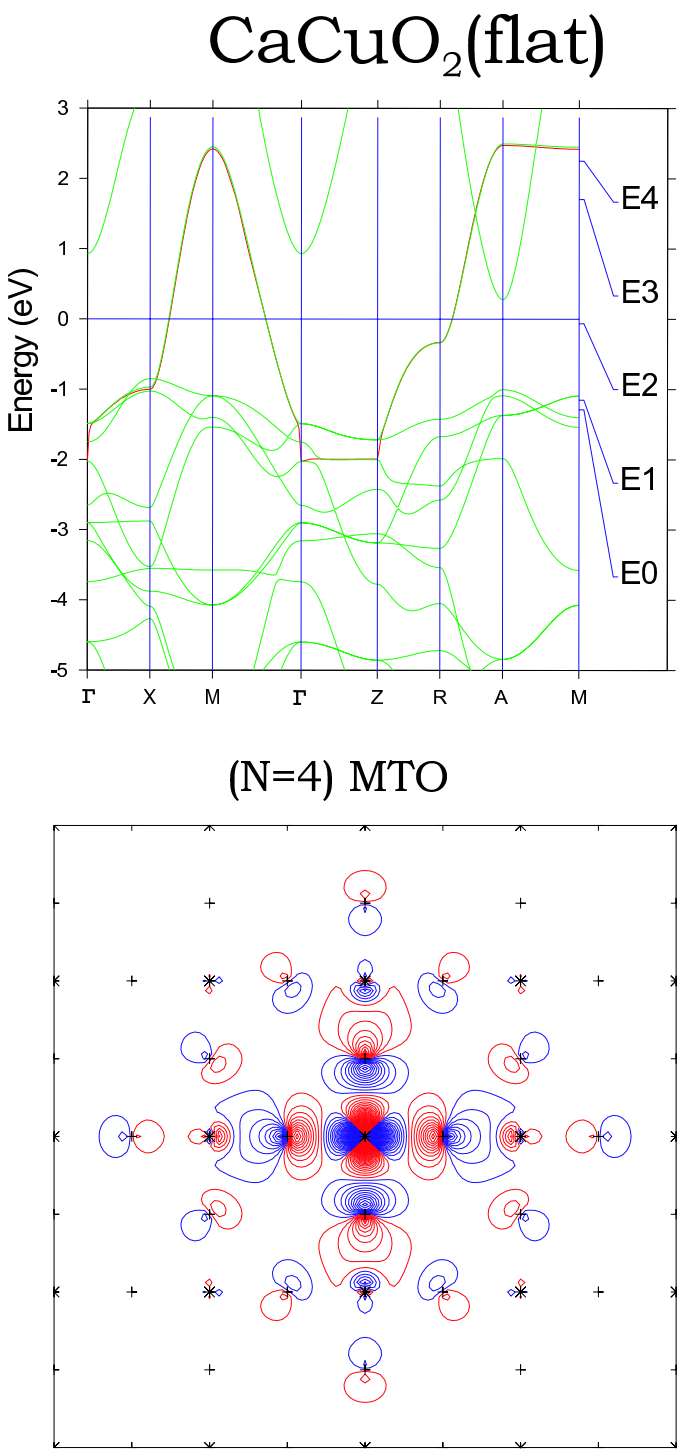

Figure 9: LDA energy bands of idealized $CaCuO_2$ with flat CuO_2-layers. The red band was obtained using the Cu $d_{x^2-y^2}$ MTO shown in the CuO_2-layer in the bottom part of the figure.

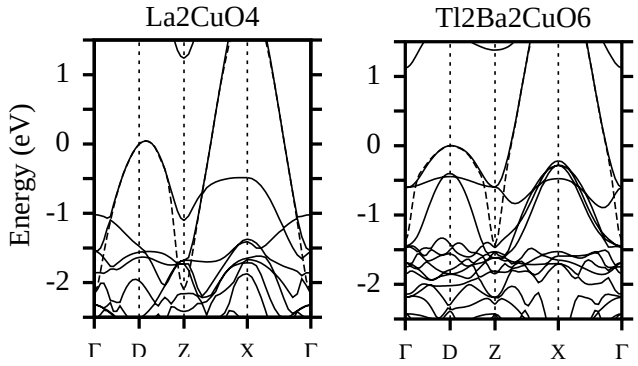

Figure 10: LDA bands calculated with the NMTO method in the bct structure. The dashed band was obtained using the Bloch sum of MTOs with N=0 and Cu $d_{x^2-y^2}$ symmetry at the central site. Γ $(0,0,0)$, D $(\pi,0,0)$, Z $(2\pi,0,0) = (0,0,2\pi/c)$, X $(\pi,\pi,0)$.

near half-filling. The low-energy bands agree with the full band structures to linear order and, in contrast to the N=4-bands in Fig. 9, head smoothly towards the pure Cu $d_{x^2-y^2}$-levels at Γ and Z, extrapolating across a multitude of other bands. Now, the hopping integrals t, t', t'', ... may be obtained by expanding the low-energy band as a Fourier series. This yields: $t = 0.43\,\mathrm{eV}$ in both cases, $t'/t = 0.17$ for La_2CuO_4 and 0.33 for $Tl_2Ba_2CuO_6$, and also many further inter- and intralayer hopping integrals [22].

That all these hopping integrals and their materials-dependence can be described with a generalized four-orbital model is conceivable from the appearance of the conduction-band orbital for La_2CuO_4 shown in Fig. 11 in the xz-plane perpendicular to the layer. Starting from the central Cu atom and going in the x-direction, we see $3d_{x^2-y^2}$ antibond to neighboring O_a $2p_x$, which itself bonds to $4s$ and antibonds to $3d_{3z^2-1}$ on the next Cu. From here, and in the z-direction, we see $4s$ and $3d_{3z^2-1}$ antibond to O_c $2p_z$, which itself bonds to La orbitals, mostly $5d_{3z^2-1}$. In the y-direction, $4s$ antibonds and $3d_{3z^2-1}$ bonds to O_b $2p_y$. For the 85 K superconductor $Tl_2Ba_2CuO_6$, we find about the same amount of Cu $3d_{x^2-y^2}$ and $O_{a/b}$ $2p_{x/y}$ character, but more Cu $4s$, negligible Cu $3d_{3z^2-1}$, much less O_c $2p_z$, and Tl $6s$ instead of La $5d_{3z^2-1}$ character. That is, in $Tl_2Ba_2CuO_6$ the axial part is mainly Cu $4s$. The situation is essentially the same in the simple tetragonal 90 K superconductor $HgBa_2CuO_4$. This is seen in Fig. 12: there is essentially no apical-oxygen character, but substantial Cu $4s$ as recognized from the node it cuts in the plane-oxygen orbital.

Calculations with larger basis sets than one MTO per CuO_2 now confirm that, in order to localize the orbitals to the extent that only nearest-neighbor hoppings are essential, one needs to add *one* orbital, Cu axial, to the three standard ones [22]. This axial (N=0)MTO obtained from calculations with Cu $d_{x^2-y^2}$, O_a p_x, O_b p_y, and Cu s chosen as active is shown in Fig. 13 for $HgBa_2CuO_4$ (left) and La_2CuO_4 (right). The corresponding four-orbital Hamiltonian is therefore the one described above in Fig. 8 and in Eqs. (58)-(59). Note that we continue to call the energy of the axial orbital ε_s, and its hopping integral with $O_{a/b}\,p_{x/y}$ for t_{sp}. Calculations with this basis set for many different materials show that, of all the parameters, only ε_s varies significantly [22]. This variation can be understood in terms of the couplings between the constituents of the axial orbital sketched in the right-hand panel of Fig. 11: We first form the

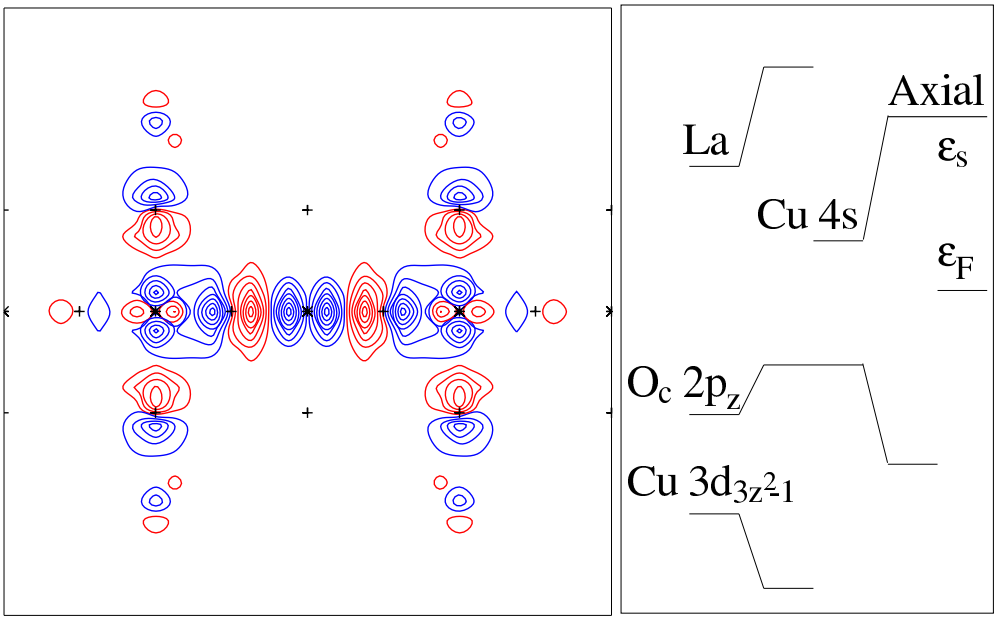

Figure 11: *Left:* N=0 MTO describing the Cu $d_{x^2-y^2}$-like conduction band in La_2CuO_4. The plane is perpendicular to the layers and passes through Cu, O_a, O_c, and La. *Right:* Schematic diagram giving the energy ε_s of the *axial* orbital in terms of the energies of its constituents and their couplings.

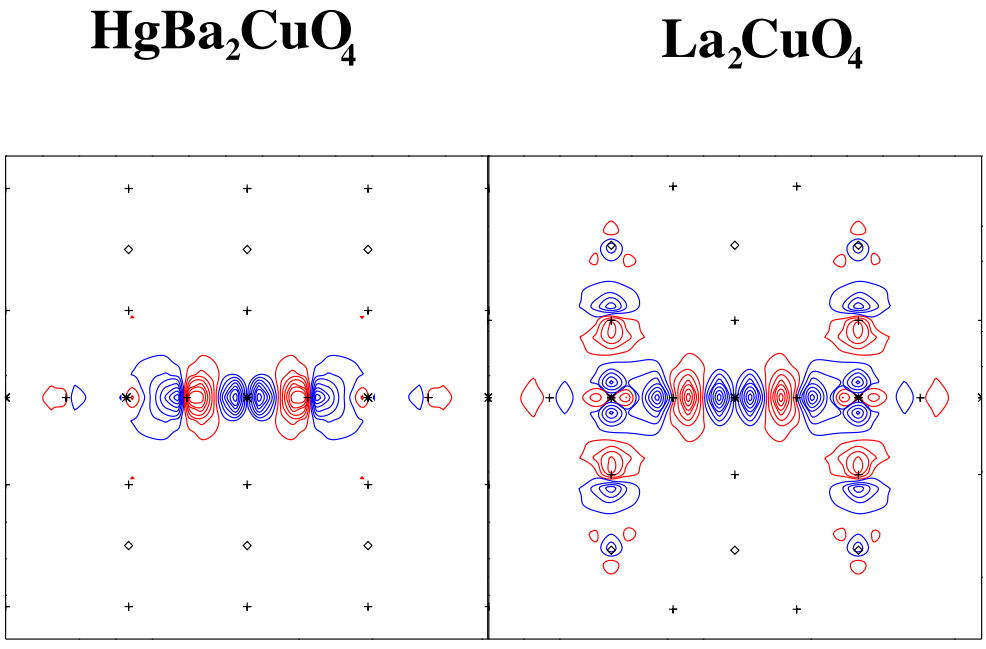

Figure 12: As left-hand side of Fig. 11 and including the conduction-band orbital for $HgBa_2CuO_4$.

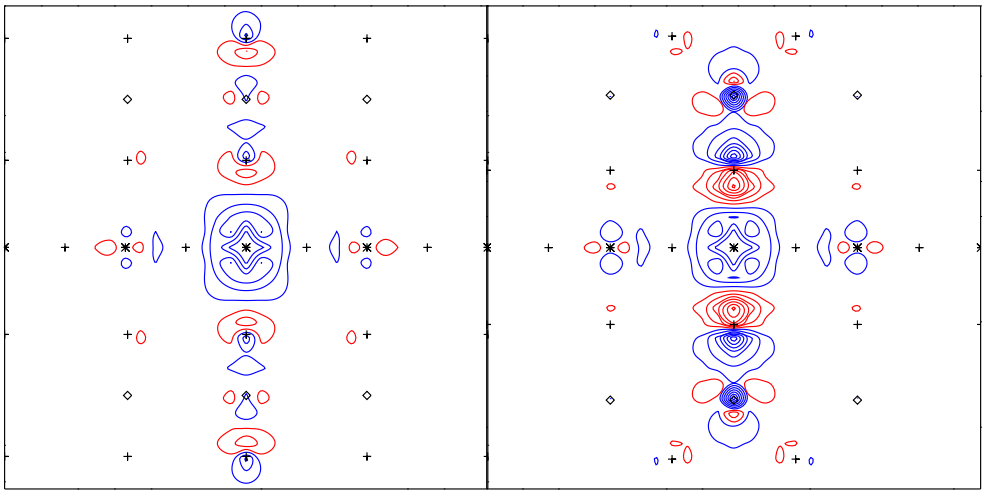

Figure 13: Axial orbital (KPW) for $HgBa_2CuO_4$ (left) and La_2CuO_4 (right) in the xz-plane perpendicular to the CuO_2 layer.

appropriate $O_c\,p_z$-like 5-atom hybrid Cu d_{3z^2-1} - 2$O_c\,p_z$ - 2 La with the energy [22]

$$\varepsilon_c = \varepsilon_{\bar{c}} + \left(1 + \frac{t_{sc}}{t_{sp}}\frac{t_{pz^2}}{t_{cz^2}}\right)^2 \frac{4\bar{r}t_{cz^2}^2}{\varepsilon_F - \varepsilon_{z^2}} - \frac{t_{cLa}^2}{\varepsilon_{La} - \varepsilon_F}, \tag{60}$$

and then we couple this to the Cu s-orbital to yield the energy

$$\varepsilon_s = \varepsilon_{\bar{s}} + \frac{2t_{sc}^2}{\varepsilon_F - \varepsilon_c}$$

of the axial orbital. Here, the energies of the pure Cu s- and $O_c\,p_z$-orbitals are denoted $\varepsilon_{\bar{s}}$ and $\varepsilon_{\bar{c}}$, respectively, while their hopping integral is t_{sc}. The energy of the Cu d_{3z^2-1}-orbital is ε_{z^2} and its hopping integrals to $O_{a/b}\,p_{x/y}$ and $O_c\,p_z$ are respectively t_{pz^2} and t_{cz^2}. In deriving [22] Eqs. (58)-(60), we have exploited that

$$\frac{t_{pz^2}^2}{t_{sp}^2} \ll \frac{\varepsilon_F - \varepsilon_{z^2}}{\varepsilon_{\bar{s}} - \varepsilon_F} \qquad \text{and} \qquad \frac{t_{pd}^2}{t_{sp}^2} \ll \frac{\varepsilon_F - (\varepsilon_p + \varepsilon_d)/2}{\varepsilon_F - (\varepsilon_p + \varepsilon_s)/2}.$$

Although specific for La_2CuO_4, Eq. (60) is easy to generalize.

In Fig. 14 we plot the r-values for single-layer materials against the distance d_{Cu-O_c} between Cu and apical oxygen. r increases with d_{Cu-O_c} because ε_s is lowered towards ε_F when the coupling between $O_c\,p_z$ and Cu d_{3z^2-1}/s is weakened. Since $t_{cz^2} \propto d_{Cu-O_c}^{-4}$ and $t_{sc} \propto d_{Cu-O_c}^{-2}$, increasing the distance suppresses the Cu d_{3z^2-1} content, which is then important in La_2CuO_4, but negligible in $Tl_2Ba_2CuO_6$ and $HgBa_2CuO_4$. This is also reflected in the slopes of the lines in Fig. 14 which give r vs. d_{Cu-O_c} for each material. The strong slope for La_2CuO_4 explains the findings of Seo *et al.* [19], provided that r correlates with superconductivity. That the Bi-point does not fall on the La-line is an effect of Bi being different from La: Bi $6p_z$ couples stronger to $O_c\,2p_z$ than does La $5d_{3z^2-1}$. The figure shows that upon reaching $HgBa_2CuO_4$, r is saturated, $\varepsilon_s \sim \varepsilon_{\bar{s}}$, and the axial orbital is almost purely Cu $4s$.

Fig. 14 hints that for single-layer materials r might correlate with the observed $T_{c\max}$. But the experimental uncertainties of both $T_{c\max}$ and the structural parameters are such that we

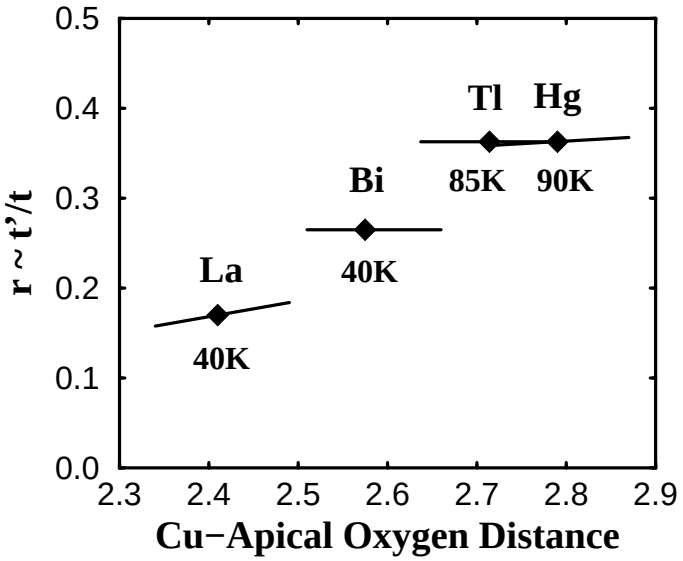

Figure 14: Calculated range parameter, r, for single-layer materials vs. the distance (in Å) between Cu and O_c. The lines result from rigid displacements of O_c.

need better statistics. Therefore, we plot the observed $T_{c\max}$ against the calculated r-values for 15 different HTSC families in Fig. 15. For the single-layer materials we observe a strong correlation between r and $T_{c\max}$, which seems to be continued in the *bonding* subband for the multilayer materials (filled squares). This indicates that the electrons are delocalized over the multilayer [25], and that $T_{c\max}$ increases with the number of layers for the *same* reason that it increases among single-layer materials; the multilayer is simply a means of lowering ε_s further, through the formation of Cu $4s$-Cu $4s$ bonding states. This is consistent with the celebrated pressure-enhancement [24] of T_c in $HgBa_2Ca_2Cu_3O_8$. One might attempt to increase $T_{c\max}$, say for $YBa_2Cu_3O_7$, by substituting Y with a smaller cation, *e.g.* Sc. This has not been done, but a *larger* cation, La, was recently inserted [23] and caused $T_{c\max}$ to drop from 92 K to 50 K. Using the observed structure of $LaBa_2Cu_3O_7$, we have calculated the r-values and included them in Fig. 15. Here again, the bonding subband is seen to follow the trend! That $T_{c\max}$ eventually drops for an increasing number of layers, is presumably caused by loss of phase coherence.

Interlayer coupling in bct La_2CuO_4 mainly proceeds by hopping from $O_c\, p_z$ at $(0,0,zc)$ to its four nearest neighbors at $\left(\pm\frac{1}{2},\pm\frac{1}{2},\left(\frac{1}{2}-z\right)c\right)$, and is therefore taken into account by adding to $\varepsilon_{\bar{c}}$ on the right-hand side of (60) the term

$$-8t_{cc}^{\perp}\cos\frac{1}{2}k_x\cos\frac{1}{2}k_y\cos\frac{1}{2}ck_z.$$

In primitive tetragonal materials, the corresponding term is merely proportional to $\cos ck_z$ because the CuO_2-layers are stacked on top of each other, *e.g.* in $HgBa_2CuO_4$, the interlayer coupling proceeds from $O_c\, p_z$ at $(0,0,zc)$ via Hg $6s/6p_z$ at $(0,0,c/2)$ to $O_c\, p_z$ at $(0,0,(1-z)\,c)$. Periodic interlayer coupling thus makes ε_s depend on k_z, and this passes onto the conduction band a k_z-dispersion proportional to $v^2\cos\frac{1}{2}k_x\cos\frac{1}{2}k_y\cos\frac{1}{2}ck_z$ in bct, and to $v^2\cos ck_z$ in tetragonal structures. Fig. 15 shows how the k_z-dispersion of r decreases with contraction of the axial orbital onto the (multi)layer.

Our identification of an electronic parameter, r or ε_s, which correlates with the observed $T_{c\max}$

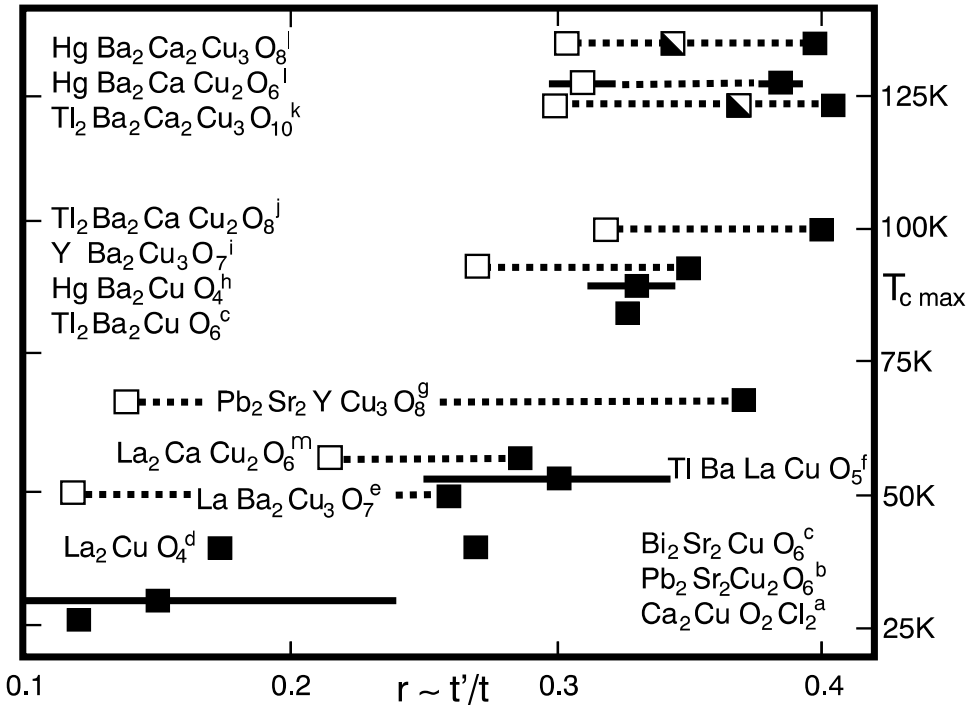

Figure 15: Correlation between calculated r and observed $T_{c\max}$. *Filled squares:* Single-layer materials and most bonding subband for multilayers. *Empty squares:* Most antibonding subband. *Half-filled squares:* Non-bonding subband. *Dotted lines* connect subband-values. *Bars* give k_z-dispersion of r in primitive tetragonal materials.

for all known types of hole-doped HTSC materials should be a useful guide for materials synthesis and a key to understanding the mechanism of HTSC. With current **k**-space renormalization-group methods one could for instance investigate the effect of the band shape on the leading correlation-driven instabilities [26]. Moreover, the possibility that a longer hopping-range leads to better screening of the Coulomb repulsion, maybe even to overscreening, could be studied. Increased diagonal hopping t' might lead to higher $T_{c\,\max}$ by suppression of static stripe order [27]. The Van Hove scenario [28] finds no support in Fig. 15 because it is the saddlepoint of the *anti*-bonding band which is at the LDA Fermi level in $YBa_2Cu_3O_7$; the bonding band is about half-filled and enhances spin-fluctuations with $\mathbf{q} \approx (\pi, \pi)$ [29]. The propensity to buckling is increased by pushing the conduction band towards the $O_{a/b}\,p_z$-level [20] by lowering of ε_s, but recent structural studies [23] as well as Fig. 15 disprove that static buckling enhances $T_{c\,\max}$, although dynamical buckling might. The interlayer-pair-tunnelling mechanism [30] is ruled out by the fact that the additional factor $\cos\frac{1}{2}k_x \cos\frac{1}{2}k_y$ attained by $t^{\perp}(\mathbf{k})$ in bct materials suppresses the interlayer pair-tunnelling in $Tl_2Ba_2CuO_6$ compared with $HgBa_2CuO_4$, and yet, $T_{c\max} \sim 90\,\mathrm{K}$ in both cases. That the axial orbital is *the* channel for coupling the layer to its surroundings is supported [31] by the observations that the **k**-dependence of the scattering in the normal state is v^2-like [21] and that the c-axis transport is strongly suppressed by the opening of a pseudogap [32] with similar **k**-dependence. The axial orbital is also *the* non-correlated vehicle for coupling between oxygens in the layer. Therefore it seems plausible that contraction of the axial orbital around the CuO_2-layer, away from the non-stoichiometric layers, will strengthen the phase coherence and thus increase $T_{c\max}$. Thermal excitation of nodal quasiparticles [33]

is, on the other hand, hardly the mechanism by which the superconducting state is destroyed, because the axial orbital does not influence the band in the nodal direction.

Finally we note that the correlation between r and $T_{c\,\max}$ does not extend to electron-doped cuprates, where the mechanism for superconductivity thus seems to be different.

Conclusion

We have solved the long-standing problem [34] of deriving energy-independent, short-ranged orbitals from scattering theory. What in the 1st-generation of the LMTO formalism was possible only through the Ansatz of neglecting the energy dependence in the interstitial, was solved in the 2nd and 3rd generations through an exact screening transformation. By treating the interstitial on the same footing as the MT-spheres, the direct relation to scattering theory, efficient downfolding through screening, and the extension to overlapping, but short-ranged potentials comes 'for free.' However, since the energy ϵ_0 around which the partial waves are expanded is now global, Taylor expansion to linear order is not always sufficient. The final step was therefore to generalize to arbitrary order and discrete meshes. By application of the NMTO formalism to a few examples, we hope to have indicated how it may become of considerable practical importance.

References

[1] J. Korringa, Physica **13,** 392 (1947); W. Kohn and J. Rostoker, Phys. Rev. **94,** 1111 (1954).

[2] O.K. Andersen, O. Jepsen, and G. Krier in *Lectures on Methods of Electronic Structure Calculations,* edited by V. Kumar, O.K. Andersen, and A. Mookerjee (World Scientific Publishing Co., Singapore, 1994), pp. 63-124.

[3] O.K. Andersen, C. Arcangeli, R.W. Tank, T. Saha-Dasgupta, G. Krier, O. Jepsen, and I. Dasgupta in *Tight-Binding Approach to Computational Materials Science,* Eds. L. Colombo, A. Gonis, P. Turchi, Mat. Res. Soc. Symp. Proc. Vol. 491 (Materials Research Society, Pittsburgh, 1998) pp 3-34.

[4] R.W. Tank and C. Arcangeli, phys. stat. sol. (b) **217**, 89-130 (2000).

[5] O.K. Andersen, T. Saha-Dasgupta, R.W. Tank, C. Arcangeli, O. Jepsen, and G. Krier in *Electronic Structure and Physical Properties of Solids. The Uses of the LMTO Method,* Ed. H. Dreysse (Springer Lecture Notes in Physics, New York, 2000) pp. 3-84.

[6] O.K. Andersen and C. Arcangeli (unpublished); C. Arcangeli and O.K. Andersen (unpublished).

[7] D. Savrasov and O.K. Andersen (unpublished).

[8] L. Vitos, H.L. Skriver, B. Johansson, et al., Comp. Mater. Sci. **18,** 24 (2000).

[9] Pavarini E., I. Dasgupta, T. Saha-Dasgupta, O. Jepsen, O.K. Andersen, Phys. Rev. Lett. **87**, 047003 (2001).

[10] O.K. Andersen and T. Saha-Dasgupta, Phys. Rev. B **62,** R16 219 (2000).

[11] For a review, see F. Aryasetiawan *et al.,* Rep. Prog. Phys. **61,** 237 (1998).

[12] L. Tsetseris, O. Jepsen, and O.K. Andersen (unpublished).

[13] O.K. Andersen, A.V. Postnikov, and S. Yu. Savrasov, in *Applications of Multiple Scattering Theory to Materials Science,* eds. W.H. Butler, P.H. Dederichs, A. Gonis, and R.L. Weaver, MRS Symposia Proceedings No. 253 (Materials Research Society, Pittsburgh, 1992) pp 37-70.

[14] Our energy windows are limited in size by the requirement, that for two energies within the window, $\phi_{RL}(\varepsilon, \mathbf{r})$ and $\phi_{RL}(\varepsilon', \mathbf{r})$ cannot be orthogonal. Hence, the present NMTOs do not carry principal quantum numbers.

[15] In Eq. (6) of Ref. [10], $-(\varepsilon - \epsilon_N)$ is misprinted as $+(\varepsilon - \epsilon_N)$.

[16] T.F.A. Müller *et al.,* Phys. Rev. B **57**, R12655 (1998); D.D. Sarma *et al.*, Phys. Rev. Lett. **85**, 2549 (2000); R. Valenti *et al.*, cond-mat/0101282.

[17] For a recent review, see J. Orenstein and A.J. Millis, Science **288**, 468 (2000), and further articles in that volume.

[18] V.J. Emery and S.A. Kivelson, Nature **374**, 434 (1995).

[19] J.W. Seo *et al.*, 18th EPS-CMD Conference, Montreux, p 363 (2000); J.-P. Locquet *et al.* Nature **394**, 453 (1998) and H. Sato *et al.,* Phys. Rev. **61**, 12 447 (2000).

[20] O.K. Andersen *et al.*, J. Phys. Chem. Solids **56**, 1573 (1995); J. Low. Temp. Physics **105**, 285 (1996).

[21] Z.X. Shen and D.S. Dessau, Phys. Rep **253**,1 (1995); H.H. Fretwell *et al.*, Phys. Rev. Lett. **84**, 4449 (2000); S.V. Borisenko *et al.*, Phys. Rev. Lett. **84**, 4453 (2000).

[22] I. Dasgupta *et al.* (to be published).

[23] D. Godschmidt *et al.*, Phys. Rev. B **48**, 532 (1993); O. Chmaissem *et al.*, Nature **397,** 45 (1999).

[24] C.W. Chu *et al.,* Nature **365**, 323 (1993); M. Nunez-Regueiro *et al.,* Science **262**, 97 (1993).

[25] This is consistent with the observation of bilayer splitting by D.L. Feng *et al.*, cond-mat/0102385.

[26] C.J. Halboth and W. Metzner, Phys. Rev. B **61**, 7364 (2000); C. Honerkamp *et al.,* cond-mat/9912358.

[27] M. Fleck *et al.,* cond-mat/0102041.

[28] D.M. Newns *et al.*, Com.Cond.Mat.Phys. **15,** 273 (1992).

[29] V.S. Oudovenko *et al.,* Physica C **336**, 157 (2000).

[30] S. Chakravarty *et al.,* Science **261**, 337 (1993).

[31] A.Z. Zheleznyak *et al.,* Phys.Rev. B **57**, 3089 (1998); L.B. Ioffe and A.J. Millis, Phys. Rev. B **58,** 11631 (1998).

[32] D. Basov *et al.*, Phys. Rev. B **50**, 3511 (1994); C.C. Holmes *et al.*, Physica C **254**, 265 (1995).

[33] P.A. Lee and X.G. Wen, Phys. Rev. Lett. **78**, 4111 (1997).

[34] See for instance, J. Hubbard, Proc. Phys. Soc. London. **92,** 921 (1967).